Probing the biological functions and interactions of the Fkh1 FHA domain in *Saccharomyces cerevisiae*

By

Antoinette M. Dummer

A dissertation submitted in partial fulfillment of

the requirements for the degree of

Doctor of Philosophy

(Cellular and Molecular Biology)

at the

UNIVERSITY OF WISCONSIN-MADISON

2016

Date of final oral examination: 05/13/2016
The dissertation is approved by the following members of the Final Oral Committee:

Elizabeth A. Craig, Professor, Biochemistry
Catherine A. Fox, Professor, Biomolecular Chemistry
Melissa M. Harrison, Assistant Professor, Biomolecular Chemistry
Michael D. Sheets, Professor, Biomolecular Chemistry
David A. Wassarman, Professor, Medical Genetics

Abstract

Probing the biological functions and interactions of the Fkh1 FHA domain in *Saccharomyces cerevisiae*

The *Saccharomyces cerevisiae* Fkh1 protein is a multifunctional protein with roles in cell-cycle regulated transcription, DNA replication timing, as well as a role in recombination donor preference during mating-type switching. While Fkh1 has been implicated in many processes, very little is known about the mechanisms or interactions that govern its functions. The phosphothreonine-binding FHA domain of Fkh1 has been shown to be sufficient for regulating donor preference during mating-type switching. A model posits that Fkh1 mediates a long-range chromosomal interaction to promote recombination between two distant loci and that this requires an interaction between the FHA domain and a phosphorylated partner protein(s), but to date no relevant partner has been described. I have shown that the FHA domain is required for Fkh1's interaction with multiple partner proteins and is important for many different Fkh1 functions. In my studies I have found that Fkh1's interaction with the Mph1 DNA repair helicase regulated donor preference during mating-type switching. I have identified two threonines within Mph1 that were particularly important for this interaction. Yeast-2-hybrid analysis and *in vitro* binding experiments indicated that at least one of these threonines had to be phosphorylated for efficient

Fkh1 binding. Substitution of these two threonines with alanines (*mph1-2TA*) specifically abolished the Fkh1-Mph1 interaction and altered donor preference during mating-type switching without affecting other functions of Mph1 in genome stability. Deletion of a second gene encoding a Fkh1-interacting protein, *FDO1*, also resulted in a change in Fkh1-dependent donor preference that was additive with deletion or mutation of *MPH1*. However, deletion of both genes did not result in a change in donor preference as drastic as that resulting from mutation of *FKH1*, suggesting Fkh1 must interact with additional proteins to accomplish this role. I also found that the FHA domain was important for Fkh1's role in cell-cycle regulation, but no single interaction partner could account for this role. I propose that Fkh1 must interact with multiple different proteins to accomplish its role in donor preference as well as other roles in which Fkh1 has been implicated.

Acknowledgements

First I would like to thank the members of the Fox lab, both current and former. I want to especially thank my advisor, Catherine Fox, as well as Tim Hoggard, and Rachel Cherney. I also would like to thank my collaborators outside of the Fox lab, Zhangli Su, John Denu, and Xiaolan Zhao. I would like to thank the members of my committee, Betty Craig, Jim Keck, Mike Sheets, and David Wassarman, as well as Melissa Harrison for filling in on my final thesis committee.

Table of Contents

List of Tables and Figures

Chapter 1

Chapter 2

Chapter 1

Introduction

1.1 The Eukaryotic Cell Cycle and the Fkh1 and Fkh2 proteins

1.1.1 The yeast cell cycle

The cell cycle is the universal program that eukaryotic cells use to organize distinct cellular events necessary for cell division. There are four defined phases of the cell cycle. In the G1-phase cells take in nutrients, grow, and sense their environment to determine if there are enough resources to commit to cell division. After G1-phase, cells enter S-phase to duplicate their chromosomes. In G2-phase, cells make sure DNA replication is completely finished and that any mistakes have been repaired. Finally, during M-phase cells segregate their duplicated chromosomes and undergo cytokinesis to form two new daughter cells that will re-enter the cell cycle in the G1-phase (Figure 1-1). The cell cycle is highly regulated to ensure that the appropriate molecular events occur in the correct order and without errors. Deregulation of cell cycle events can lead to catastrophic damage such as cancer or cell death. To prevent such damage, cells contain complex networks of transcription factors, kinases, and other regulators that program the cell cycle and ensure that these cellular processes are properly regulated. Many of these factors and regulatory networks are universally conserved among eukaryotic organisms.

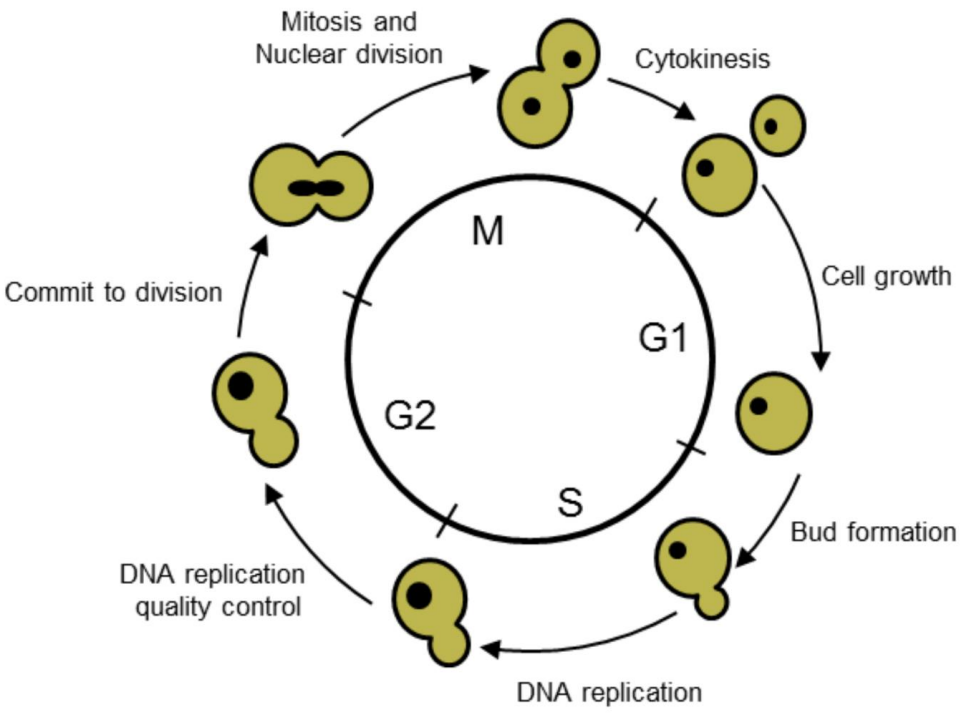

Figure 1-1. The yeast cell cycle. The yeast mitotic cell cycle is divided into four distinct phases. During the G1-phase cells grow and determine whether or not there are sufficient resources to divide. DNA replication occurs in S-phase and the daughter cell bud begins to form. During the G2-phase cells ensure that their DNA has been properly replicated. Finally, during M-phase the nucleus divides and the cell undergoes cytokinesis in which it separates into two cells. Unlike metazoans, yeast have a "closed mitosis" in which the nuclear membrane remains intact and divides independently from the rest of the cell during M-phase.

1.1.2 Cyclins and CDK

Cyclin-dependent kinases (CDKs), which phosphorylate target proteins that carry out cell cycle phase-specific actions, are the main drivers of the cell cycle. CDK activity is composed of a distinct kinase in close association with a cyclin protein that endows the CDK with specificity for protein targets. The availability of different cyclin subunits changes during the cell cycle, allowing for a single CDK to phosphorylate different targets throughout the cell cycle. The budding yeast *Saccharomyces cerevisiae* has a single CDK (Cdc28) that associates with one of nine different cyclins, each of which guides the CDK to particular targets during different phases of the cell cycle (Figure 1-2) [1].

The G1 cyclin genes *CLN1*, *2*, and *3* are highly transcribed during the G1-phase of the cell cycle and direct many cellular events that occur in the G1-phase. For example, Cln-Cdc28 kinase activity is responsible for targeting the Clb-kinase inhibitor Sic1 for degradation, which is required for entry into S-phase [2]. The S-phase cyclins, Clb5 and Clb6 are highly expressed in G1 phase, but are not active until early S-phase after the degradation of Sic1. These cyclins guide CDK to phosphorylate proteins that function in the initiation of DNA replication in S-phase. For example, Clb5 guides CDK to phosphorylate target proteins that function directly in DNA replication, such as ORC, the complex that binds to DNA replication origins [3]. The M-phase cyclins Clb3 and Clb4 accumulate during S-phase to promote the G2/M phase transition, while Clb1 and Clb2 accumulate in the G2-phase of the cell cycle to promote the molecular events required for mitosis and cytokinesis [2]. Because the concentrations of specific cyclins drive cell phase-specific molecular events, mechanisms that control the periodic levels and activity of cyclin proteins are critical. These mechanisms include periodic transcriptional activation and repression, as well as targeted degradation and inhibition. The factors that regulate the cyclins are also cell-cycle

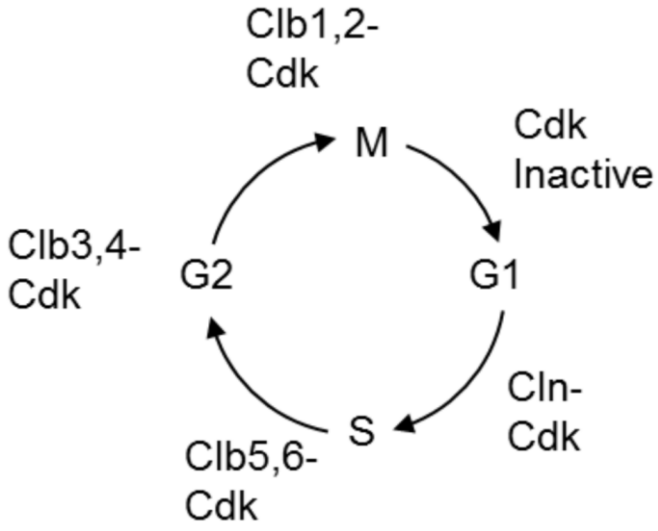

Figure 1-2. Cdk complexes active at different phases of the cell cycle.

regulated, creating self-reinforcing waves of expression of both cyclins and their regulators that define the different stages of the cell cycle.

1.1.3 The CLB2-*cluster*

A group of genes called the *CLB2*-cluster are highly transcribed in the G2-phase of the cell cycle. This cluster consists of over 30 genes that encode proteins required for M-phase, including many required for mitosis and cytokinesis [4]. For example, the *BUD4* gene is included within this *CLB2*-cluster and the Bud4 protein is required for axial budding in haploid yeast [5]. The promoter of three of these *CLB2*-cluster genes, *CLB1*, *CLB2*, and *SWI5*, have been characterized in detail. These promoters share common sets of DNA sequence elements responsible for their periodic transcription [6–8]. One of these elements binds the MADS-box transcription factor, Mcm1. Mcm1 forms a ternary complex with these promoters and another factor, originally dubbed 'Swi5 factor' (SFF) based on its ability to promote periodic transcription of the *SWI5* gene [6]. Both Mcm1 and SFF are required for the periodic activation of these genes in late G2 and early M phase.

1.1.4 Identification of Fkh1 and Fkh2 as regulators of CLB2-*cluster transcription*

The molecular identity of SFF was revealed over ten years after its initial discovery as the Fkh2 (forkhead homology 2) protein. The identification was challenging in part because Fkh2 has a paralog in *S. cerevisiae*, Fkh1 that can largely substitute for the function of Fkh2 in *fkh2*Δ cells. In *FKH2* cells, Fkh1 has a poorly understood role in attenuating the *CLB2*-cluster expression cycle.

A number of independent studies provide evidence that Fkh1 and 2 are important for and have redundant/overlapping roles in *CLB2*-clutser transcription and cell cycle regulation. In particular, deletion of both *FKH* genes to create *fkh1*Δ*fkh2*Δ cells, but not deletion of either gene

alone, causes a major defect in the transcription of the *CLB2* gene and other *CLB2*-cluster genes [9–11]. In *fkh1*Δ*fkh2*Δ cells, the expression of *CLB2*-clutser genes is delayed relative to the G1-S-phase transition and the peak level of expression is substantially reduced. Moreover, in wild type cells *CLB2*-cluster gene expression is fully repressed in G1, but in *fkh1*Δ*fkh2*Δ (and *FKH1fkh2*Δ) cells these genes remain expressed, albeit at low levels. The end result is that *fkh1*Δ*fkh2*Δ exhibit a much shallower CLB2-cluster expression cycle compared to wild type cells (Figure 1-3A). In addition, *fkh1*Δ*fkh2*Δ cells exhibit a major cell cycle defect that manifests itself in elongated cells that grow in chains and penetrate solid agar media. This pseudohyphal-like morphology is reminiscent of the phenotype caused by deletion of *CLB1* and *CLB2* (Figure 1-3B) [9–15]. These and other data suggest that the cell cycle and morphological defects of *fkh1*Δ*fkh2*Δ cells are caused by the loss of transcription of *CLB2*-cluster and possibly other genes.

While *FKH1* and *FKH2* clearly had overlapping roles in *CLB2*-cluster expression and cell cycle regulation, subsequent biochemical studies established that Fkh2, and not Fkh1, is the major DNA-binding component of SFF. Indeed, direct biochemical purification of SFF followed by mass spectrometry revealed the presence of Fkh2, but not Fkh1 [10]. In addition, Fkh2 binds to *CLB2*-cluster promoters in a cooperative manner with Mcm1 whereas Fkh1 shows no cooperative interactions with Mcm1 [10,12,13,16]. These and other data described below support the conclusion that Fkh2, and not Fkh1, is the major transcription factor responsible for *CLB2*-cluster expression. Nevertheless, both Fkh1 and Fkh2 bind to *CLB2*-cluster gene promoters *in vivo*, consistent with the finding that these proteins have similar DNA binding domains (DBDs) and in fact are extremely similar throughout the length of the smaller Fkh1 protein (Figure 1-4). However, *fkh1*Δ also show differences in *CLB2* expression compared to wild type cells, albeit subtle

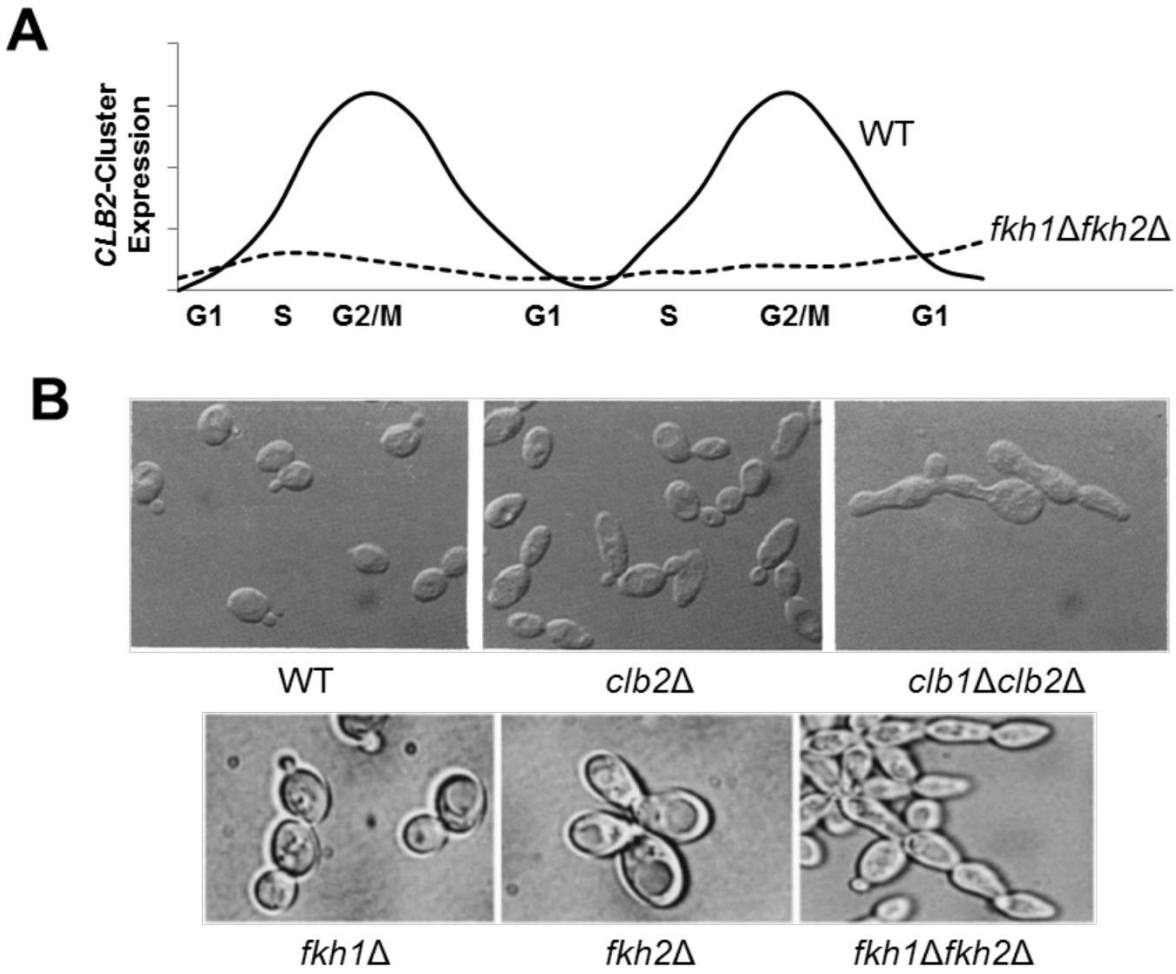

Figure 1-3. *CLB2*-cluster transcriptional defect and morphological defect in *FKH* mutants. (**A**) Cartoon depiction of *CLB2*-cluster transcript levels throughout the cell cycle of WT and *fkh1*Δ*fkh2*Δ yeast. Levels of *CLB2*-cluster transcription are much lower in *fkh1*Δ*fkh2*Δ yeast and their levels peak later in the cell cycle. (**B**) Images of WT, *clb2*Δ, and *clb1*Δ*clb2*Δ mutant yeast from [14]. Images of *fkh1*Δ, *fkh2*Δ, and *fkh1*Δ*fkh2*Δ mutant yeast from [9]. Pseudohyphal growth is observed in both *fkh1*Δ*fkh2*Δ and *clb1*Δ*clb2*Δ yeast.

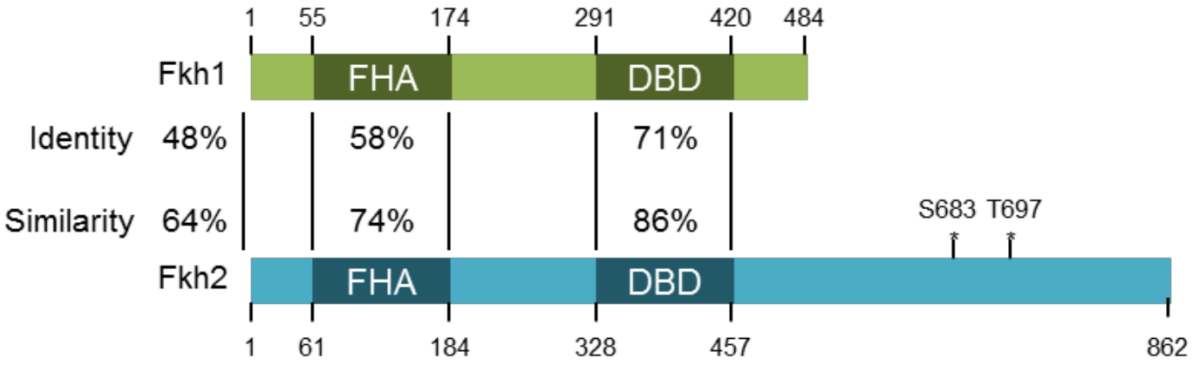

Figure 1-4. Primary amino acid sequence comparison of Fkh1 and Fkh2. Adapted from [10]. Boundaries of the phosphothreonine-binding Forkhead-associated (FHA) domains were determined based on my own homology modeling and alignment (discussed in Chapter 2 and Appendix B). Boundaries of the DNA binding domains (DBDs) were based on [9]. Identity and similarity calculated using BLAST P [17]. Fkh2 phosphorylation sites [18] are marked with asterisks**.**

compared to either *fkh2*Δ or *fkh1*Δ*fkh2*Δ cells [9]. All together these and other data indicate that *FKH2* is likely the main regulator of *CLB2*-cluster transcription, with *FKH1* playing an accessory and perhaps attenuating role in wild-type cells. However, in the absence of Fkh2, Fkh1 can clearly substitute to a large extent for Fkh2 functions, though the precise mechanisms by which Fkh1 plays this role are unclear.

1.1.5 Mechanisms of transcriptional regulation by Fkh1 and Fkh2

The mechanism by which Fkh2 regulates transcription of *CLB2*-cluster genes has been worked out in some detail (Figure 1-5). Fkh2-Mcm1 cooperative binding requires a small region of Fkh2 N-terminal of its DNA binding domain that is not present on Fkh1 [19]. This binding requires residue Y315 of Fkh2 and V69 of Mcm1 [19]. This Fkh2-Mcm1 complex remains bound to promoters throughout the entirety of the cell cycle and acts as a landing pad for other regulatory proteins that activate or repress transcription of target genes at various stages of the cell cycle. Fkh1 also remains bound to *CLB2*-cluster promoters throughout the cell cycle and, because *CLB2*-cluster promoters often contain multiple *FKH* binding sites, may bind to these promoters simultaneously with Fkh2, though this postulate has not been tested directly [16,20].

Both Fkh1 and Fkh2 have been shown to associate with the Sir2 histone deacetylase at *CLB2*-cluster promoters throughout the G2-, M- and G1-phases of the cell cycle, repressing transcription of target genes [21]. Deletion of *FKH1*, *FKH2*, and *SIR2* is lethal, suggesting that Sir2 must also be able to function by some other mechanism in the absence of Fkh1 and Fkh2 [21]. Fkh2 also binds the Sin3/Rpd3 histone deacetylase complex through the same phases of the cell cycle and represses transcription of target genes [22,23]. The N-terminus of Fkh2 is required for Sin3/Rpd3 association with promoters [22]. This region is similar between Fkh1 and 2, but the

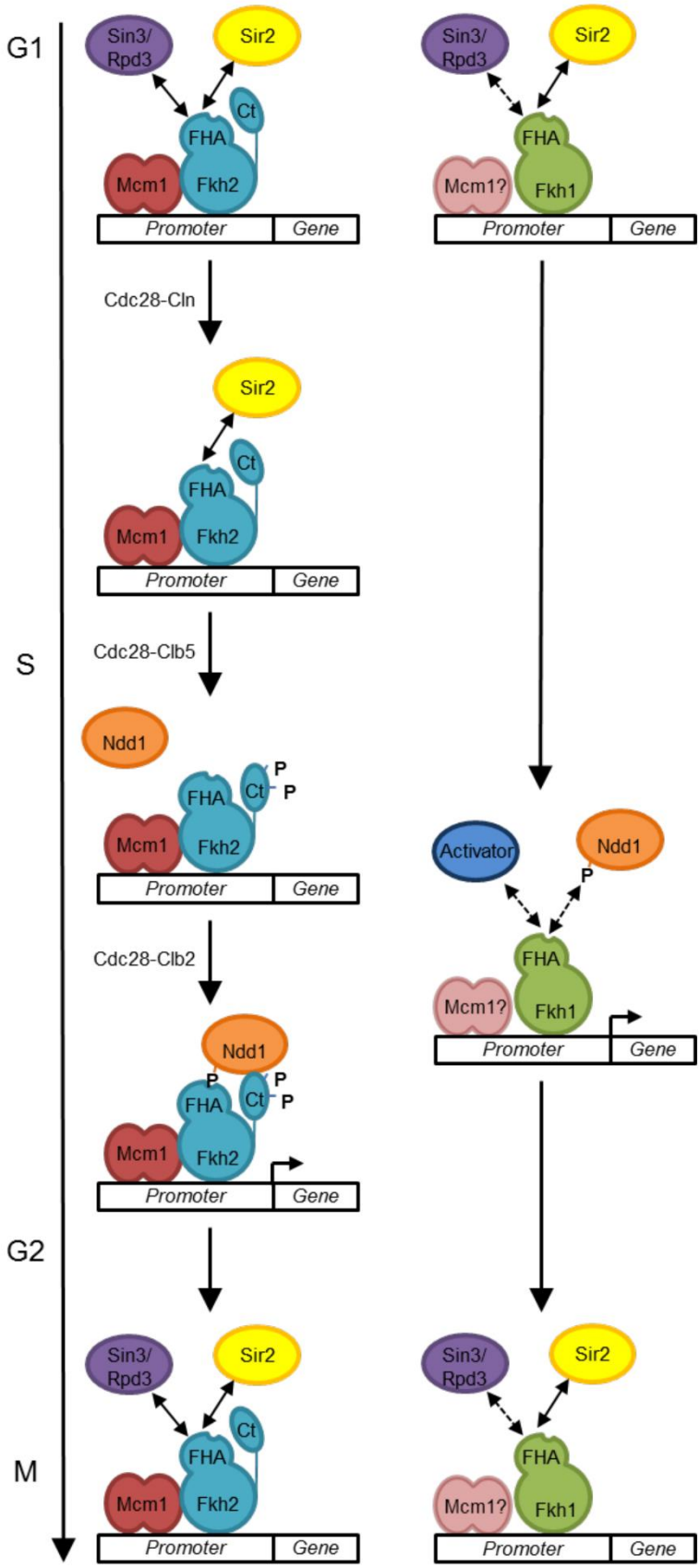
G1
S
G2
M
Sin3/
Rpd3
Sir2
Ct
FHA
Mcm1
Fkh2
Promoter
Gene
Cdc28-Cln
Cdc28-Clb5
Cdc28-Clb2
Ndd1
P
Mcm1?
Fkh1
Activator

Figure 1-5. Fkh-regulated transcription. Mcm1 and Fkh2 cooperatively bind to target promoters throughout the cell cycle. Fkh1 also binds to promoters throughout the cell cycle. It does not bind cooperatively with Mcm1, but it is not known whether Mcm1 is also able to bind in the presence of Fkh1. Through the G2-, M-, and G1-phases of the cell cycle Sin3/Rpd3 and Sir2 bind to Fkh1 and 2 and represses transcription of target genes. While Sir2 associates with both Fkh1 and 2 it is unknown whether Sin3/Rpd3 associates with Fkh1 under wild-type conditions or only in the absence of Fkh2. Cln-kinase activity is required for removal of Sin3/Rpd3 from Fkh2. Fkh2 is phosphorylated on S683 and T697 by the Cdc28-Clb5 kinase early in S-phase. Ndd1 is then phosphorylated by Cdc28-Clb2 and binds directly to the Fkh2 FHA domain and activates transcription of target genes. It is unclear what role Fkh1 plays in S-phase. Fkh1 is able to recruit Ndd1 in the absence of Fkh2, but it is unknown whether this association occurs in wild-type cells. It is also unknown whether Fkh1 is able to bind additional transcriptional activators. It is possible that in wild-type cells the normal function of Fkh1 is to attenuate Fkh2-transcription through repression. Adapted from [18,21–23].

exact residues that are required for Sin3/Rpd3-Fkh2 binding are unknown and may not be conserved between Fkh1 and 2. However, Sin3/Rpd3 are able to be recruited by Fkh1 at some promoters in the absence of Fkh2 [23]. The G1 CDK is required in late G1 to remove Sin3/Rpd3 from Fkh2 and promoter regions, releasing inhibition of transcription. However, release of Sin3/Rpd3 from these promoters is not sufficient to activate transcription of target genes [22].

To activate transcription, Fkh2 recruits the Ndd1 protein in S-phase. In contrast to *FKH2*, *NDD1* is an essential gene and its deletion is lethal [24]. However, deletion of *FKH2*, but not *FKH1*, suppresses the lethality of *ndd1*Δ [12,19,25], suggesting Ndd1 is necessary for activation of transcription when Fkh2 is bound to promoters, but that some alternative mechanism must exist in Fkh2's absence. Additionally, deletion of the Fkh2 C-terminus, which is not shared with Fkh1, suppresses the lethality of *NDD1* deletion, suggesting a role for the Fkh2 C-terminus in Ndd1-regulated transcription [25]. Indeed, the C-terminus of Fkh2 is phosphorylated on S683 and T697 by Cdc28-Clb5 in G1/S-phase, enhancing binding to Ndd1 [18]. It is unclear whether this effect is achieved through direct binding of Ndd1 to phosphorylated sites on Fkh2 or if phosphorylation causes a conformational change in Fkh2, allowing more efficient Ndd1 binding. The phosphothreonine-binding FHA domain of Fkh2 also promotes Ndd1 binding [26]. Consistent with the Fkh2 FHA domain's interaction with Ndd1, Ndd1 is phosphorylated on T319 by Cdc28-Clb2 and this phosphorylation is required for binding Fkh2 [25]. Once Ndd1 is bound to Fkh2, it is this Mcm1-Fkh2-Ndd1 complex that activates transcription of target genes. Both Fkh2 and Fkh1 are capable of recruiting Ndd1 to promoters, although they may not use the same molecular interactions to do so, and Fkh1 likely recruits Ndd1 only when Fkh2 is absent [12].

In summary, the existing evidence points to Fkh1 being the main regulator of *CLB2*-cluster transcription and the major component of SFF. However, it is clear that Fkh1 must also be able to

regulate transcription of these genes in the absence of Fkh2, as both genes need to be deleted to observe the most substantial *CLB2*-cluster transcription and cell cycle and cell morphology defects. However, the mechanisms by which Fkh1 regulates *CLB2* transcription in either the presence or absence of Fkh2 remain unclear.

1.2 FHA Domains

1.2.1 Role of FHA domains in biology

Forkhead-associated (FHA) domains are protein-protein interaction domains with a high specificity for binding phosphothreonines [27]. Over 2000 proteins in prokaryotes and eukaryotes contain FHA domains [28]. In eukaryotes these domains are especially prevalent among regulatory proteins such as kinases, phosphatases, and transcription factors. They play a crucial role in DNA damage sensing and repair, chromatin remodeling, cell cycle regulation, DNA replication, and transcription [29–32]. Many FHA domain-containing proteins play important roles in disease, such as NBS1, which plays a role in the human disease Nijmegen breakage syndrome [33,34], the kinesin family protein KIF13A, which has been shown to play a role in anxiety in mice [35], and Chk2, which plays a role in human cancers [36].

1.2.2 Structure of FHA domains

FHA domains are unique among phosphopeptide binding domains in that they specifically bind phosphothreonine peptides and have little to no affinity for phosphoserine peptides [37]. Though the primary amino acid sequence of FHA domains is not well conserved, the structure is conserved. The structure of an FHA domain consists of a β sandwich comprised of at least 11 β

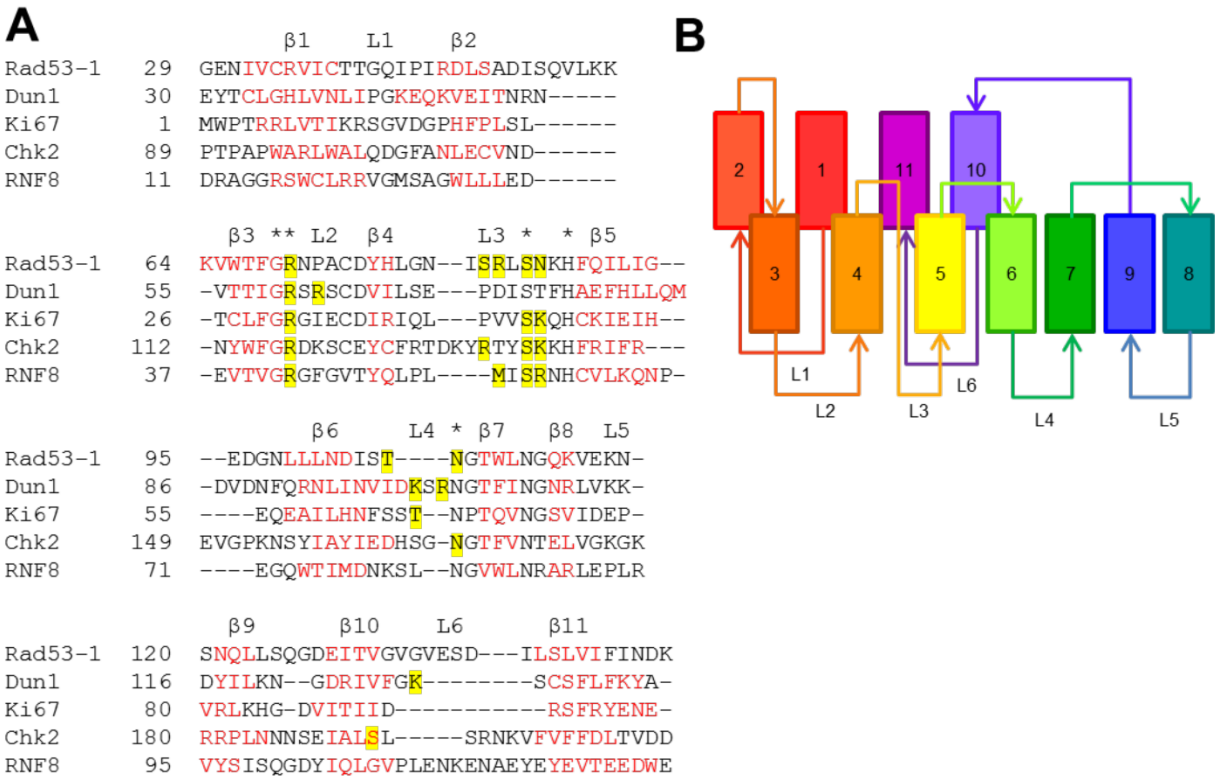

Figure 1-6. FHA domain structure. (**A**) Structure-based sequence alignment of different FHA domain-containing proteins. Beta strands are in red letters. Numbered beta strands and loops are labeled above the corresponding sequence. The five conserved FHA residues which comprise the pT binding pocket are marked with asterisks. Residues in each protein shown to be important for binding phosphopeptides are highlighted. Adapted from [38] with additional information from [39–43]. (**B**) The conserved FHA domain fold contains 11 β strands linked by loops. The peptide binding interface is on loops labeled 1-6. Adapted from [38].

strands, with loops between β strands acting as the protein-protein binding interface (Figure 1-6). Some FHA domains contain additional structures within the loops, but the overall fold of the β sandwich remains intact. There are five amino acids conserved among all FHA domains which comprise the phosphothreonine binding pocket (Figure 1-6A, starred). These amino acids are located within loops 2, 3, and 4 (Figure 1-6). A number of interactions between these loops increase their rigidity and stabilize the phosphothreonine binding pocket [38].

1.2.3 Determinants of FHA-phosphopeptide binding specificity

Most FHA domains interact with very short peptides within proteins, making contact with only a few amino acids N- and C-terminal to the phosphothreonine. Some of the first FHA domains characterized display a preference for a specific amino acid at the position 3 amino acids C-terminal to the phosphothreonine (pT+3). This led to different FHA domains being grouped according to the type of amino acid preferred at the pT+3 position. There are FHA domains that prefer a negatively charged residue at the pT+3 position (including the N-terminal FHA domain of the DNA damage response checkpoint kinase Rad53 [39]), those with a preference for an aliphatic residue (including the C-terminal Rad53 FHA domain [39]), and those with a preference for a hydrophobic residue (including the E3 ubiquitin ligase RNF8 [43]). However, even within these groups there is flexibility in what types of peptides FHA domains can bind. For example, the N-terminal FHA domain of Rad53 generally prefers an aspartic acid at the pT+3 position, but has been shown to efficiently bind peptides containing an isoleucine at this position (See Table 1-1 for binding affinities) [44]. More recently FHA domains with no preference for a particular pT+3 residue have been characterized. For example, the checkpoint kinase Dun1 has a preference for a dual phosphothreonine peptide, with one binding to the canonical pT binding pocket, and a second

Table 1-1. Binding affinities of different FHA domains and phosphothreonine peptides. The phosphothreonine residue that binds within the main pT binding pocket is shown in bold.

Protein	Peptide sequence	K_d (μM)	Ref.
Rad53-1	LEV(**pT**)EADATFAK	0.53	[39]
Rad53-1	NDPD(**pT**)LEIYS	15	[44]
Dun1	NI(pT)QP(**pT**)QQST	0.3-1.2	[40]
Ki67	KTVD(pS)QGP(**pT**)PVC(pT)PTFLERRKSQVAELNDDDKDDEIVFKQPISC	0.077	[45]
Chk2	RHFD(**pT**)YLIRR	0.9	[42]
Chk2	DDDSASEADSTD(**pT**)ELFETG	0.869	[46]
RNF8	DDDSASEADSTD(**pT**)ELFETG	0.833	[46]

pT residue at the pT-2 position binding in a secondary binding pocket [40]. The human cell cycle protein Ki67 has an additional binding interface on β strand 4 that interacts with an extended peptide, providing specificity far outside of the traditional pT peptide [45].

There have been at least two reports of FHA domains that do not require a phosphothreonine for binding. One of these is the *Mycobacterium tuberculosis* Rv1827 FHA domain, which has been shown to bind partner proteins in a phospho-independent manner. However, phosphorylation of a threonine residue within Rv1827 triggers an intramolecular interaction between this phosphopeptide and the Rv1827 FHA domain. This intramolecular interaction is stronger than the phospho-independent interactions and precludes Rv1827 from binding these other partners [47]. Thus, while Rv1827 is able to bind non-phosphorylated proteins, its affinity for phosphorylated proteins is much higher. The second phospho-independent interaction is that between Rad53 and Dbf4. This interaction appears to occur on a different interface of the N-terminal Rad53 FHA domain than phosphothreonine binding, as a mutant form of Rad53 that doesn't have the ability to bind phosphopeptides (Rad53-R70A) is still able to bind Dbf4 [48]. Additionally, crosslinking a phosphothreonine peptide to Rad53 does not inhibit interaction with Dbf4. This Rad53-Dbf4 interaction requires β strands 1, 7, 10, and 11 of the Rad53 FHA domain. This interaction surface is different from that on Ki67 which binds an extended peptide. Thus, while most characterized FHA interactions are phosphothreonine dependent and occur on the pT binding interface, it is possible for FHA domains to interact through other interfaces.

1.3 Fkh1 role in mating-type switching

1.3.1 Yeast mating types and switching

In the haploid form yeast exist as one of two distinct mating types, *MAT***a** or *MAT*α. Diploids are formed by the conjugation of opposite mating-types to form *MAT***a**/*MAT*α. Yeast mating-types are determined by the genes encoded at the *MAT* locus on chromosome III. *MAT***a** cells have the a1 and a2 genes at the *MAT* locus while *MAT*α cells have the α1 and α2 genes (Figure 1-7). These genes encode proteins that regulate the transcription of mating-type, haploid, and diploid specific genes. Additional copies of these mating-type genes are also located at the two silent mating loci located at either end of the same chromosome as *MAT*. *HML*, which is located on the left end of chromosome III, normally contains alpha mating-type sequences (*HML*α). *HMR*, which is located on the right end of chromosome III, normally contains **a** mating-type sequences (*HMR***a**). Both the *HML* and *HMR* loci are encased in silent chromatin, such that their genes are not expressed and yeast act as a haploid of whatever mating-type is dictated by the genes at the *MAT* locus.

Yeast are able to divide mitotically as both haploids and diploids. However, only diploids are able to undergo meiosis and produce spores, a process that is advantageous in cases of nutrient limitation. To be able to self-diploidize yeast have evolved the ability to change their mating-type in a specialized DNA repair process called mating-type switching [49]. To switch mating-types, the *MAT* locus is cleaved by the HO endonuclease. The resulting double strand break is then repaired through homologous recombination using the mating-type genes located at either *HML* or *HMR* as donor template sequences [50,51]. Wild-type yeast are able to undergo this process up to once per generation. In G1-phase, the mother cell from the previous generation switches mating-type while the daughter does not due to the presence of an inhibitor of *HO* expression [52,53]. This

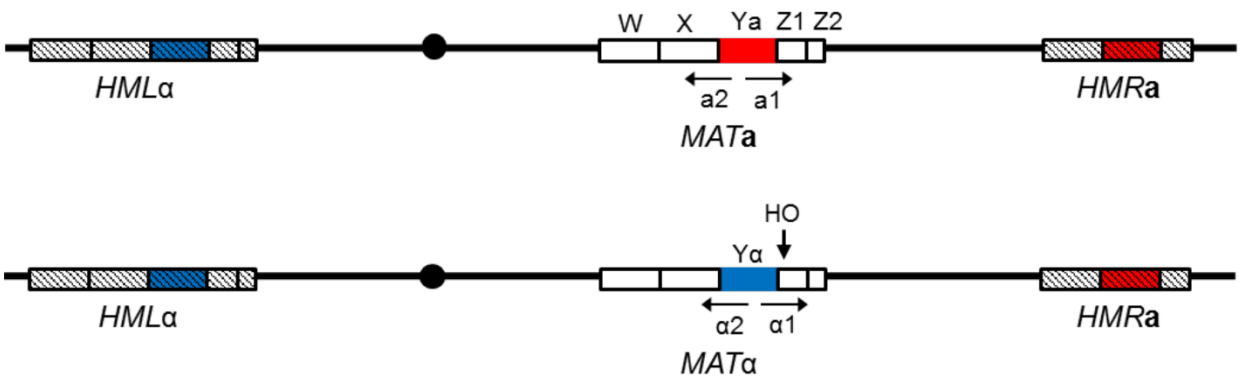

Figure 1-7. Yeast chromosome III. Mating-type is determined by the sequences in the Y region of the *MAT* locus. Regions W, X, Z1, and Z2 are identical in *MAT***a** and *MAT*α cells. The HO endonuclease cleavage site is located within the Z1 region of *MAT*. In wild-type yeast *HMR* contains *MAT***a** sequences, while *HML* contains *MAT*α sequences. Both *HMR* and *HML* are encased in heterochromatin and therefore are resistant to HO endonucleolytic cleavage and do not express their mating-type genes.

results in one cell of each mating-type, allowing for diploid formation between mother and daughter cells.

1.3.2 Directionality of mating-type switching and the recombination enhancer

To ensure that this process results in a change in mating-type, the yeast must choose the proper donor for recombination. In fact, *MAT***a** cells favor recombination with *HML*α ~90% of the time, while *MAT*α cells choose *HMR***a** as a donor ~90% of the time, resulting in a high frequency of mating-type switching (Figure 1-8A). The choice of mating-type donor, that is the directionality of mating-type switching, does not depend on the mating-type genes located at the silent mating-type loci *HMR* or *HML*, but rather their position on chromosome III. In fact, *HMR***a** can be completely replaced with *HML*α and *MAT*α cells will still choose the right arm (which now contains *MAT*α sequences) as a donor ~90% of the time [54].

A regulatory *cis*-element called the recombination enhancer (RE), a chromosomal region located between the *MAT* and *HML* loci, regulates donor preference in *MAT***a** cells [55]. Deletion of RE in *MAT***a** cells leads to a change in donor preference such that *HMR* is the preferred donor in ~90% of cells, similar to the preference seen in *MAT*α cells [55]. The sequence of RE contains a Matα2-Mcm1 operator, a Swi4-Swi6 binding site, and multiple Fkh1 binding sites (Figure 1-8B) [56]. In *MAT*α cells RE is bound by the Matα2-Mcm1 repressor complex, which recruits highly positioned nucleosomes that prevent binding of other factors [57,58]. In *MAT***a** cells chromatin remains open and RE is bound by Mcm1, Swi4-Swi6, and Fkh1. Deletion of any of these binding sites or *trans*-acting factors in *MAT***a** cells reduces *HML* usage, suggesting all of these proteins play a role in regulating donor preference [56,58,59]. However, the entirety of RE can be replaced with multimers of region A, D, or E (all of which contain Fkh1 binding sites) in

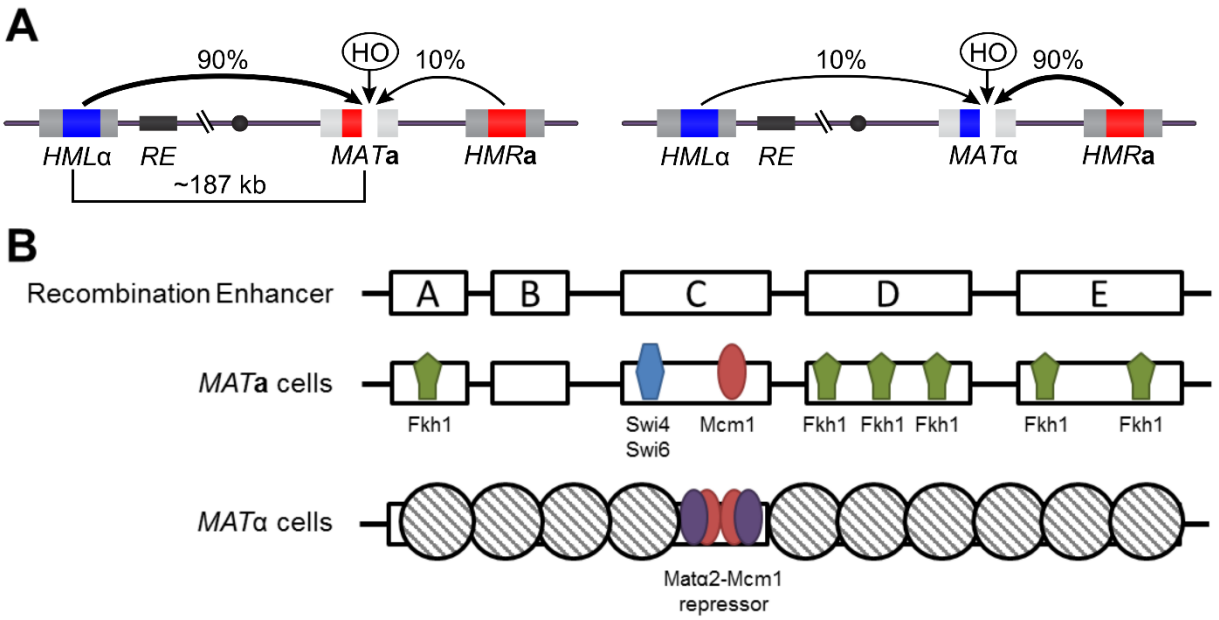

Figure 1-8. Directionality of mating-type switching and the recombination enhancer. (**A**) Donor choice during mating-type switching is different in *MAT***a** and *MAT*α cells. In *MAT***a** cells *HML*α is used as the donor ~90% of the time, whereas in *MAT*α cells *HMR***a** is used as the donor ~90% of the time. Adapted from [59]. (**B**) There are five consensus elements in the recombination enhancer that are conserved among multiple yeast species. In *MAT***a** cells Mcm1 facilitates the binding of Swi4-Swi6 and multiple copies of Fkh1. In *MAT*α cells the Matα2-Mcm1 repressor complex is bound to RE and nucleosomes are highly positioned such that other factors are unable to bind. Adapted from [51].

*MAT***a** cells and donor preference is maintained, suggesting that the presence of multiple copies of Fkh1 is sufficient for RE function [56].

1.3.3 Role of the Fkh1 FHA domain in mating-type switching

To further examine how Fkh1 is able to regulate donor preference, the Haber lab constructed a strain that could study the effects of Fkh1 on RE function in isolation [60]. In this strain, Fkh1 is expressed as a LexA fusion protein. This Fkh1-LexA fusion is fully functional in regulating donor preference if RE is replaced with LexA binding sites. Truncation experiments using this Fkh1-LexA fusion revealed that the N-terminal 120 amino acids of Fkh1, which include the FHA domain, are sufficient for conferring donor preference. As discussed above, FHA domains are phosphothreonine binding domains, and, consistent with a role for the Fkh1 FHA domain in RE function, mutation of casein kinase II, a Ser/Thr kinase, also reduces preference for *HML* in this system. These data support a model in which Fkh1 bound to RE binds to proteins phosphorylated on threonines present at the double strand break at *MAT* (Figure 1-9). The model posits that this association brings *HML* in close proximity to *MAT*, leading to a preference for using *HML* as a donor for recombination.

1.4 Fkh1 role in DNA replication

1.4.1 Eukaryotic DNA replication origins and timing

In the vast majority of cells, DNA replication initiates at specific chromosomal loci called origins. Eukaryotes have multiple origins per chromosome and replication at these origins is regulated both spatially and temporally. Replication at some origins initiates early in S-phase,

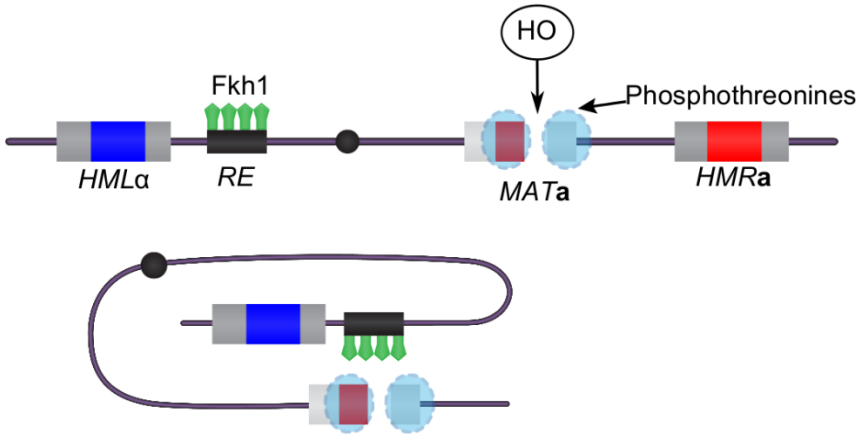

Figure 1-9. Model of Fkh1-regulated mating-type switching. The HO endonuclease cuts at *MAT***a**, where the model proposes that a protein(s) bound to the double-strand break is phosphorylated on threonines. Fkh1 bound to RE then binds to these phosphorylated proteins, causing a conformational change in the chromosome that leads to an increased preference for recombination with *HML*. Adapted from [60].

while at others it initiates later in S-phase or not at all (Figure 1-10). Generally, in yeast DNA replication is initiated earlier at origins located near centromeres and later at origins located in telomeric regions. However, there are "early" and "late" firing origins at all different loci throughout the genome. In multicellular organisms, this temporal replication pattern is associated with normal cellular proliferation [61]. Perturbation of this pattern can lead to genome instability, a hallmark of cancer. Therefore, the mechanisms that regulate the timing of activation at different origins are important for understanding basic biology as well as human disease. However, the mechanisms underlying this type of control remain fairly obscure, though recent advances at the level of molecular mechanism have been made in some cases [62].

Eukaryotic replication origins are recognized by a heterohexameric protein complex called the origin recognition complex (ORC) [63]. ORC binds to origin DNA and recruits the proteins necessary to initiate DNA replication. In *Saccharomyces cerevisiae* ORC recognizes a specific DNA sequence element. However, while ORC in metazoans still binds DNA, it appears to have no sequence specificity [64,65]. Several studies indicate that metazoan ORC likely recognizes origins through interactions with chromatin features, although these features have not been well-defined [66]. Studies from our lab have demonstrated that while yeast ORC does have sequence specificity, it is also able to recognize sequence independent features or origins [67,68]. In fact, a study in our lab has shown that origins that rely less on DNA sequence and more on chromatin features for ORC binding tend to replicate earlier in S-phase [68]. However, the identities of these chromatin features remain mostly unknown.

1.4.2 Role of Fkh1 and Fkh2 in replication timing

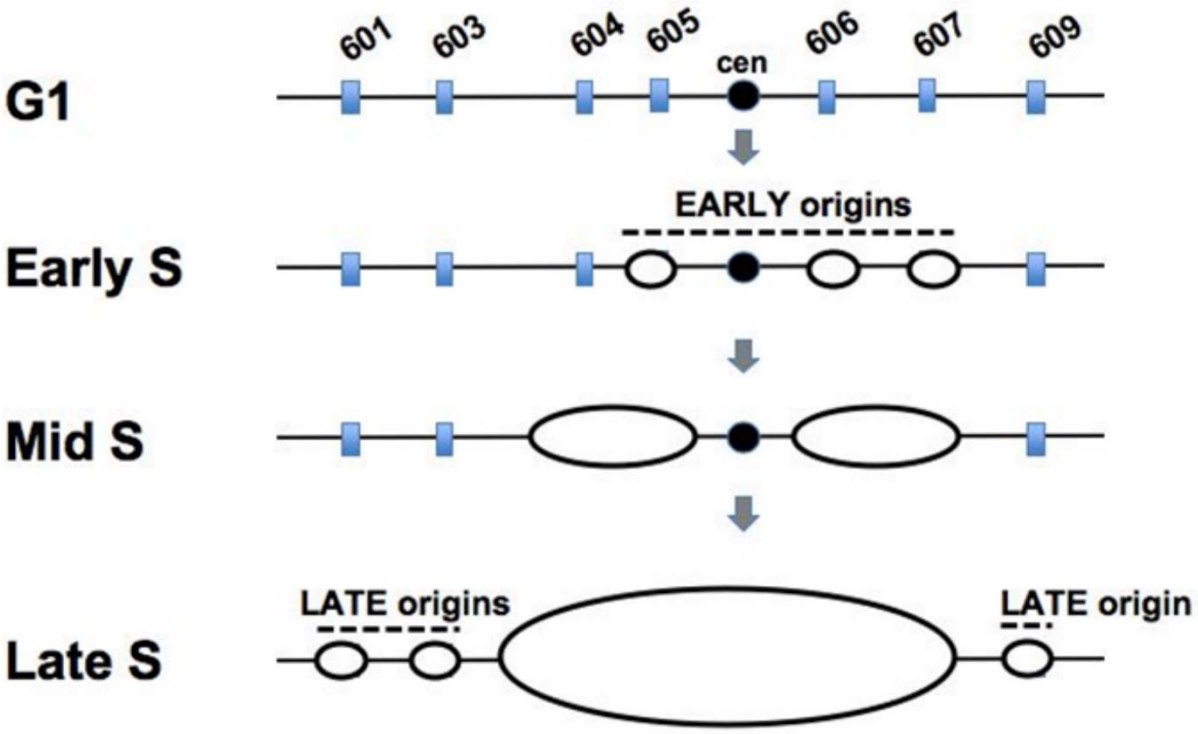

Figure 1-10. Origin activation timing of yeast chromosome VI. The origins of yeast chromosome VI (blue) are activated in a characteristic temporal order, creating a distinct replication profile.

Fkh1 and Fkh2 have both been implicated in the regulation of timing of DNA replication initiation. Deletion of *FKH1* and *FKH2* alters the activation timing of multiple origins throughout the genome [69]. Specifically, in *fkh1*Δ*fkh2*Δ cells the activation of normally early firing origins is delayed, while the activation of late firing origins is advanced. Fkh1 appears to be the main regulator of this activity, as replication timing is affected more drastically in *fkh1*Δ cells than in *fkh2*Δ cells, although *fkh1*Δ*fkh2*Δ cells display the most drastic phenotypic change [69]. Fkh binding sites were found to be enriched near origins that fired earlier in S-phase. Genome-wide binding analysis shows that Fkh1 binds the majority of these origin-associated sites, with Fkh2 binding many fewer origins [20]. Fkh-associated origins fire early in S-phase even when relocated to a normally late-firing area of the genome [70]. However, mutation of Fkh binding sites near early-firing origins delays their activation time, suggesting that Fkh binding is responsible for earlier activation time [69,70]. Origins not associated with Fkh1/2 fire earlier in *fkh1*Δ*fkh2*Δ cells. However, this is thought to be an indirect effect due to an increased availability of rate-limiting factors that would otherwise be localized to early Fkh-associated origins. Indeed, overexpression of Fkh1 and 2 advances activation timing across the genome, suggesting Fkh1/2 may act as rate-limiting factors themselves or aid in the recruitment of rate-limiting factors [71].

Chromosome conformation capture-on-chip (4C) analysis demonstrated that some Fkh-activated origins were in close association with each other and that this association was lost upon deletion of *FKH1* and *FKH2* [69]. A model proposed by the Aparicio lab posits that Fkh1/2 act to cluster origins into “replication factories” in the nucleus where the relative concentration of rate-limiting replication factors is high. Fkh1 interacts physically with ORC [69]. However, it is not known if Fkh1 is interacting with ORC in *cis* (i.e. Fkh1 and ORC bound to the same origin) or in *trans* (i.e. Fkh1 bound to the Fkh binding site at one origin and ORC bound to a different origin).

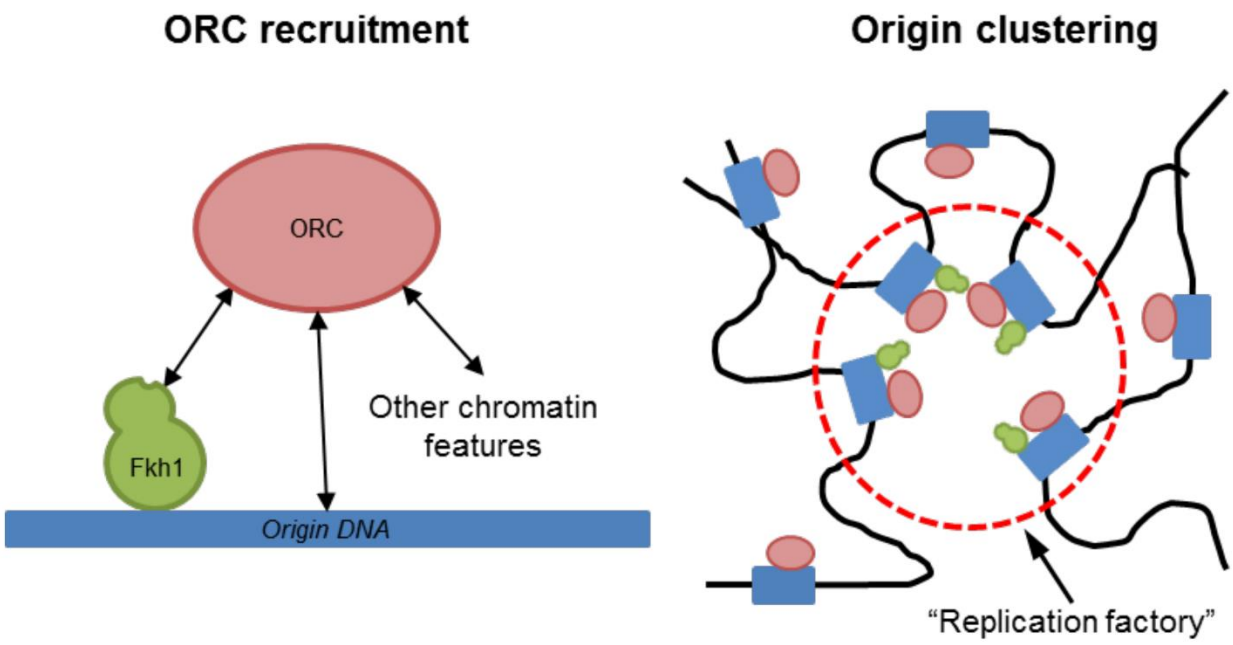

Figure 1-11. Models for regulation of origin timing by Fkh1. Fkh1 bound to origin DNA may serve as an additional mechanism to recruit ORC in addition to ORC-DNA interactions and ORC interaction with other chromatin features. Fkh1 may also serve to cluster origins into replication factories within the nucleus where the concentration of rate-limiting factors required for DNA replication initiation is proposed to be high. One model posits that this is through Fkh1 (green) interactions with ORC (red) bound to different origins. However, other Fkh1 interactions or Fkh1-independent interactions could be responsible for this clustering.

This model further posits that Fkh1-ORC binding in *trans* could serve as a mechanism for clustering origins. However, Fkh1 that binds ORC in *cis* could serve as a chromatin feature that ORC uses to recognize origin DNA, which may also affect replication timing (Figure 1-11). These two possibilities are not mutually exclusive. Fkh1 may be able to bind ORC both in *cis* and *trans*. It is also possible that the Fkh1-ORC interaction occurs exclusively in *cis* and that origin clustering observed at these early origins is due to an independent mechanism. However, whether the timing or clustering effects could be due to global changes in cell cycle transcription has not been investigated fully and could be a possibility, as well.

1.5 The FOX family of transcription factors

The *Saccharomyces cerevisiae* Fkh1 protein is a member of the FOX (forkhead box) family of proteins defined by their winged-helix DNA binding domains. FOX family transcription factors are evolutionarily conserved in eukaryotic organisms from yeast to humans and are important for their roles in regulating the cell cycle and differentiation [72]. Humans have 50 FOX family proteins divided into 19 subfamilies [73]. These proteins regulate transcription through diverse actions (reviewed in [74]). For example, the FOXA subfamily primarily act as pioneer factors, which are able to directly promote nucleosome de-compaction to allow other transcriptional regulators access to bind. Members of the FOXP family act as classical transcription factors by binding to promoters and recruiting chromatin modifying enzymes which regulate transcription. Some FOX subfamilies, such as the FOXO subfamily, are able to act as both pioneer factors and classical transcription factors.

Like yeast Fkh1 and Fkh2, many of these FOX family transcription factors play important roles in cell cycle regulatory transcription. Like Fkh1 and 2, the FOXM proteins play an important role in regulating the G2/M transition in the human cell cycle [75]. Due to their importance in regulating the cell cycle and differentiation, many human FOX genes are implicated in cancer and other human diseases [75,76]. FOX genes can act as both oncogenes and tumor suppressor genes [75,77,78]. For example, deletion of FOXO1 is observed in many human prostate cancers, suggesting it may play a role in suppressing these cancers [79]. Amplification of the FOXM1 locus is associated with multiple different cancers, suggesting it acts as an oncogene [80–82]. FOX proteins also play crucial roles in normal development and cellular differentiation in humans, as well as in other areas of disease such as insulin response and speech acquisition (reviewed in [76]).

While the cell cycle regulatory transcriptional roles of *S. cerevisiae* FOX proteins Fkh1 and Fkh2 are clearly important, there is increasing evidence, especially for Fkh1, that these proteins are able to regulate processes independent of transcription. Data from my work and others have shown an importance for the FHA domain in many of these processes, including mating-type switching, DNA replication, and transcription [25,26,60,71]. However, the only FOX proteins in humans that contain FHA domains are FOXK1 and FOXK2 and very little is known about the function the FOXK FHA domains play in human biology.

FOXK1 is required for the proliferation of muscle stem cells and muscle generation [83,84]. A recent study provides evidence for a central role for FOXK1 in mTOR-signaling-controlled transcriptional regulation of autophagy genes [85]. In response to mTOR signaling, FOXK1-containing complexes at gene promoters disassemble and FOXK1 moves out of the nucleus and remains stably “stored” in the cytoplasm. These steps contribute to the activation of autophagy genes in part by relieving basal repression and in part by allowing the activating FOXO3

protein to bind autophagy gene promoters and induce the autophagy program. FOXK1 in the nucleus represses transcription at these promoters through the recruitment of Sin3A-HDAC complexes [85]. Fkh1 and 2 have been shown to recruit the yeast Sin3A homolog, Sin3, to promoters and repress transcription, showing some functional conservation with the FOXKs [22,23]. Further investigation into how Fkh1 functions in yeast may lead to important insights for how the FOXKs or other FOX proteins function in human development and disease.

Chapter 2

Binding of the Fkh1 Forkhead Associated Domain to a Phosphopeptide within the Mph1 DNA Helicase Regulates Mating-Type Switching in Budding Yeast

2.1 Preface

This chapter has been accepted for publication in PLoS Genetics [86]. Some of the figure panels have been moved to incorporate supplemental figures into the main text. I (with the help of my advisor, Catherine Fox) conceived and designed all of the experiments. Zhangli Su analyzed the fluorescence anisotropy data and generated the model of Fkh1 electrostatic potential. Rachel Cherney aided in the construction of yeast strains and performed some of the dissections shown in Figure 2-5. Ulrika Müller performed the initial 2-hybrid screen. Xiaolan Zhao and Koyi Choi contributed yeast strains containing various *MPH1* alleles. Catherine Fox and Xiaolan Zhao helped with the writing of the manuscript.

2.2 Abstract

The *Saccharomyces cerevisiae* Fkh1 protein has roles in cell-cycle regulated transcription as well as a transcription-independent role in recombination donor preference during mating-type

switching. The conserved FHA domain of Fkh1 regulates donor preference by juxtaposing two distant regions on chromosome III to promote their recombination. A model posits that this Fkh1-mediated long-range chromosomal juxtaposition requires an interaction between the FHA domain and a partner protein(s), but to date no relevant partner has been described. In this study, we used structural modeling, 2-hybrid assays, and mutational analyses to show that the predicted phosphothreonine-binding FHA domain of Fkh1 interacted with multiple partner proteins. The Fkh1 FHA domain was important for its role in cell-cycle regulation, but no single interaction partner could account for this role. In contrast, Fkh1's interaction with the Mph1 DNA repair helicase regulated donor preference during mating-type switching. Using 2-hybrid assays, co-immunoprecipitation, and fluorescence anisotropy, we mapped a discrete peptide within the regulatory Mph1 C-terminus required for this interaction and identified two threonines that were particularly important. *In vitro* binding experiments indicated that at least one of these threonines had to be phosphorylated for efficient Fkh1 binding. Substitution of these two threonines with alanines (*mph1-2TA*) specifically abolished the Fkh1-Mph1 interaction *in vivo* and altered donor preference during mating-type switching to the same degree as *mph1*Δ. Notably, the *mph1-2TA* allele maintained other functions of Mph1 in genome stability. Deletion of a second Fkh1-interacting protein encoded by *YMR144W* also resulted in a change in Fkh1-FHA-dependent donor preference. We have named this gene *FDO1* for **F**orkhead one interacting protein involved in **do**nor preference. We conclude that a phosphothreonine-mediated protein-protein interface between Fkh1-FHA and Mph1 contributes to a specific long-range chromosomal interaction required for mating-type switching, but that Fkh1-FHA must also interact with several other proteins to achieve full functionality in this process.

2.3 Introduction

The *Saccharomyces cerevisiae* Fkh1 (forkhead homolog 1) protein is a member of the FOX (forkhead box) family of proteins defined by their winged-helix DNA binding domains. The FOX family proteins are best known for their transcriptional roles in regulating the cell cycle and differentiation [72]. For example, the Fkh1 paralog, Fkh2, controls the cell-cycle regulated transcription of the *CLB2*-cluster genes required for the proper execution of M-phase events [4,9–13,18,19,22,25,26]. Fkh1 appears to play an accessory role here, as deletion of both *FKH1* and *FKH2*, but not either gene alone, causes severe cell-cycle dysfunction. However, its molecular functions and the mechanisms by which Fkh1 participates in this process remain poorly understood [9,16]. Accumulating evidence indicates that Fkh1 and 2 also play a transcription-independent role in regulating the timing profile for DNA replication origin activation [69,70]. In addition, Fkh1 has a unique role not shared with Fkh2 in recombination-mediated mating-type switching [56,59], but the molecular mechanisms of this Fkh1 function are not completely understood.

Mating-type switching allows haploid cells of one mating-type to switch to the other, consequently enabling two neighboring haploids to mate and undergo sexual reproduction [49]. Mating-type switching is a critical aspect of yeast biology and evolution that has been used as a model to better understand the repair of double-strand breaks (DSBs) through homologous recombination [51]. During mating-type switching, a DSB is generated by the HO endonuclease at the *MAT* locus that contains either **a**- or alpha- mating-type genes. This break is repaired through homologous recombination using donor template sequences located at the silent mating-type loci, *HML* or *HMR*, at the opposite ends of the same chromosome as *MAT* (Figure 2-1A) [50,51]. *HML* and *HMR* contain a repressed copy of alpha (*HML*α) or **a** genes (*HMR***a**), respectively. Productive mating-type switching requires the proper choice between these two donor loci so that the opposite

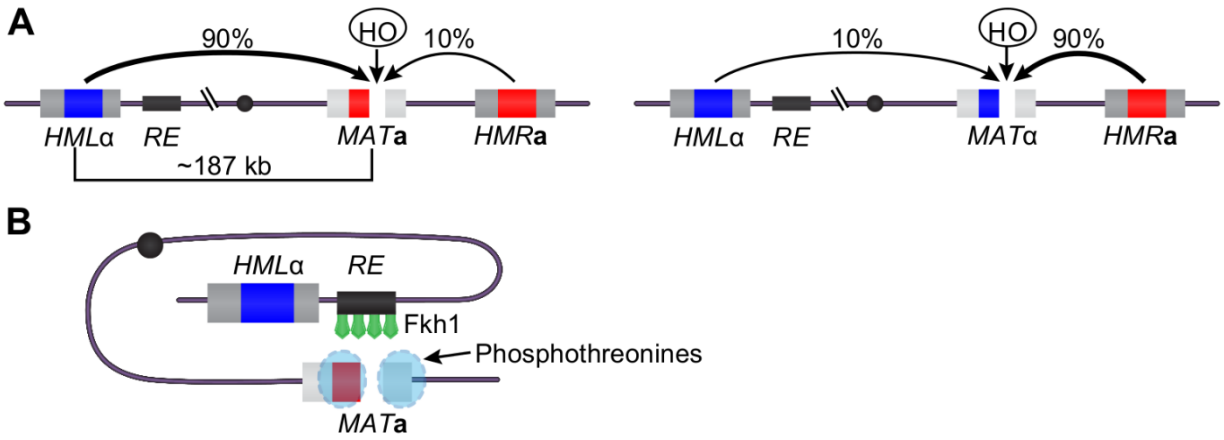

Figure 2-1. Donor preference during mating-type switching is regulated by Fkh1 through the recombination enhancer. (**A**) *MAT***a** cells primarily use *HML*α as a donor, while *MAT*α cells use *HMR***a** as a donor, resulting in a high frequency of mating-type switching. Adapted from [59,87]. (**B**) Model of Fkh1-regulated mating-type switching. Adapted from [60]. The HO endonuclease cuts at *MAT***a**, and a protein(s), phosphorylated on specific threonine residues binds to the double-strand break (DSB). Fkh1 bound to the RE interacts with these phosphorylated proteins. These interaction(s) bring *HML* close to the DSB at *MAT* and result in substantial preference for recombination between *MAT* and *HML*.

mating-type gene is inserted at *MAT*. Thus *MAT***a** cells favor recombination with *HML*α ~90% of the time, while *MAT*α cells choose *HMR***a** as a donor ~90% of the time (Figure 2-1A). The choice of mating-type donor, that is the directionality of mating-type switching, does not depend on the mating-type genes themselves, but on the protein-DNA complex that forms at a regulatory *cis*-element called the recombination enhancer (RE), a chromosomal region located between the *MAT* and *HML* loci [55]. Fkh1 has been shown to regulate the directionality of mating-type switching by binding to RE in *MAT***a** cells and establishing a strong preference for *HML*α for repair (Figure 2-1B) [56]. The forkhead associated (FHA) domain of Fkh1 is sufficient for this function as a LexA-Fkh1-FHA domain fusion is fully functional in regulating donor preference if RE is replaced with LexA binding sites [60].

FHA domains are present in many proteins involved in chromosomal functions and serve as protein-protein interaction modules that specifically recognize phosphorylated threonine residues [27,29–31,37]. This property of FHA domains and the involvement of the Fkh1 FHA domain in donor preference during mating-type switching support a model in which the Fkh1 FHA domain controls the directionality of mating-type switching through direct interactions with a phosphorylated protein partner(s) (Figure 2-1B). This model posits that the presumed partner protein(s) likely binds the DSB at *MAT***a**, and through an interaction with Fkh1 bound to RE, localizes *HML*α, the donor locus, near the DSB, allowing for efficient strand invasion to occur [60]. Currently, the identities of this Fkh1 partner protein(s) is unknown, and the possible roles of this protein(s), or the Fkh1 FHA domain, in Fkh1's other cellular roles are also unknown.

To address these issues, we performed a 2-hybrid interaction screen that identified five Fkh1-interacting proteins. Domain analyses revealed that Fkh1 interacted with each of these proteins via its FHA domain. Mutation of key residues within this domain revealed that it was

important for Fkh1's role in cell-cycle regulation, though no single interacting partner could account for this role. In addition, our genetic analyses indicate that functions of the FHA domain outside of its phosphopeptide binding activity contribute to Fkh1's cell cycle role. Focusing on one Fkh1 binding partner, Mph1, we found that its loss altered donor preference during mating-type switching. Using multiple approaches, we defined a peptide within Mph1 that interacted directly and efficiently with purified Fkh1 *in vitro* and in a manner that depended on the phosphorylation state of two threonines within the peptide. Mph1 also interacted with Fkh1 in cells and this interaction required the same threonines that mediated the Fkh1-Mph1-peptide interaction. Alanine substitutions of the two threonines in Mph1 (*mph1-2TA*) caused a defect in donor preference during mating-type switching similar to that caused by *mph1*Δ. However, *mph1-2TA* cells did not share other cellular defects caused by *mph1*Δ, such as sensitivity to MMS or an elevated rate of mutation. Because *MPH1* could only partially explain Fkh1-FHA's role in mating-type switching, we examined the role of a second Fkh1-interacting protein identified in our screen, encoded by *YMR144W*. A *ymr144W*Δ also altered mating-type switching directionality, and *ymr144W*Δ *mph1*Δ reduced the efficiency of this process beyond that of either mutation alone. We have named this gene *FDO1* for **F**orkhead one interacting protein involved in **do**nor preference. Thus we have delineated a specific cellular role for Fkh1 and Mph1 mediated by an FHA-phosphothreonine interaction, and provided evidence that Fkh1-FHA bound to the RE likely must recognize several proteins at the DSB for full function in mating-type switching directionality.

2.4 Results

2.4.1 Yeast 2-hybrid screen identified five proteins that interact with Fkh1

Table 2-1. Fkh1 2-hybrid interacting proteins.

Name	Description	Region identified in screen (aas)	Fkh1-FLAG interactor? [94]
MPH1	DNA repair helicase	762-993	Yes
ECM30	Putative protein involved in cell wall biosynthesis	1005-1183	No
GLN3	Transcriptional activator of genes regulated by nitrogen catabolite repression	20-189	No
URE2	Transcriptional regulator that acts by inhibition of GLN3 transcription in good nitrogen source	84-354	Yes
FDO1 (YMR144W)	Putative nuclear protein of unknown function	98-342	Yes

To identify proteins that interact with Fkh1, we used a 2-hybrid interaction screen in which a Fkh1-Gal4 DNA binding domain (Fkh1-GBD) fusion protein served as bait and a library of Gal4 activation domain (GAD) fusions served as prey [88]. This Fkh1-GBD fusion protein contained the entire Fkh1 coding sequence except for its forkhead DNA binding domain, as this domain was replaced with GBD. Five proteins were identified as positive interactors from this screen (Table 2-1). These included the DNA helicase Mph1 that is involved in recombinational repair, the Gln3 and Ure2 proteins involved in transcriptional control, and the two uncharacterized proteins with unclear functions [89–93]. Mph1, Ure2, and Fdo1 (formerly Ymr144w) were identified in a previous proteomic screen as proteins that co-purified with a Fkh1-FLAG fusion protein [94], verifying the effectiveness of our screen.

2.4.2 The FHA domain of Fkh1 interacted with the C-terminal domain of Mph1

To define how Fkh1 interacts with the proteins identified in our screen, we tested which regions of Fkh1 interacted with Mph1, the yeast homolog of the human FANCM helicase [95,96]. The Fkh1-Mph1 interaction was of particular interest because both proteins are implicated in recombinational repair, though each protein also has other functions [51,56,60,95,96]. Our 2-hybrid screen identified the C-terminal region of Mph1 (amino acids 762-993, henceforth referred to as Mph1-Ct), which has been shown to act as a regulatory domain on this protein, providing interaction sites for numerous proteins that regulate its function [97–100]. To define the region of Fkh1 that interacts with Mph1-Ct, we tested several GBD constructs containing different regions of Fkh1 (Figure 2-2A) and found that amino acids 50-202 of Fkh1, the majority of which is comprised of the FHA domain, was sufficient for interaction with Mph1-Ct (Figure 2-2B). Conversely, the fkh1(Δ50-202) mutant did not interact with Mph1-Ct. Thus, the region of Fkh1

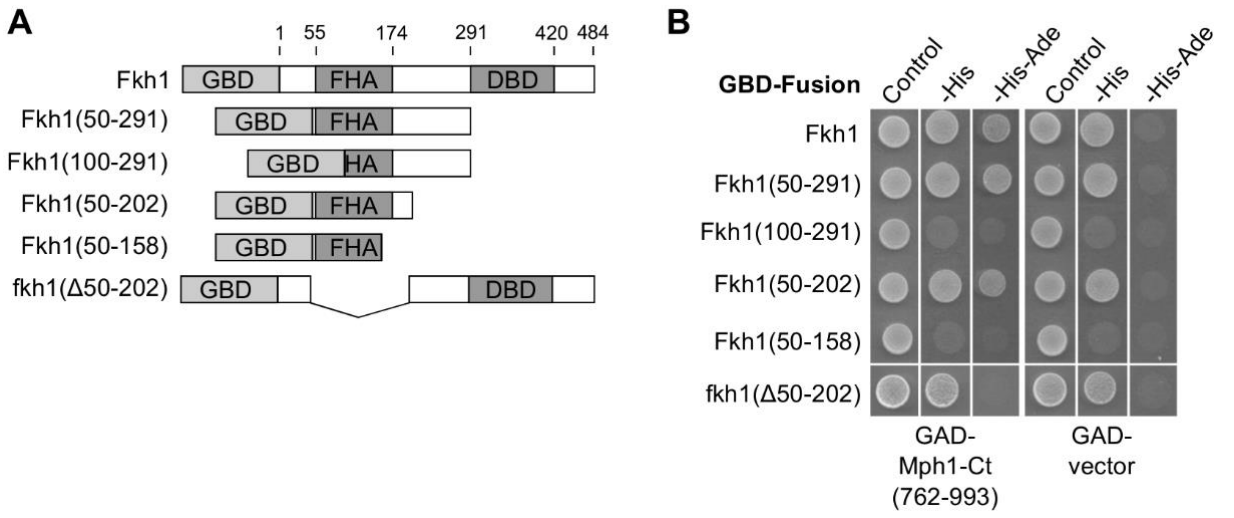

Figure 2-2. Fkh1 interacted with Mph1 through the FHA domain. (**A**) Diagram of GBD-Fkh1 fusions used in panel (B). (**B**) Yeast 2-hybrid assays performed using various regions of Fkh1 as bait (shown in panel (A)). Interaction was assessed by selection for activation of reporter genes *HIS3* and *ADE2* on media lacking histidine or both adenine and histidine. Note that many GBD-Fkh1 fusion proteins were able to activate transcription of the *HIS3* reporter gene in the absence of an interaction partner. Therefore, interaction was defined as the ability to grow on selective media only in the presence of an interaction partner, and not the GAD alone. For most constructs analyzed, interaction was determined by growth on media lacking both histidine and adenine

containing amino acids 50-202 (henceforth referred to as Fkh1-FHA) was necessary and sufficient to interact with Mph1-Ct.

2.4.3 Modeling of the FHA domain of Fkh1 defined residues predicted to be important for phosphothreonine binding

Next, we examined whether the predicted phosphothreonine binding ability of Fkh1-FHA was required for binding Mph1. To this end, we performed homology modeling (Fig 2-3A-D) using published structures of multiple FHA domains as template (see Table 2-2). Of the homology models generated, the one using the well-characterized N-terminal FHA domain of the checkpoint protein Rad53 [39] as template yielded the highest quality model (Table 2-2). Using this information, as well as additional secondary structure prediction [104] of the regions not modeled, we generated a structure-based sequence alignment of the Fkh1 and Rad53 FHA domains. Upon generation of the homology model and alignment, we found that the FHA domain of Fkh1 is ~50 amino acids larger than previous studies have reported [10,60], as it contains two extra predicted β-strands in addition to the 11 β-strands which comprise the core FHA domain fold [38] (Figure 2-3). In addition, this approach allowed for identification of several amino acids predicted to be on or near the phosphopeptide binding surface of Fkh1 (Figure 2-3). Five of these residues (Figure 2-3E, boxed) form the phosphothreonine binding pocket and are conserved among FHA domains [113]. In addition, multiple residues within loops two, three, and four of this domain can make direct contacts with phosphopeptide binding partners in other FHA domains and are less well conserved, allowing different FHA domains to have distinct binding specificities [38]. We note that the predicted phosphopeptide binding surface of Fkh1 FHA is predominantly positively

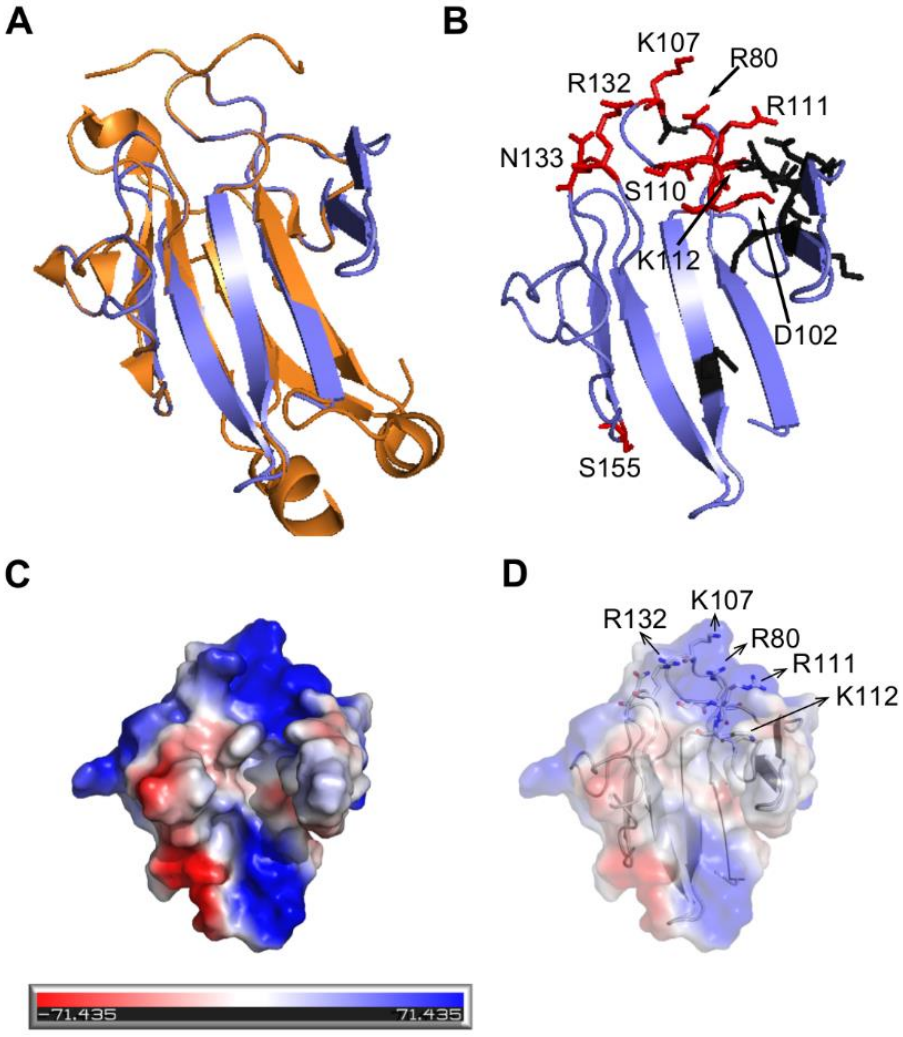

E

```
                        β1        L1        β2
Rad53-1   29    GENIVCRVICTTGQIPIRDLSADISQVLK
Fkh1      55    EVNAYAKIA-----GCDWTYYVQ------
                        β3      L2
Rad53-1   58    EKRSIKKV-WTFGRNPA---------------
Fkh1      73    ------KLEVTIGRNTDSLNLNAVPGTVVKKN
                  β4    L3          β5        β6
Rad53-1   74    CDYHLGNISRLSNKHFQILLGEDGNLLLNDI
Fkh1      99    IDIDLGPAKIVSRKHAAIRFNLESGSWELQI
                 L4   β7   β8    L5    β9      β10
Rad53-1   105   -SINGTWLNGQK---VEKNSNQLLSQGDEITV
Fkh1      130   FGRNGAKVNFRRIPTGPDSPPTVLQS--GCII
                  L6      β11
Rad53-1   133   GVGVESDILSLVIFINDK
Fkh1      160   DIGG---VQMIFILPEQE
```

Figure 2-3. Homology modeling and structure-based sequence alignment of the Fkh1 FHA domain. (**A**) A predicted structure for amino acids 72-170 of the Fkh1 FHA domain was generated by SWISS-MODEL using the N-terminal Rad53 FHA domain as a template (PDB 1G6G) [39,101–103]. See Table 2-2 for a table of other templates used for homology modeling. The Rad53 structure with associated peptide is shown in orange and was chosen for this comparison because it produced the highest quality model (as determined by QMEAN Z-scores-see Table 2-2). The predicted Fkh1 FHA domain structure is shown in blue. (**B**) Predicted structure for the Fkh1 FHA domain. Residues analyzed that were required for binding Mph1 in the 2-hybrid context are shown in red and labeled by their residue number. Residues analyzed that were not required for binding Mph1 are shown in black (See Figure 2-4 for 2-hybrid data). (**C**) Model of electrostatic potential of the Fkh1 FHA domain. Blue indicates positively charged regions. Red indicates negatively charged regions. (**D**) The positively charged region on the phosphopeptide interaction surface contains residues R80, K107, R111, K112, and R132. (**E**) Structure-based sequence alignment between the N-terminal Rad53 FHA domain (Rad53-1) and the Fkh1 FHA domain (Fkh1). Alignment was generated using structural predictions of the Fkh1 FHA domain, which include a combination of the Rad53-based homology model and secondary structure prediction [104]. Conserved FHA domain β-strands and the loops which comprise the peptide binding site are labeled [38]. Rad53 β-strands are shown in red. Fkh1 β-strands predicted in the homology model are shown in red and those predicted from secondary structure prediction are shown in blue. The five conserved FHA residues that comprise the phosphothreonine binding pocket are boxed. Fkh1 residues shown to be required for binding to Mph1 are highlighted yellow and residues from Rad53 that make direct contact with a Rad9-derived peptide are highlighted green. Fkh1 residues that were tested but not required for Mph1 binding are underlined.

Table 2-2. Template structures used for homology modeling of the Fkh1 FHA domain. QMEAN4 scores provided by SWISS-MODEL [105].

Protein Name	PDB ID	Ref	QMEAN4 Raw Score	QMEAN4 Z-Score
Chfr-Native	1LGQ	[106]	0.417	-3.691
Chfr-Tungstate bound	1LGP	[106]	0.302	-4.772
Chk2-P2 form	3I6W	[107]	0.323	-4.571
Chk2-$P2_12_12_1$ form	3I6U	[107]	0.417	-3.688
Chk2	1GSC	[42]	0.496	-2.98
Ki67	2AFF	[41]	0.419	-3.633
Ki67	1R21	[45]	0.357	-4.23
PNK3-P	2BRF	[108]	0.183	-5.6
PNK	1YJM	[109]	0.405	-3.4
Rad53-1	1G6G	[39]	0.491	-2.773
Rad53-1	1J4P	[110]	0.409	-3.237
Rad53-2	1J4K	[111]	0.439	-3.41
Rad53-2	1DMZ	[112]	0.256	-5.07
RNF8	2PIE	[43]	0.392	-3.51

charged, suggesting a preference for binding to a peptide with negatively charged residues (Figure 2-3C, D).

2.4.4 Putative phospho-binding residues of the Fkh1 FHA domain were important for associating with Mph1

Based on this structural and alignment information we engineered several single amino acid substitutions in Fkh1-FHA and assessed their ability to interact with Mph1-Ct in 2-hybrid assays. We found that several amino acids predicted to be on the phosphopeptide binding surface, as well as a more distal residue (S155), were important for interaction with Mph1 (Figure 2-3B-red, 2-3E-highlighted yellow, and 2-4A). For example, Fkh1 R80 is conserved in all FHA domains and the analogous residue in Rad53 makes direct contact with its partner peptide [39,113]. Substitution of alanine for Fkh1 R80 abolished the interaction between Fkh1-FHA and Mph1-Ct (Figure 2-3B, E and Figure 2-4A). In contrast, amino acid substitutions in several amino acids predicted not to be on the phosphopeptide binding interface of Fkh1-FHA had no effect on the Fkh1-FHA-Mph1-Ct 2-hybrid interaction, including substitutions within the extended loop two (Figure 2-3B-black, 2-3E-underlined, and 2-4B). Taken together, these mutagenesis studies suggest that the predicted phosphopeptide-interaction surface of the FHA domain of Fkh1 is important for interaction with Mph1.

2.4.5 Fkh1 interacted with five partner proteins via its conserved FHA domain

To test whether the FHA domain of Fkh1 is also involved in interacting with other proteins recovered from our 2-hybrid screen, we examined their binding to Fkh1-FHA and the mutant constructs described above in the 2-hybrid assay (Figure 2-4A, C). Fkh1-FHA was necessary and

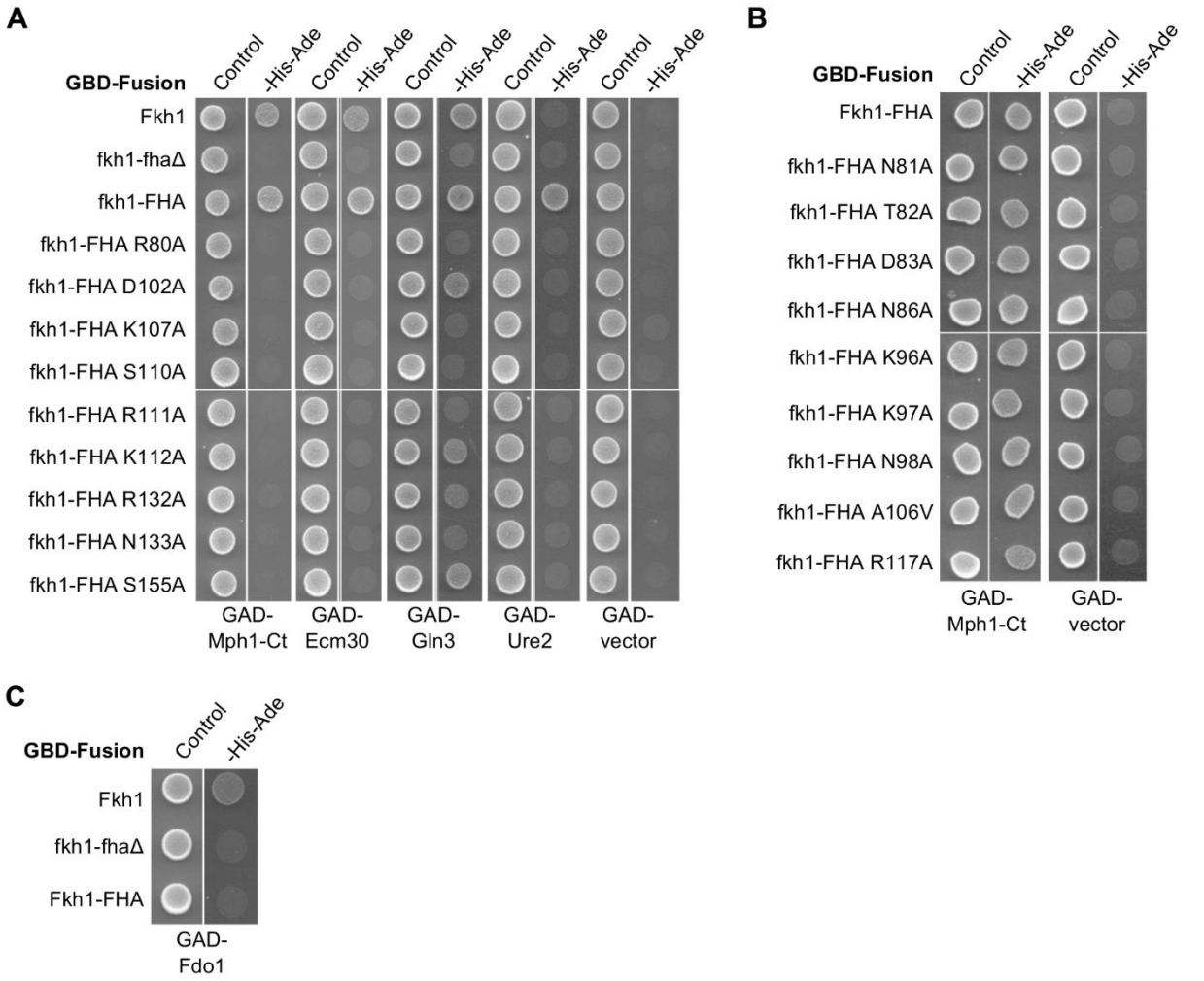

Figure 2-4. Phosphothreonine binding capability of the Fkh1 FHA domain was required for interaction with multiple partner proteins. (**A-C**) Yeast 2-hybrid assays using different mutant forms of Fkh1 bait. The FHA domain is defined as amino acids 50-202. GAD constructs contain the segment of each protein identified in the original 2-hybrid screen (listed in Table 2-1) or the GAD alone.

sufficient to interact with Ecm30(1005-1183), Gln3(20-189) and Ure2(84-354) (Figure 2-4A). In addition, with only a few exceptions for assays with Gln3, the amino acid substitutions that abolished Fkh1-FHA-Mph1-Ct binding also abolished the interaction with these other proteins. Finally, a region containing the FHA domain of Fkh1 was necessary but not sufficient to interact with Fdo1, suggesting the involvement of additional regions for their interaction (Figure 2-4C). Thus Fkh1 can interact with a number of distinct proteins via its conserved FHA domain.

2.4.6 The FHA domain contributed to Fkh1's overlapping role with Fkh2 in the regulation of cell growth

To understand the biological functions of protein interactions observed with the Fkh1 FHA domain, we investigated whether this domain was required for the functions shared between Fkh1 and 2, namely the regulation of the cell cycle and colony morphology. Deletion of both *FKH1* and *FKH2*, but not either gene alone, causes cell-cycle dysfunction that leads to a pseudohyphal-like growth that produces rough, chalky colonies that scar solid agar medium [9–13]. While the FHA domain of Fkh2 is important for *FKH2* function [25,26], the role of the Fkh1 FHA domain in *FKH1* function in these phenotypes has not been reported. Therefore, we determined whether mutant versions of Fkh1 examined above (referred to as *fkh1-m*) resulted in these defects in a *fkh2*Δ background (Figure 2-5A). We note that all the examined *fkh1-m* proteins were expressed at levels similar to that of wild type Fkh1 (Figure 2-5B), indicating that any observed defects are not due to a loss of Fkh1 protein.

By examining spore clones generated from diploids heterozygous for both *fkh1-m* and *fkh2*Δ, we first confirmed previous findings that *fkh1*Δ *fkh2*Δ and *fkh1-dbd*Δ *fkh2*Δ yeast grew slowly and produced a colony that scarred the agar medium (Figure 2-5C) [9]. We also found that

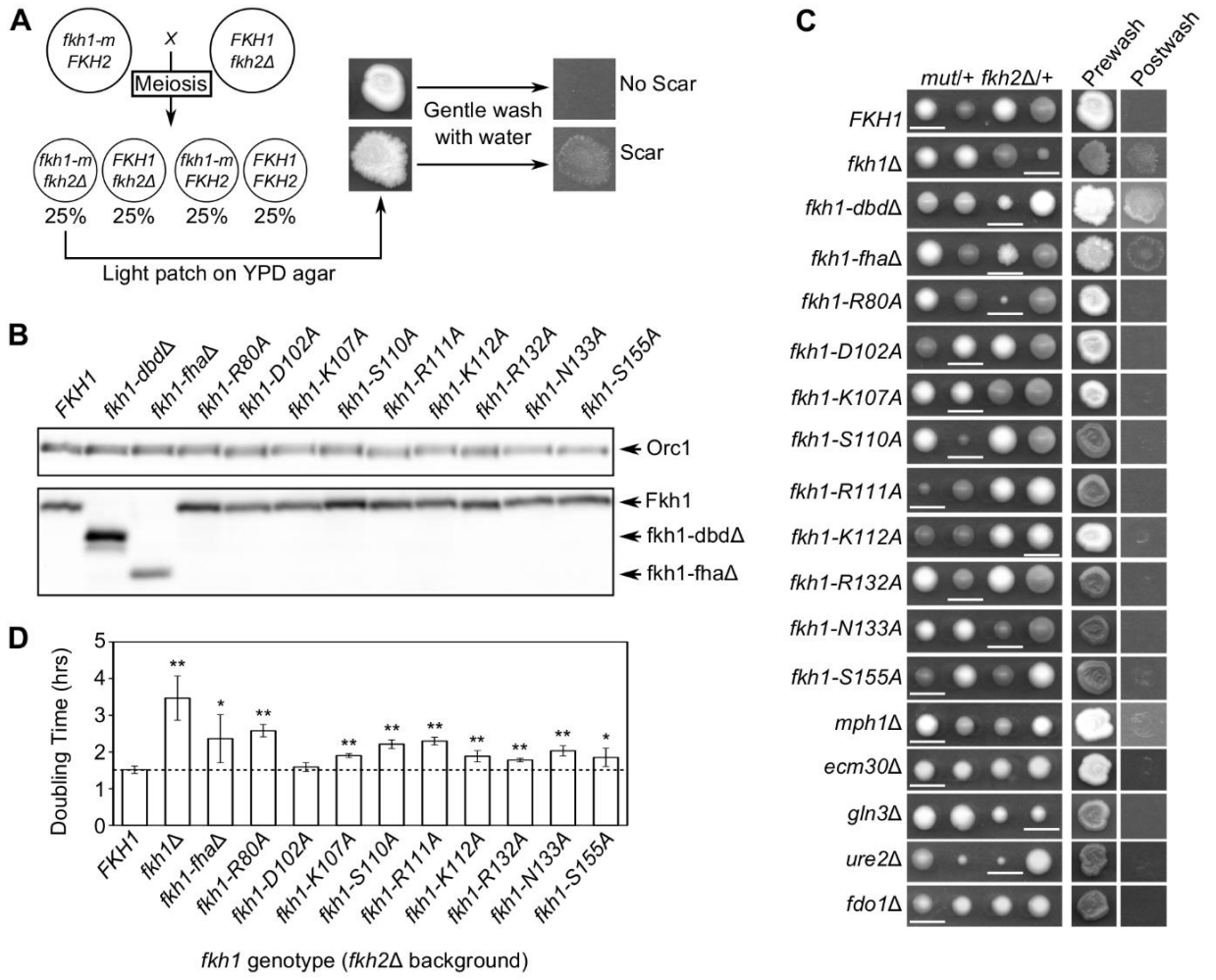

Figure 2-5. The FHA domain of Fkh1 was involved in maintaining proper cell morphology and growth rate. (**A**) Schematic of morphology experiment. Haploids expressing the indicated mutant were crossed to *fkh2*Δ haploid yeast to form heterozygous *fkh1-m*/+ *fkh2*Δ/+ diploids. Diploids underwent meiosis and tetrads were dissected. Spore clones containing both the indicated mutation and *fkh2*Δ were assessed for morphology differences by agar scarring assays. All pertinent genotypes were assessed by PCR. Agar scarring was assessed by gently patching haploid strains onto YPD and washing with H_2O after three days. (**B**) Protein immunoblot of *fkh1-m* strains using anti-Fkh1 antibody. Orc1 detected with an anti-Orc1 antibody [114] served as a loading control. (**C**) Morphology assays as described in panel (A). Representative tetrads in which all four

possible allelic combinations are present are shown. Spore clones containing both the indicated mutation and *fkh2*Δ are underlined. Agar scarring assays were performed on the underlined spore. (**D**) Doubling times of *fkh1-m fkh2*Δ strains in liquid YPD media. Averages are based on at least 3 replicates. Error bars represent 1 standard deviation. Asterisks indicate level of statistical significance compared to *fkh2*Δ cells. P-value of 0.05-0.001=*, p-value <0.001=**.

a *fkh1* allele lacking the FHA domain coding region (Δ50-202, *fkh1-fha*Δ), when combined with *fkh2*Δ, produced the same phenotype as *fkh1*Δ and *fkh1-dbd*Δ (Figure 2-5C). Thus, this N-terminal region including the Fkh1 FHA domain (residues 50-202) was important for Fkh1's role in cell cycle regulation. The single residue substitution alleles examined, *fkh1-R80A*, *fkh1-S110A* and *fkh1-R111A* produced smaller colonies when combined with *fkh2*Δ, indicating that these single amino acids were also essential for wild-type Fkh1 function in this assay (Figure 2-5C). Each of these residues is predicted to be critical for the phosphopeptide binding function of the Fkh1 FHA domain. The remainder of the *fkh1-m* alleles examined in this assay caused no discernible defect when combined with *fkh2*Δ (Figure 2-5C). However, most of the alleles did reduce mitotic growth rates in liquid culture when combined with *fkh2*Δ, suggesting a defect in functions that overlap with Fkh2 (Figure 2-5D). The different effects of *fkh1*-fhaΔ versus the *fkh1-m* alleles suggest that Fkh1 residues 50-202 have functions beyond phosphopeptide binding activity in cell cycle regulation. Regardless, most single amino acid substitutions predicted to reduce or abolish FHA phosphopeptide binding activity caused mitotic growth defects, supporting a role for the Fkh1 FHA domain in Fkh1's overlapping roles with Fkh2 in the yeast cell cycle.

2.4.7 Fkh1's overlapping role with Fkh2 did not depend on any single binding partner identified in the 2-hybrid screen

The data presented above supported the hypothesis that Fkh1's role in cell-cycle regulation is mediated through the Fkh1 FHA domain's interaction with one or more partner proteins. To test if any of the putative partners defined in the 2-hybrid screen were important for this role, we examined whether deletions of genes encoding these proteins phenocopied a *fkh1-fha*Δ or the *fkh1-m* alleles, such as *fkh1-R80A*, using the same genetic logic as in Figure 2-5A. A complete deletion

of the protein coding regions for *MPH1*, *ECM30*, *GLN3*, *URE2* or *FDO1* did not reduce colony size when combined with a *fkh2*Δ, the diagnostic for Fkh1 function in this assay (Figure 2-5C). A *ure2*Δ did slow colony formation after dissection, but this effect did not require a *fkh2*Δ mutation. Therefore, no single Fkh1 interaction partner identified in the 2-hybrid screen could explain how the FHA domain contributed to Fkh1's overlapping role with Fkh2 in cell-cycle regulation and morphology.

2.4.8 The Fkh1-Mph1 interaction required either one of two specific threonines within the C-terminus of Mph1

An important transcription-independent function of Fkh1 lies in the regulation of recombination-mediated mating-type switching [56,60]. Only one Fkh1-interaction partner identified in our 2-hybrid screen, Mph1, has an established role in recombinational repair [95,96,115]. Therefore, we focused on gaining a better molecular understanding of the Fkh1-Mph1 interaction. First, we confirmed this interaction using co-immunoprecipitation. Fkh1 was recovered in an immunoprecipitation with anti-FLAG antibodies only in cells expressing Mph1-FLAG (Figure 2-6A). Conversely, Mph1-FLAG was recovered in an immunoprecipitation with anti-Fkh1 antibodies only in cells expressing Fkh1 (Figure 2-6B). We found that this co-immunoprecipitation interaction depended on the region containing the FHA domain of Fkh1 (Figure 2-6B), validating our 2-hybrid results. In addition, 2-hybrid assays using different GBD-Mph1 fusions showed that amino acids 762-993 of Mph1 were both necessary and sufficient for its interaction with Fkh1-FHA, a result consistent with our finding in the original 2-hybrid screen (Figure 2-7A). Moreover, a smaller Mph1 fragment composed of amino acids 751-810 was sufficient to interact with Fkh1-

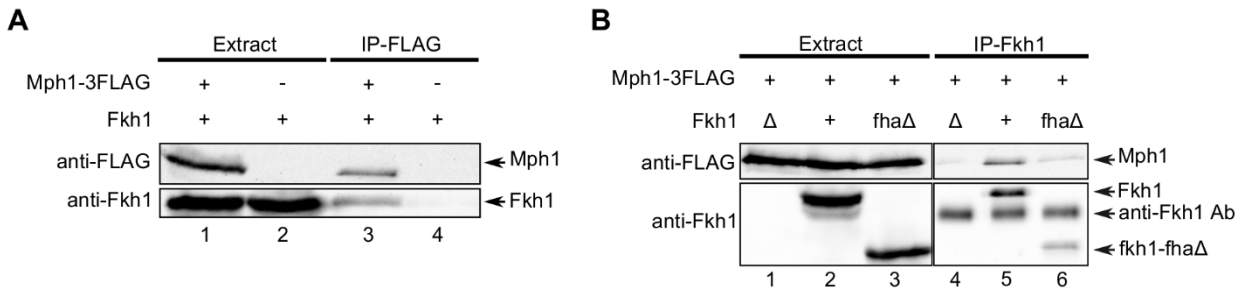

Figure 2-6. Fkh1 and Mph1 interacted in yeast cell extracts. (**A**) Co-immunoprecipitation using anti-FLAG antibodies. Anti-FLAG antibodies were used to immunoprecipitate proteins from *MPH1-FLAG* (+) or *MPH1* (-) cells. The starting extract (extract) and immunoprecipitated proteins (IP) were then examined by protein immunoblotting using either anti-FLAG or anti-Fkh1 antibodies. (**B**) Anti-Fkh1 antibodies were used to immunoprecipitate proteins from *FKH1* (+), *fkh1*Δ (Δ), or *fkh1-fha*Δ (fhaΔ) cells and proteins were examined as described in panel (A).

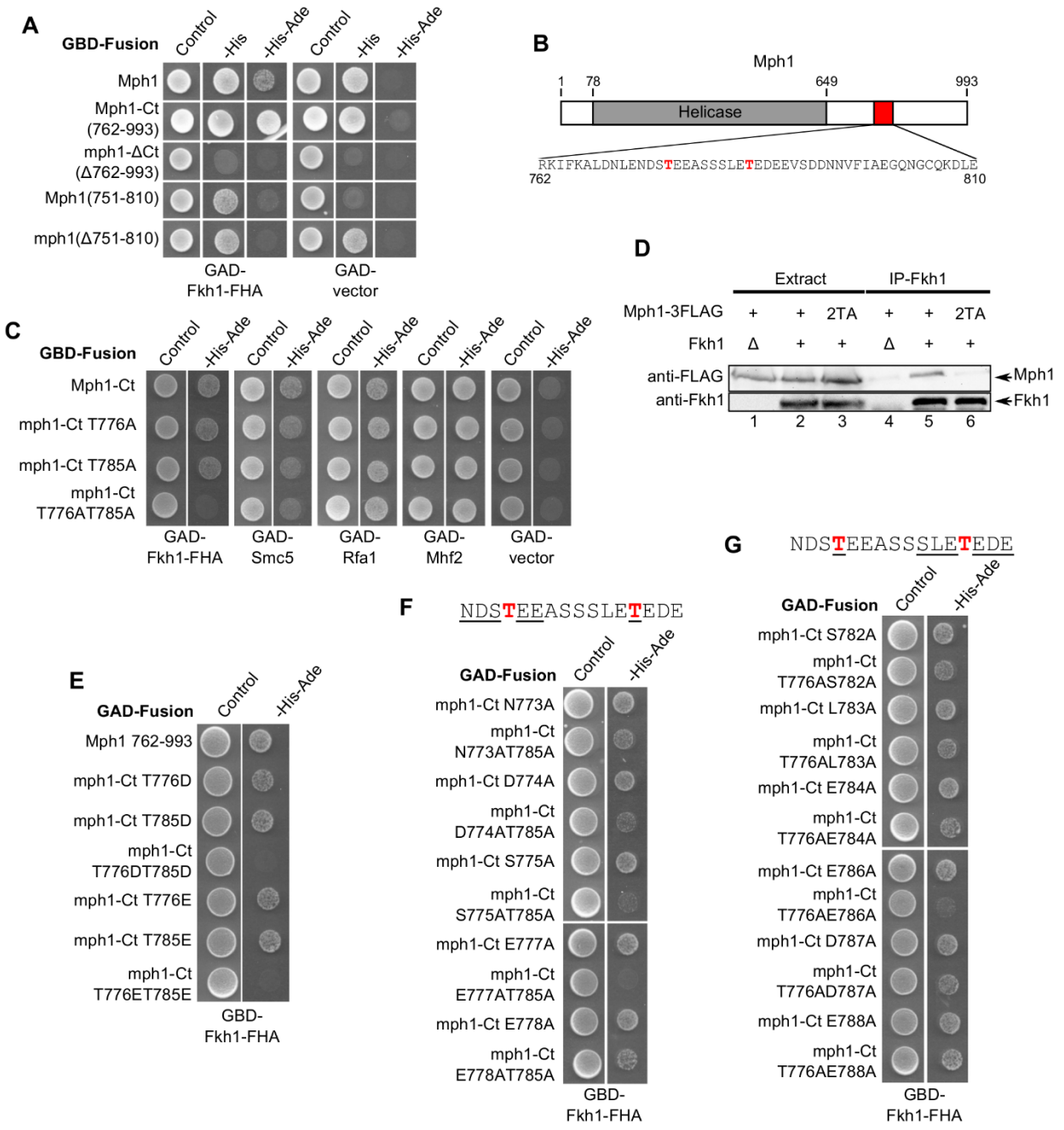

Figure 2-7. The Fkh1-Mph1 interaction required either one of two closely spaced threonines within the C-terminus of Mph1. (**A**) Yeast 2-hybrid assays performed using the indicated regions of Mph1 as bait. Note that many GBD-Mph1 fusion proteins were able to activate transcription of the *HIS3* reporter gene in the absence of an interaction partner. Therefore, interaction was defined as the ability to grow on selective media only in the presence of an interaction partner, and not the

GAD alone. (**B**) Diagram of Mph1 primary structure [116]. The Mph1 region that interacts with Fkh1 occurs at the overlap between amino acids 751-810 and 762-993 (762-810, boxed in red) based on data in panel (A). The sequence of this region is displayed, with the two threonines it contains, T776 and T785, shown in red. (**C**) Yeast 2-hybrid assays using mutant forms of GBD-Mph1-Ct (amino acids 762-993) as bait and several known Mph1 interaction partners as prey. (**D**) Anti-Fkh1 antibodies were used to immunoprecipitate proteins from cells expressing *MPH1-FLAG* (+) or *mph1-2TA-FLAG* (2TA) in *FKH1* (+) or *fkh1*Δ (Δ) backgrounds as described in Figure 2-6. (**E-G**) Yeast 2-hybrid assays using GBD-Fkh1-FHA (amino acids 50-202) and mutant forms of GAD-Mph1-Ct (amino acids 762-993) as indicated.

FHA, albeit to a weaker extent than Mph1-Ct (amino acids 762-993), while Mph1 lacking this region was unable to bind the Fkh1 FHA domain (Figure 2-7A).

Previous studies of FHA domains [27,37,113] and the alignment and mutagenesis described in Figure 2-3, 4 led to the prediction that the Fkh1 FHA domain binds partner proteins through contact with a phosphothreonine residue. To test this idea, we used the 2-hybrid assay to examine if any threonine in Mph1 was required for binding Fkh1. We focused on the overlapping 49 residues between Mph1(751-810) and Mph1(762-993), which contained only two threonines (Figure 2-7B). Substitution of alanine for both of these threonines (T776AT785A), but not either single T→A substitution, abolished the Mph1-Fkh1 interaction (Figure 2-7C). This finding was confirmed by co-immunoprecipitation, as Fkh1 failed to pull down mph1-T776AT785A in an immunoprecipitation experiment (Figure 2-7D). Both assays suggest that the Fkh1-Mph1 interaction required one of two threonines (T776 and T785) within Mph1. These residues are located within a highly acidic region of Mph1. The modeled structure of Fkh1-FHA showed a strongly positively charged concave surface, mainly formed by R80, K107, R111, K112, and R132 (Figure 2-3C, D), all of which were required for binding Mph1, suggesting Fkh1 uses this lysine-arginine-rich region to help recognize Mph1 through electrostatic interactions. The Mph1-Ct region serves as a regulatory hub on the Mph1 multifunctional helicase, directing its interactions with several partner proteins, including a subunit of the Smc5/6 complex (Smc5), the large subunit of RPA (Rfa1), and a subunit of the histone fold complex (Mhf2) [97–100]. To determine whether T776 and T785 were involved in these previously reported interactions, 2-hybrid assays were performed with the same series of Mph1 variants examined for interaction with Fkh1. Mph1-T776AT785A was able to interact with all three tested proteins (Figure 2-7C). Thus T776 and

T785 directed a specific interaction between Fkh1 and Mph1 that was distinct from Mph1's interaction with several other protein partners.

To better establish how Fkh1-FHA interacted with Mph1 we performed 2-hybrid assays in which T776 and/or T785 of Mph1 were replaced with aspartic acid or glutamic acid (Figure 2-7E). These negatively charged residues can act as phosphomimetics, and thus it was possible that if the role of these two threonine residues were fulfilled via their phosphorylation, that T→D or E substitutions would support the Fkh1-Mph1 2-hybrid interaction via electrostatic contributions alone. However, substitution of these threonines with aspartic acid or glutamic acid, but not the single substitutions, abolished interaction with Fkh1, indicating that T→D or E substitutions were as disruptive to the Fkh1-Mph1 interaction as the T→A substitutions we examined (Figure 2-7E). These data provide evidence that the threonine residue identities are particularly important, supporting the conclusion that the Fkh1 FHA domain is interacting with this region of Mph1 via classical FHA-phosphothreonine peptide contacts and not merely electrostatic interactions.

Many FHA domains (including the Rad53 N-terminal FHA domain) display a preference for particular amino acids at the pT +3 residue, while other FHA domains have a preference for particular amino acids at other positions [38,117]. As a first step toward understanding the binding preferences of the Fkh1 FHA domain we looked at how substitution of alanine for residues surrounding the two threonines in Mph1 affected Fkh1 binding. We found that substitution of alanine for any of these residues alone did not abolish Fkh1 binding, consistent with the finding that any single T→A substitution (T776A or T785A) did not abolish the Fkh1-Mph1 interaction. However, substitution of alanine for residues surrounding T776 in combination with a T785A substitution did reduce the Fkh1 2-hybrid interaction (Figure 2-7F). In particular, substitution of alanine for the aspartate at position 774, the serine at position 775, or the glutamate at position 777

in combination with T785A reduced or abolished the Fkh1-Mph1 interaction. Thus the region surrounding T776, including residues D774, S775 and E777, contributed to the Fkh1-Mph1 interaction. We used the same approach to define important residues surrounding T785, analyzing alanine substitutions in combination with T776A (Figure 2-7G). These data provided evidence that the region surrounding T785, most notably residue E786 but also to a lesser degree residue S782 and E784, contributed to the Fkh1-Mph1 interaction. These data provide additional evidence that this region of Mph1 contains two separate and independent FHA-binding motifs and that both motifs have similar features, including a preference for glutamic acid at the pT+1 position.

2.4.9 Recombinant Fkh1 interacted directly with phosphorylated Mph1-derived peptides

Next, we tested whether Fkh1 interacted directly with Mph1 through the region containing T776 and T785 and if this interaction was controlled by phosphorylation of these threonines. To this end, recombinant Fkh1-6xHis was purified from *E. coli* and its ability to bind an 18-residue peptide representing Mph1(772-789) was assessed by fluorescence anisotropy (Figure 2-8). The peptide that was phosphorylated on both T776 and T785 bound purified Fkh1 efficiently, with a K_d of 2.2 μM, well within range of other FHA-phosphopeptide interaction affinities [38]. The non-phosphorylated version of the peptide bound Fkh1 with a >100-fold reduced affinity (K_d of 270.8 μM). In addition, and consistent with the effects observed in the 2-hybrid assays in Figure 2-7C, mono-phosphorylated forms of the peptide (i.e. containing phosphorylation on only T776 or T785) also bound Fkh1, albeit with modestly reduced affinities. These data support the conclusion that Mph1 contained two independent Fkh1-FHA binding motifs, each having a similar affinity for Fkh1.

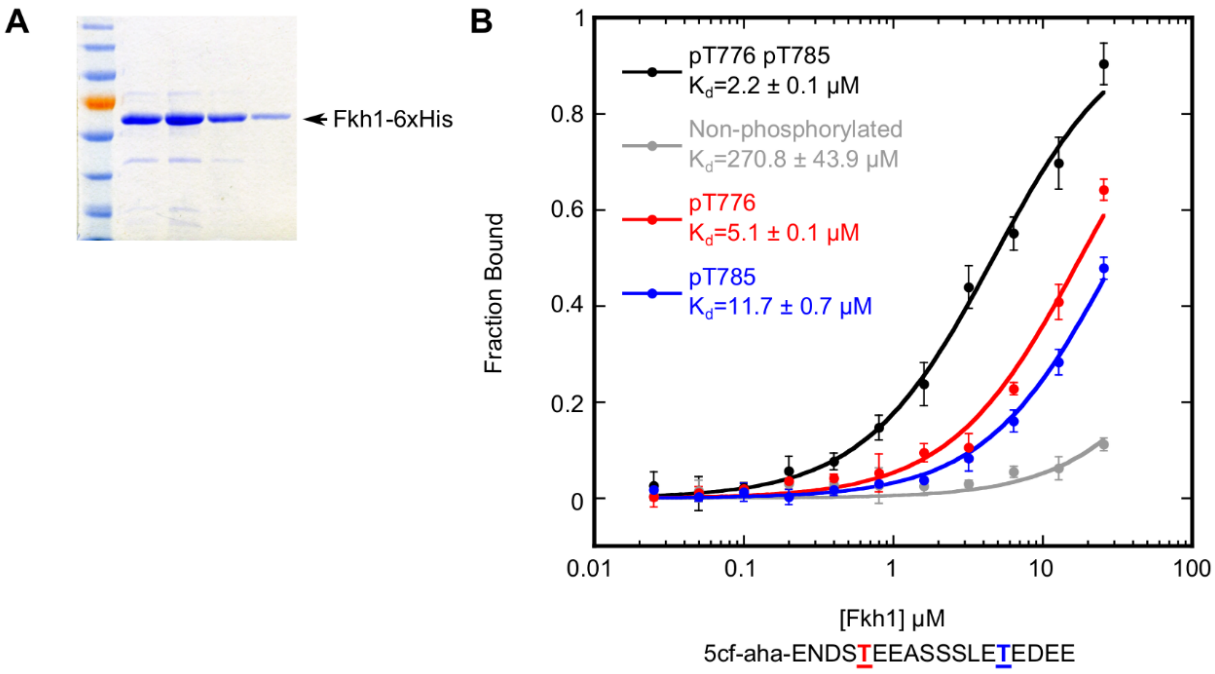

Figure 2-8. Recombinant Fkh1 directly bound to an Mph1-derived peptide in a phosphorylation-dependent manner. (**A**) Polyacrylamide gel showing recombinant Fkh1-6xHis protein used for peptide binding in panel (B). (**B**) Peptide binding assay of Fkh1-6xHis and Mph1-derived peptides using fluorescence anisotropy. Binding reactions contained the indicated concentration of purified His-tagged Fkh1 and 3 nM 5-carboxyfluorescein labeled Mph1-derived peptide (5cf-aha-ENDSTEEASSSLETEDEE) with threonines phosphorylated or unmodified, as indicated.

2.4.10 The Fkh1-Mph1 interaction contributed to the directionality of mating-type switching but not to MPH1*'s role in tolerance for MMS-induced DNA damage or genome stability*

After establishing that the Fkh1-Mph1 interaction was mediated by the FHA domain of Fkh1 and one of two phosphothreonines on Mph1, we assessed whether this interaction was important for Fkh1's role in mating-type switching. Fkh1 regulates donor preference during mating-type switching by directly binding to the recombination enhancer (RE) and promoting recombination between an HO-induced DSB at *MAT* and the donor locus *HML*. In a previous study, the N-terminal region of Fkh1 containing the FHA domain was shown to be sufficient to direct RE function [60]. This point was elucidated by engineering a strain in which RE was replaced with LexA binding sites and a LexA-Fkh1-FHA fusion protein was expressed [60]. In this Fkh1-dependent assay, the **a**-mating-type genes located at *HMR* were replaced by *MAT*α sequences that contained a unique *BamH*I restriction site (*HMR*α-B), such that repair of a DSB generated by the HO endonuclease at *MAT***a** will always result in a *MAT*α cell, and those using the *HMR*α-B donor sequence can be cut by *BamH*I, while those using *HML*α cannot. Thus donor preference can be examined by testing the relative abundance of the two different repair products through a PCR reaction that amplifies *MAT*α sequences followed by a *BamH*I restriction digest (Figure 2-9A). Consistent with a previous finding [60], *HML* was the preferred donor, as it was used as template for repair in >90% of cells, while in a strain containing a mutant version of LexA-FHA containing the R80A substitution (LexA-FHA-R80A), recombination between *MAT***a** and *HML* was reduced to less than 20% (Figure 2-9B). We found that *mph1*Δ reduced the function of RE, as *HML* now acted as the donor in <80% of cells (Figure 2-9B). While this level of reduction was not equivalent to that caused by loss of Fkh1-FHA function, it was highly reproducible. Moreover, *mph1-2TA* phenocopied the effect of the *mph1*Δ allele and reduced *HML* usage to

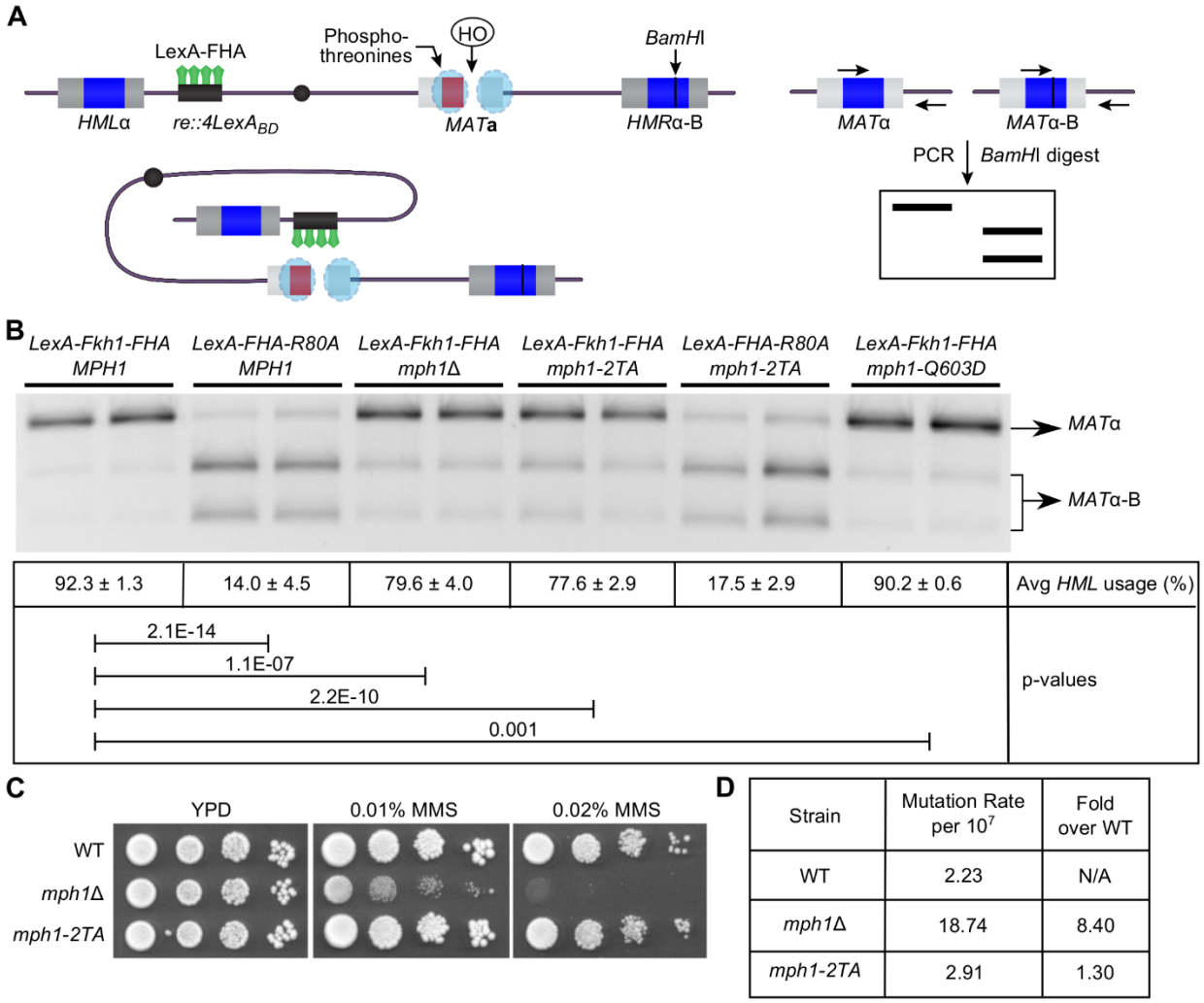

Strain	Mutation Rate per 10^7	Fold over WT
WT	2.23	N/A
mph1Δ	18.74	8.40
mph1-2TA	2.91	1.30

Figure 2-9. The Fkh1-Mph1 interaction contributed to the regulation of donor preference during mating-type switching. (**A**) Schematic showing Fkh1-dependent PCR-based switching assay and model proposed in [60]. A galactose-inducible HO endonuclease cuts at *MAT***a**. The resulting double strand break is repaired through recombination with either *HML* or *HMR*, both of which contain *MAT*α sequence, but with the insertion of a unique *BamH*I restriction site in *HMR* (*HMR*α-B). Directionality is controlled through the recombination enhancer (RE), which has been replaced by 4 LexA binding domains. LexA-fused Fkh1-FHA binds to RE causing a preference for recombination with *HML*. Primers that specifically amplify *MAT*α were used to amplify the repaired *MAT* locus by PCR. The PCR products were then digested with *BamH*I and donor

preference was calculated as *MAT*α / (*MAT*α + *MAT*α-B). (**B**) A switching assay was performed using at least four replicates of each strain. Average *HML* usage and standard deviations were calculated and a representative gel is shown. Strains were congenic and contained all alleles represented in panel (A) unless otherwise noted. P-value significance of differences observed between strains is indicated by connecting lines. (**C**) MMS assays of *MPH1* mutant strains. Cells were grown in liquid YPD media to mid-log phase and 10-fold serial dilutions were spotted onto YPD plates containing the indicated concentration of MMS. (**D**) Mutation rate of *MPH1* mutant strains. Forward *CAN1* mutation rate was calculated using FALCOR by the Ma-Sandri-Sarkar maximum likelihood method in which the data are fit to the Luria-Delbrück distribution [118].

<80%. Additionally, *mph1-2TA* did not reduce *HML* preference further in strains expressing LexA-FHA-R80A, providing additional genetic evidence that the Fkh1-Mph1 interaction contributed to donor preference during mating-type switching. The helicase activity of Mph1 is not responsible for this activity, as a helicase defective mutant of *MPH1 (mph1-Q603D*) did not alter donor preference as drastically as deletion of *MPH1* or the *mph1-2TA* allele, although it did have a statistically small effect. This donor preference defect caused by *mph1-2TA* was specific to this function because, unlike *mph1*Δ cells, *mph1-2TA* cells did not exhibit sensitivity to MMS (Figure 2-9C) or an increase in mutation rate (Figure 2-9D). Thus the *mph1-2TA* allele caused a specific functional defect in Mph1's role in regulating RE function while leaving at least two other known roles for Mph1 intact.

2.4.11 FDO1 *also contributed to the regulation of donor preference during mating-type switching*

The reduction in *HML* usage in *mph1-2TA* strains is less than that in cells expressing LexA-FHA-R80A, suggesting there must be other Fkh1 partners required for its role in mating-type switching. To address a role for additional Fkh1-FHA partner proteins, we examined the switching profile in cells lacking Fdo1. We found that deletion of *FDO1* reduces *HML* usage to ~80%, a 10% reduction relative to the wild type control similar to the level of reduction caused by deletion of *MPH1* (Figure 2-10A). Interestingly, in contrast to the Mph1-Fkh1 interaction, the Fkh1 FHA domain was not sufficient for interaction with Fdo1 (Figure 2-4C). However, further examination of this interaction by 2-hybrid showed that, in the context of full length Fkh1, the fkh1-R80A mutation reduced the Fkh1-Fdo1 interaction, strongly suggesting that the established phosphothreonine binding function of the FHA domain was necessary for the Fkh1-Fdo1 interaction as it was for the Fkh1-Mph1 interaction (Figure 2-10B). To test whether the defects in

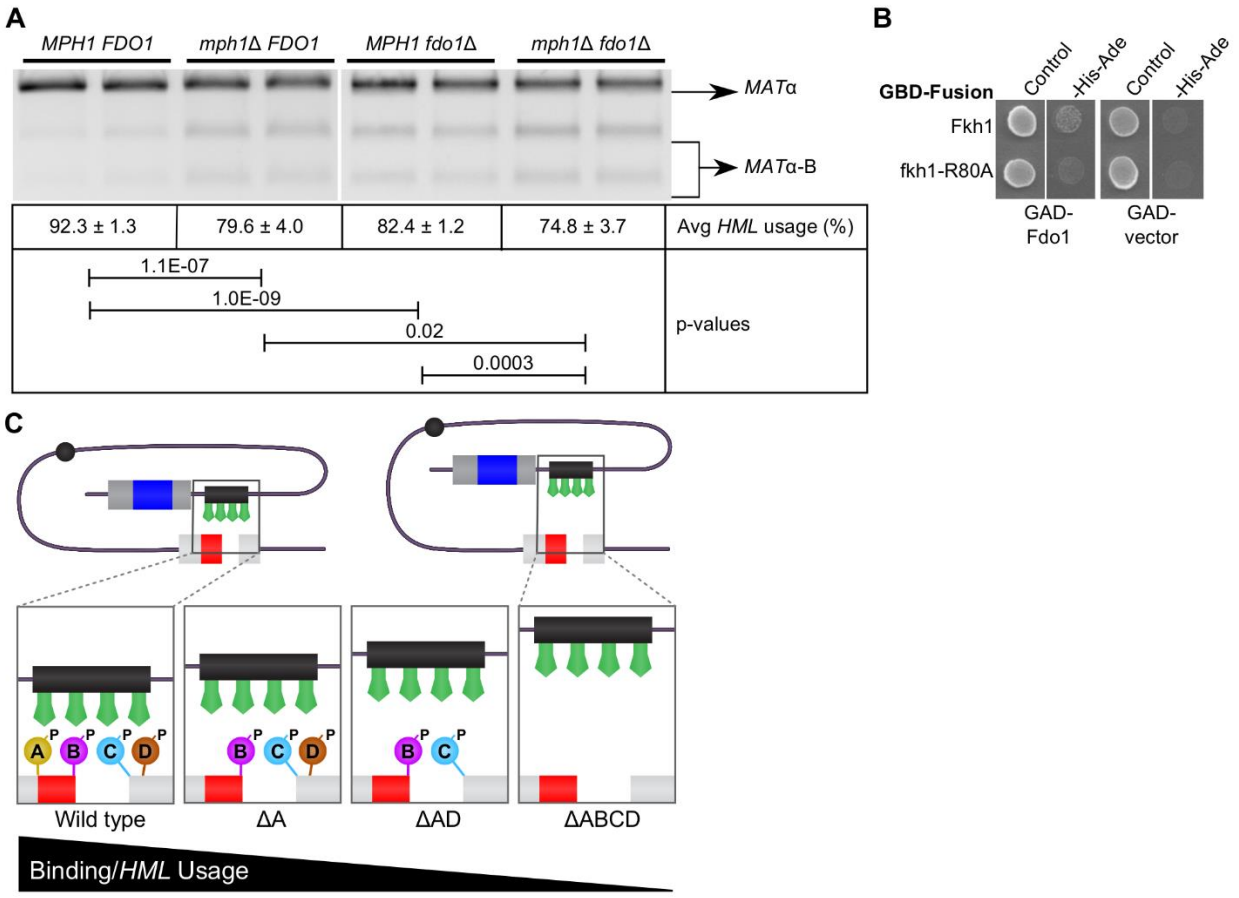

Figure 2-10. Fdo1 contributed to Fkh1-FHA-dependent regulation of donor preference during mating-type switching. (**A**) A switching assay was performed using at least four replicates of each strain. Average *HML* usage and standard deviations were calculated and a representative gel is shown. Strains were congenic and contained all alleles represented in Figure 2-9A unless otherwise noted. P-value significance of differences observed between strains is indicated by connecting lines. (**B**) Yeast 2-hybrid assays using different forms of full-length Fkh1 as bait. GAD constructs contained the region of Fdo1 identified in the 2-hybrid screen (Table 2-1) or the GAD alone. (**C**) Model for Fkh1 function at RE. Fkh1-FHA interacts with multiple proteins that associate with the DSB generated at *MAT* and are phosphorylated on threonines (we represent only 4 putative phosphoproteins). Deletion of any single Fkh1-FHA partner only slightly reduces

interaction with the DSB at MAT and, therefore, *HML* preference. Deletion of more than one partner reduces binding and *HML* preference further. Thus Fkh1-FHA's role at the RE requires its interaction with many different proteins that together define a DSB.

donor preference caused by deletions of *MPH1* and *FDO1* were additive, we also examined mating-type switching in *mph1*Δ *fdo1*Δ cells. *HML* usage was reduced in these cells to a greater degree than in cells containing either single mutation, suggesting that Mph1 and Fdo1 contribute independent Fkh1-FHA binding interactions to control Fkh1-regulated donor preference.

2.5 Discussion

This study provided evidence that Mph1 was a direct Fkh1-FHA phosphoprotein partner relevant to Fkh1's role in regulating the directionality of mating-type switching. This Fkh1-Mph1 interaction was mediated through a small peptide within the C-terminal regulatory region of Mph1 that contains two threonines each capable of directing interactions with the Fkh1 FHA domain. Mutagenesis studies show that these two threonines likely act as two independent Fkh1-FHA binding motifs, as both threonines must be substituted with alanine to abolish binding by 2-hybrid. Additionally, the amino acid sequences surrounding the two threonines are similar and highly acidic. Both motifs have a glutamic acid residue at the pT+1 position, and mutational analyses indicated that this residue was important for each motif to direct binding of the Fkh1 FHA domain to Mph1. While the 2-hybrid data cannot exclude the possibility that the +1 glutamic acid is required for phosphorylation of the relevant threonine and not directly involved in Fkh1-FHA binding, they nevertheless indicate that a TE signature is relevant to each motif's independent ability to direct an Mph1-Fkh1-FHA interaction. These observations underscore that there are two redundant Fkh1-FHA binding motifs built into this small region of Mph1. Because a mutant incapable of phosphorylation on these threonines, *mph1-2TA*, behaved as an *mph1*Δ in a mating-type switching assay, but not in other commonly used assays that assess *MPH1* function, we

propose that the Fkh1-Mph1 interaction helps establish the long-range chromosomal interaction essential for donor preference during mating-type switching.

While our data were consistent with the model for Fkh1 bound to the recombination enhancer (RE) guiding the *HML* locus to the DSB at *MAT* [60], they also raised an important new question. In particular, why does loss of Fkh1-FHA function cause a much larger defect in RE function compared to *mph1-2TA* (or *mph1*Δ), both of which abolish the Fkh1-FHA-Mph1 interaction? The simplest explanation is that Mph1 is only one of several proteins bound to the DSB at *MAT* that the Fkh1 FHA domain uses to locate this lesion. It makes sense for Fkh1 to bind several different proteins at the DSB with relatively weak affinities—in this way the RE remains close to *MAT* long enough to increase the opportunity for strand invasion into *HML*. At the same time Fkh1 is not bound so tightly to any one partner or the DSB region itself to inhibit strand invasion and the protein/DNA remodeling necessary to drive the recombination event. Therefore, we propose that there must exist other Fkh1-FHA partner proteins at the HO-induced DSB at *MAT* that contribute to the RE's ability to direct the *MAT* locus to *HML*. The multi-partner model for Fkh1 FHA function in donor preference may represent a general mechanism by which Fkh1-FHA performs its other biological functions in transcription and replication. This type of mechanism may allow for relatively high specificity but low affinity (and thus potentially highly dynamic) interactions that may be important to these complex chromosomal processes.

Based on this idea and data reported in a previous study, the CK2 kinase likely phosphorylates many Fkh1-interacting proteins involved in donor preference [60]. In this regard we note that, consistent with our observation of an interaction in asynchronous cells and within the 2-hybrid context, CK2 constitutively phosphorylates target proteins [119]. Additionally, the amino acid sequence surrounding both relevant Mph1 threonines are consistent with a CK2 target

[119]. When these phosphorylated proteins come together at a DSB, perhaps with other proteins phosphorylated in a more regulated manner by other kinases, they collectively serve to define the DSB for Fkh1-FHA. Consistent with this proposal, a deletion of *FDO1*, a gene encoding another Fkh1-FHA interaction partner identified in our screen, also reduced donor preference to a degree similar to that of *mph1-2TA* (or *mph1*Δ). Moreover, a deletion of both genes to create an *fdo1*Δ *mph1*Δ cell reduced preference for *HML* to a degree greater than deletion of either gene alone. However, a substantial amount of Fkh1-FHA-dependent donor preference remained intact even in cells carrying null mutations in both of these genes, suggesting that another protein or proteins at the DSB must interact with Fkh1-FHA. Many proteins, in addition to Mph1, bind to DSBs and would be good candidates for additional Fkh1-FHA interaction partners that regulate donor preference [120–122]. While mating-type switching is a specific form of homologous recombination, it is clear that DSB repair in diploids also requires a search for homologous regions by the DSB [123]. It will be interesting to learn whether this more generalized process uses similar protein-protein interactions to stabilize chromosomal interactions that serve to juxtapose homologous regions.

Our data provided evidence that the Fkh1 FHA domain may be controlling most, if not all, Fkh1-mediated biology in yeast. Indeed, many *fkh1-fha* single residue substitution (*fkh1-m*) mutants abolished interaction with all protein partners uncovered here and reduced Fkh1's ability to function in cell-cycle regulation with Fkh2, even though deletion of no single gene encoding an interaction partner had an effect. Based on the results with donor preference, it seems likely that multiple different Fkh1-FHA interaction partners will be needed to fully explain Fkh1-FHA's role in cell cycle regulation. A deletion of the entire FHA domain of Fkh1 (*fkh1-fha*Δ) phenocopied a *fkh1*Δ mutation in cell cycle regulation as measured by both mitotic cell division rates and

pseudohyphal-like growth and agar scarring when combined with a *fkh2*Δ allele. Because the established role of FHA domains is to bind phosphopeptides, it was perhaps unexpected that amino acid substitutions in the FHA domain predicted to abolish FHA-phosphopeptide interactions only slowed mitotic cell division in *fkh2*Δ cells without causing pseudohyphal-like growth. The Fkh1 FHA domain may play roles in Fkh1 function in addition to phosphopeptide binding by providing as yet undefined interaction surfaces for other regulators of transcription. Alternatively, the *fkh1-fha*Δ allele used in this study lacked coding information for an additional ~30 amino acids outside of the alignment-defined FHA domain that may provide surfaces for additional protein-protein interactions. Regardless, these data raise new questions about whether Fkh1's roles in regulating cell proliferation rate and suppressing pseudohyphal growth are completely separable, or whether a certain threshold of reduced transcription/altered transcriptional regulation must be met before pseudohyphal growth is also observed.

Our data provided evidence that several Fkh1-FHA interaction partners that can direct Fkh1 cellular roles remain unidentified. As we have shown, determining the role of any particular Fkh1-protein interaction is difficult through mutation of Fkh1-FHA itself, as the same FHA residues participate in multiple Fkh1-protein interactions and Fkh1 processes. For this reason, it will be important to identify other Fkh1-FHA-partner proteins and engineer mutations that specifically abolish their ability to interact with Fkh1, as we did for Mph1 in this study, to isolate the discrete mechanisms and pathways influenced by Fkh1.

2.6 Materials and methods

2.6.1 Yeast strains and plasmids

Strains used in this study were derived from the *Saccharomyces cerevisiae* strain w303 unless otherwise noted. Standard methods were used for yeast growth, strain and plasmid construction. Strains used in this study are listed in Table 2-3. Plasmids are listed in Table 2-4. Random mutagenesis of pGBDU-C1 plasmids was performed as described in [124]. Lack of interaction alleles were identified by replica plating from non-selective media to media selective for 2-hybrid interaction and identifying colonies that were no longer viable. Mutants identified by random mutagenesis were confirmed by directed mutagenesis and 2-hybrid assays.

2.6.2 Yeast 2-hybrid assays

2-hybrid assays were performed in the PJ69-4A strain as described in [88]. The strain contains two reporter genes, *HIS3* and *ADE2*. The original screen was performed using a Fkh1-GBD fusion protein in which the entire DNA binding domain was precisely replaced with the GBD. This GBD-Fkh1 fusion activated transcription of the *HIS3* reporter gene. Therefore colonies harboring potential Fkh1-interacting partners were identified on minimal media lacking both histidine and adenine.

2.6.3 Homology modeling and FHA alignment

A predicted structure for the Fkh1 FHA domain was generated using the N-terminal Rad53 FHA domain as a template using SWISS-MODEL [39,101–103]. Amino acids 72-170 were modeled. A structure-based sequence alignment of the N-terminal Rad53 FHA domain (Rad53-1) and the Fkh1 FHA domain was generated using a combination of the Rad53 crystal structure (PDB 1G6G) [39] and structural predictions of the Fkh1 FHA domain based on a combination of

Table 2-3. Yeast strains used in this study. For many assays multiple independent strains were used. For brevity only one is included in this table.

Name	Description	Source
PJ69-4A	*MATa trp1-901 leu2-3,112 ura3-52 his3-200 gal4Δ gal80Δ GAL2-ADE2 LYS2::GAL1-HIS3 met2::GAL7-lacZ*	[88]
CFY3533	*MATa ADE2+ RAD5+ CAN1+*	This study
CFY3537	*MATa ADE2+ RAD5+ CAN1+ fkh1Δ::HisG*	This study
CFY3539	*MATa ADE2+ RAD5+ CAN1+ mph1Δ::KanMX*	This study
CFY3549	*MATa ADE2+ RAD5+ CAN1+ fkh2Δ::HisG*	This study
CFY3552	*MATa ADE2+ RAD5+ CAN1+ fkh1Δ::HisG fkh2Δ::HisG*	This study
CFY3886	*MATa ADE2+ RAD5+ CAN1+ fkh1-R132A*	This study
CFY3888	*MATa ADE2+ RAD5+ CAN1+ fkh1-K107A*	This study
CFY3893	*MATa ADE2+ RAD5+ CAN1+ fkh1-D102A*	This study
CFY3894	*MATa ADE2+ RAD5+ CAN1+ fkh1-R111A*	This study
CFY3956	*MATa ADE2+ RAD5+ CAN1+ fkh1-R80A*	This study
CFY3960	*MATa ADE2+ RAD5+ CAN1+ fkh1-S110A*	This study
CFY3963	*MATa ADE2+ RAD5+ CAN1+ fkh1-S155A*	This study
CFY3969	*MATa ADE2+ RAD5+ CAN1+ fkh1-fhaΔ (Δ50-202)*	This study
CFY3971	*MATa ADE2+ RAD5+ CAN1+ fkh1-N133A*	This study
CFY3978	*MATa ADE2+ RAD5+ CAN1+ fkh1-K112A*	This study
CFY3995	*MATa ADE2+ RAD5+ CAN1+ fkh1-S110A fkh2Δ::HisG*	This study
CFY4034	*MATa ADE2+ RAD5+ CAN1+ fkh1-dbdΔ*	Modified from [9]
CFY4038	*MATa ADE2+ RAD5+ CAN1+ mph1-2TA*	This study
CFY4068	*MATa ADE2+ RAD5+ CAN1+ Mph1-3FLAG-HIS3 fkh1Δ::HisG*	Modified from [125]
CFY4069	*MATa ADE2+ RAD5+ CAN1+ Mph1-3FLAG-HIS3*	Modified from [125]
CFY4143	*MATa ADE2+ RAD5+ CAN1+ mph1-2TA-3FLAG-HIS3*	This study
CFY4246	*MATa ADE2+ RAD5+ CAN1+ fkh1-R80A fkh2Δ::HisG*	This study
CFY4248	*MATa ADE2+ RAD5+ CAN1+ fkh1-fhaΔ (Δ50-202) fkh2Δ::HisG*	This study
CFY4249	*MATa ADE2+ RAD5+ CAN1+ fkh1-D102A fkh2Δ::HisG*	This study
CFY4251	*MATa ADE2+ RAD5+ CAN1+ fkh1-K112A fkh2Δ::HisG*	This study
CFY4252	*MATa ADE2+ RAD5+ CAN1+ fkh1-S155A fkh2Δ::HisG*	This study
CFY4254	*MATa ADE2+ RAD5+ CAN1+ fkh1-K107A fkh2Δ::HisG*	This study
CFY4257	*MATa ADE2+ RAD5+ CAN1+ fkh1-R111A fkh2Δ::HisG*	This study
CFY4258	*MATa ADE2+ RAD5+ CAN1+ fkh1-R132A fkh2Δ::HisG*	This study
CFY4262	*MATa ADE2+ RAD5+ CAN1+ fkh1-N133A fkh2Δ::HisG*	This study
CFY4267	*MATa ADE2+ RAD5+ CAN1+ fkh1-fhaΔ (Δ50-202) Mph1-3FLAG-HIS3*	Modified from [125]
CFY4345	*MATa ADE2+ RAD5+ CAN1+ fkh1-dbdΔ fkh2Δ::HisG*	Modified from [9]
CFY4383	*MATa ADE2+ RAD5+ CAN1+ ade3::GAL-HO HMRα-Bre Δ::4LexA-Kan arg56::LexAFkh1FHA-LEU2 Δho*	Modified from [60]

CFY4387	*MATa ADE2+ RAD5+ CAN1+ ade3::GAL-HO HMRα-Bre*Δ*::4LexA-Kan arg56::LexAFkh1FHA-LEU2* Δ*ho mph1*Δ*::KanMX*	Modified from [60]
CFY4394	*MATa ADE2+ RAD5+ CAN1+ ecm30*Δ*::KanMX*	This study
CFY4397	*MATa ADE2+ RAD5+ CAN1+ ure2*Δ*::KanMX*	This study
CFY4400	*MATa ADE2+ RAD5+ CAN1+ fdo1*Δ*::KanMX*	This study
CFY4417	*MATa ADE2+ RAD5+ CAN1+ ade3::GAL-HO HMRα-Bre*Δ*::4LexA-Kan arg56::LexAFkh1FHA-LEU2* Δ*ho mph1-2TA*	Modified from [60]
CFY4465	*MATa ADE2+ RAD5+ CAN1+ gln3*Δ*::KanMX*	This study
CFY4500	*MATa ADE2+ RAD5+ CAN1+ ade3::GAL-HO HMRα-Bre*Δ*::4LexA-Kan arg56::LexAFkh1FHA-LEU2* Δ*ho fdo1*Δ*::KanMX*	Modified from [60]
CFY4501	*MATa ADE2+ RAD5+ CAN1+ ade3::GAL-HO HMRα-Bre*Δ*::4LexA-Kan arg56::LexAFkh1FHA-LEU2* Δ*ho fdo1*Δ*::KanMX mph1*Δ*::KanMX*	Modified from [60]
CFY4509	*MATa ADE2+ RAD5+ CAN1+ ade3::GAL-HO HMRα-Bre*Δ*::4LexA-Kan arg56::LexAFkh1FHA-R80A-LEU2* Δ*ho*	Modified from [60]
CFY4511	*MATa ADE2+ RAD5+ CAN1+ ade3::GAL-HO HMRα-Bre*Δ*::4LexA-Kan arg56::LexAFkh1FHA-R80A-LEU2* Δ*ho mph1-2TA*	Modified from [60]
CFY4522	*MATa ADE2+ RAD5+ CAN1+ ade3::GAL-HO HMRα-Bre*Δ*::4LexA-Kan arg56::LexAFkh1FHA-LEU2* Δ*ho mph1-Q603D-3FLAG-HIS3*	Modified from [60], [125]

Table 2-4. Plasmids used in this study.

Name	Description	Source
pGBDU-C1	Yeast-2-hybrid vector-Gal4 DNA Binding Domain	[88]
pGAD-C1	Yeast-2-hybrid vector-Gal4 Activation Domain	[88]
pCF577	pRS426 Fkh1-GBD (GBD in place of FKH1 DBD-used for original 2-hybrid screen)	This study
pCF2086	pGBDU-C1 Mph1 (762-993) (pGBDU-C1 Mph1-Ct)	This study
pCF2098	pGBDU-C1 Fkh1	This study
pCF2099	pGBDU-C1 Fkh1 (50-291)	This study
pCF2101	pGBDU-C1 Fkh1 (100-291)	This study
pCF2106	pGBDU-C1 Fkh1 (50-202)	This study
pCF2113	pGBDU-C1 Fkh1 (50-158)	This study
pCF2183	pGAD-C1 Fkh1 (50-202)	This study
pCF2185	pGAD-C1 Mph1 (762-993) (pGAD-C1 Mph1-Ct)	This study
pCF2203	pGBDU-C1 Mph1-Ct T785A	This study
pCF2205	pGBDU-C1 Mph1-Ct T776A	This study
pCF2297	pGBDU-C1 Fkh1 R80A	This study
pCF2299	pGBDU-C1 Fkh1 (50-202) R80A	This study
pCF2411	pGBDU-C1 Fkh1 (50-202) A106V	This study
pCF2413	pGBDU-C1 Fkh1 (50-202) R117A	This study
pCF2415	pGBDU-C1 Fkh1 (50-202) S155A	This study
pCF2422	pGBDU-C1 Fkh1 (50-202) K107A	This study
pCF2423	pGBDU-C1 Fkh1 (50-202) R111A	This study
pCF2424	pGBDU-C1 Fkh1 (50-202) R132A	This study
pCF2461	pGBDU-C1 Fkh1 (50-202) N81A	This study
pCF2463	pGBDU-C1 Fkh1 (50-202) D102A	This study
pCF2465	pGBDU-C1 Fkh1 (50-202) N133A	This study
pCF2504	pGBDU-C1 Fkh1 (50-202) T82A	This study
pCF2506	pGBDU-C1 Fkh1 (50-202) D83A	This study
pCF2508	pGBDU-C1 Fkh1 (50-202) N86A	This study
pCF2510	pGBDU-C1 Fkh1 (50-202) K96A	This study
pCF2512	pGBDU-C1 Fkh1 (50-202) K97A	This study
pCF2514	pGBDU-C1 Fkh1 (50-202) N98A	This study
pCF2516	pGBDU-C1 Fkh1 (50-202) S110A	This study
pCF2518	pGBDU-C1 Fkh1 (50-202) K112A	This study
pCF2559	pGAD-C3 Ecm30 (1005-1183)	[88]
pCF2561	pGAD-C1 Gln3 (20-189)	[88]
pCF2568	pGAD-C2 Ure2 (84-354)	[88]
pCF2570	pGAD-C2 Fdo1 (98-342)	[88]
pCF2571	pGAD-C1 Smc5	This study
pCF2573	pGAD-C1 Rfa1	This study
pCF2575	pGAD-C1 Mhf2	This study
pCF2586	pGBDU-C1 Mph1-Ct T776AT785A	This study
pCF2663	pGBDU-C1 Mph1	This study
pCF2694	pGBDU-C1 Mph1 (Δ751-810)	This study
pCF2696	pGBDU-C1 Mph1 (Δ762-993)	This study

pCF2697	pGBDU-C1 Mph1 (751-810)	This study
pCF2774	pGBDU-C1 Fkh1 (Δ50-202)	This study
pCF2958	pET28b-Fkh1 Ct His tag	This study
pCF4144	pGAD-C1 Mph1-Ct N773A	This study
pCF4146	pGAD-C1 Mph1-Ct N773AT785A	This study
pCF4148	pGAD-C1 Mph1-Ct D774A	This study
pCF4150	pGAD-C1 Mph1-Ct D774AT785A	This study
pCF4152	pGAD-C1 Mph1-Ct S775A	This study
pCF4153	pGAD-C1 Mph1-Ct S775AT785A	This study
pCF4154	pGAD-C1 Mph1-Ct E777A	This study
pCF4156	pGAD-C1 Mph1-Ct E777AT785A	This study
pCF4157	pGAD-C1 Mph1-Ct E778A	This study
pCF4159	pGAD-C1 Mph1-Ct E778AT785A	This study
pCF4160	pGAD-C1 Mph1-Ct S782A	This study
pCF4161	pGAD-C1 Mph1-Ct T776AS782A	This study
pCF4162	pGAD-C1 Mph1-Ct L783A	This study
pCF4164	pGAD-C1 Mph1-Ct T776AL783A	This study
pCF4166	pGAD-C1 Mph1-Ct E784A	This study
pCF4168	pGAD-C1 Mph1-Ct T776AE784A	This study
pCF4170	pGAD-C1 Mph1-Ct E786A	This study
pCF4172	pGAD-C1 Mph1-Ct T776AE786A	This study
pCF4174	pGAD-C1 Mph1-Ct D787A	This study
pCF4175	pGAD-C1 Mph1-Ct T776AD787A	This study
pCF4177	pGAD-C1 Mph1-Ct E788A	This study
pCF4179	pGAD-C1 Mph1-Ct T776AE788A	This study
pCF4207	pGAD-C1 Mph1-Ct T776D	This study
pCF4209	pGAD-C1 Mph1-Ct T785D	This study
pCF4211	pGAD-C1 Mph1-Ct T776DT785D	This study
pCF4213	pGAD-C1 Mph1-Ct T776E	This study
pCF4215	pGAD-C1 Mph1-Ct T785E	This study
pCF4217	pGAD-C1 Mph1-Ct T776ET785E	This study

the homology model and secondary structure predicted using JPred [104]. Electrostatic potential was generated by PyMol v 1.7 [126].

2.6.4 Determining morphology and growth rates

Heterozygous *fkh1-m*/+ *fkh2*Δ/+ diploids expressing Fkh1 mutants were dissected and scanned after three days growth. Agar scarring was assessed by gently patching haploid strains onto YPD and washing with H_2O after three days. Growth curves were generated by growing to saturation in YPD media, diluting to an OD_{600} of 0.1 in a 96-well plate, and monitoring growth by measuring the OD_{600} every three minutes over a 24 hour period in a Biotek Synergy 2 plate reader shaking at 30°C. Doubling times were calculated by exponential regression of data generated from growth curves during log-phase [127].

2.6.5 Co-immunoprecipitation and Western blotting

Cell extracts for Western blotting were prepared as described in [128]. Cell extracts for co-immunoprecipitation were prepared by breaking cells by the glass bead method in CoIP buffer (50 mM HEPES pH 7.5, 140 mM NaCl, 1 mM EDTA, 1% TX-100, protease inhibitors (Calbiotech)). Lysates were then diluted 1:1 in CoIP buffer and incubated with the appropriate antibody. Beads were washed with CoIP buffer without detergents followed by washes with the same buffer with 200 mM NaCl.

Co-immunoprecipitation of Fkh1 and FLAG-tagged Mph1 (modified from [125]) were performed using Anti-FLAG antibodies (ANTI-FLAG M2 Affinity Gel, Sigma) or Protein A sepharose-linked anti-Fkh1 antibodies [129]. The starting extract and immunoprecipitated proteins were examined by protein immunoblotting using either anti-FLAG (ANTI-FLAG M2 monoclonal,

Sigma) or anti-Fkh1 antibodies. Orc1 detected with an anti-Orc1 antibody [114] served as a loading control.

2.6.6 Fluorescence anisotropy

C-terminally His-tagged full length Fkh1 protein was expressed from a pET28b expression vector in Rosetta *E. coli*. *E. coli* were broken with modified B-PER (Thermo Fisher) diluted 1:1 in wash buffer (50 mM Tris pH 7.0, 5 mM $MgCl_2$, 5 mM ATP, 10% glycerol, 1M NaCl, 5 mM BME, 20 mM imidazole, protease inhibitors (Calbiotech)) with 1 mM EDTA. His-tagged Fkh1 protein was purified using nickel chromatography (Qiagen) and eluted in buffer (Wash buffer with 200 mM NaCl, 500 mM imidazole, and without ATP). Peptides (synthesized by the University of Wisconsin-Madison and the Tufts University Core Facility) were labeled on the N-terminus with 5-carboxy fluorescein and an aminohexanoic acid linker. Peptides (constant final concentration of 3 nM) were mixed with titrations of purified Fkh1-6xHis protein in binding buffer (50 mM HEPES pH 7.0, 200 mM KCl, 10% glycerol, 5 mM BME, 1 mM EDTA, 1 mM EGTA, 5 mM MgOAc, 0.02% NP-40, protease inhibitors (Calbiotech)). Polarization at each concentration was measured in triplicates in 384-well polystyrene black microplates (Thermo Fisher Scientific #262260) by a Biotek Synergy H4 multimode plate reader (light source: xenon flash, offset from top: 7 mm, sensitivity: 60 %, excitation: 485/20 nm, emission: 528/20 nm, both parallel and perpendicular, normal read speed). Fraction bound (Fb) at each concentration was calculated based on the corresponding polarization values (P): $Fb_c = (P_c - P_{min}) / (P_{max} - P_{min})$, where P_{min} is the polarization value of the no-protein control and P_{max} is the polarization value of the saturation value for that peptide. Dissociation constants (K_d) were derived by KaleidaGraph (version 4.1.3) using the following equation: $Fb = [protein] / ([protein] + K_d)$.

2.6.7 Mutation rate analysis and MMS assays

Mutation rates were calculated by fluctuation analysis as in [130]. Briefly, single colonies were inoculated into minimal media lacking arginine and grown overnight, diluted 1:10,000 and aliquoted into a 96-well plate. Cells were then incubated, without shaking, at 30°C for 2 days. 24 of the 96 samples were pooled and plated in triplicate to determine the number of viable cells. The remaining 72 samples were spotted onto 10x canavanine plates (minimal media lacking arginine + 0.6 g/L canavanine). Mutation rate was analyzed using FALCOR by the Ma-Sandri-Sarkar maximum likelihood method in which the data are fit to the Luria-Delbrück distribution [118]. For MMS assays, cells were grown to mid-log phase, diluted so that the OD_{600} was 0.5 and 10-fold serial dilutions were spotted onto YPD plates containing the indicated concentration of MMS. MMS plates were poured fresh on the day of each experiment. Plates were imaged three days after plating.

2.6.8 Mating-type switching assays

Donor preference during mating-type switching was determined by a PCR-based method as described in [60]. Briefly, cells were grown in YP-lactate medium to mid-log phase. Expression of the HO endonuclease was induced by addition of 2% galactose and incubated for one hour. Induction was stopped by the addition of 2% glucose and the cells were allowed to recover for 24 hours. DNA was then isolated using quick genomic DNA extraction [131] and PCR was used to amplify *MAT*α sequences using primers Yalpha105F and MAT-dist4R [60]. 700 ng of PCR DNA was then cut with *BamH*I and the resulting digest was run on an agarose gel. Relative densities of the different bands were determined using ImageJ [132], and donor preference (as *HML* usage) was calculated using the formula *MAT*α / (*MAT*α+*MAT*α-B).

Chapter 3

Summary and Future Directions

3.1 Summary

I have demonstrated that the phosphothreonine binding FHA domain of Fkh1 is involved in many Fkh1-protein interactions and likely governs most, if not all, Fkh1 biology. Fkh1 interacts with several proteins through its FHA domain, and these interactions require the phosphopeptide binding capability of Fkh1. Substitution of alanine for multiple different residues within the Fkh1 FHA domain also affects Fkh1 transcription. Doubling times in *fkh1* mutant yeast in a *fkh2*Δ background were significantly increased compared to *FKH1* yeast. This phenotype was not recapitulated by deletion of any single gene that I identified in my 2-hybrid screen as one that encoded a Fkh1-FHA interaction protein. These findings suggest that the Fkh1 FHA domain's role in the cell cycle may require interaction with an unidentified protein, or possibly multiple different protein partners. They also show that creating mutants in Fkh1 (such as the R80A mutant that is unable to interact with phosphopeptides) likely affects multiple different Fkh1-protein interactions and, therefore, multiple different Fkh1-related processes.

Further examination of the interaction between Fkh1 and one interacting protein, Mph1, demonstrated that these two proteins interact via a canonical FHA-phosphopeptide interaction. My data suggest that Mph1 contains two independent FHA binding motifs that are close together

within a small region of Mph1, each of which can be recognized by the FHA domain of Fkh1. Both of these FHA recognition motifs must be disrupted to abolish Fkh1-Mph1 binding. I was unable to assign a role for this interaction in any Mph1-associated genome maintenance roles, including resistance to DNA damaging agents and replication fork reversal (see Appendix A). However, I was also unable to rule out the possibility that the Fkh1-Mph1 interaction may also be involved in these processes.

The Fkh1-Mph1 interaction was important for regulating donor preference during mating-type switching. Disrupting this interaction via mutation of *MPH1* led to a change in donor preference, albeit one significantly less severe than that caused by mutation of *FKH1*. This result indicated that while the Fkh1-Mph1 interaction is involved in regulating donor preference, there must exist other Fkh1-protein interactions to fully explain the role of Fkh1 in this process. Deletion of another gene encoding a previously uncharacterized Fkh1-interacting protein, *YMR144W*, also led to a change in donor preference that was additive with deletion of *MPH1*. This result led us to name this gene *FDO1* for **F**orkhead one interacting protein involved in **do**nor preference. However, these two genes still do not fully explain Fkh1's role in regulating donor preference, indicating there must be additional proteins with which Fkh1 interacts to fulfill its role.

It is clear that the Fkh1 FHA domain interacts with multiple proteins to control multiple different processes. I have assigned a role in regulating donor preference to two distinct Fkh1-protein interactions, but Fkh1 must interact with additional as yet unidentified proteins to carry out this role. Additionally, I have shown that the FHA domain is important for Fkh1's role in the cell cycle (presumably through interactions with other proteins) but was unable to identify the partner protein(s) involved in this process. I have also identified additional Fkh1-FHA-protein interactions for which there is currently no assigned role. These results indicate that Fkh1 interacts with

multiple different proteins via the same interface to accomplish different goals. The identities of many of these proteins remain unknown. Identification of these proteins will aid in the characterization of the mechanisms involved in Fkh1 biology.

3.2 Characterizing the Fkh1-Fdo1 interaction and Fdo1's role in mating-type switching

3.2.1 Characterizing the Fkh1-Fdo1 interaction

I have shown that Fdo1 (formerly Ymr144w) plays a role in regulating donor preference during Fkh1-dependent mating-type switching. However, as little is known about any roles Fdo1 plays in cells an interesting future direction would be to further investigate its role in this process, as well as its interaction with Fkh1. Fdo1 interacts with Fkh1 and loss of this interaction in *fdo1*Δ cells is the likely cause of alteration in donor preference. However, I have not definitively shown that this defect is caused by a loss of interaction rather than being an indirect effect of loss of a different, as yet undefined, *FDO1* function. Therefore, it would be best to examine donor preference in a strain, similar to *mph1-2TA*, in which Fdo1 is still present but is unable to interact with Fkh1.

Fdo1 was previously found to interact with Fkh1 in an affinity-capture mass spectrometry screen, validating that this interaction likely occurs in cells [94]. I showed by 2-hybrid that this interaction depends on the phosphopeptide binding capability of Fkh1, suggesting that, like the Fkh1-Mph1 interaction, the Fkh1-Fdo interaction may be a classical FHA-phosphopeptide interaction. As a first step to engineering mutations in *FDO1* that abolish interaction with Fkh1 I would examine the need for threonines in Fdo1 by 2-hybrid. While many serines have been shown to be phosphorylated in this protein, no threonines have yet been found to be phosphorylated

[133,134]. The original region of Fdo1 pulled out of the 2-hybrid screen (amino acids 98-342) contains 18 threonines (Figure 3-1). Of these threonines only one, T288, has a glutamate at the +1 position, which I have shown to be important for Fkh1 interaction with Mph1. I would start by substituting alanine for this threonine to see if interaction with Fkh1 is weakened or lost. A region containing the Fkh1 FHA domain (amino acids 50-202) was found to not be sufficient for interaction with Fdo1. This could indicate that the interaction is more complicated than a simple FHA-pT interaction, similar to the way the Ki67 FHA domain interacts with a longer phosphopeptide through the canonical FHA-pT interface and an additional interface on the Ki67 FHA domain [45]. However, it is also possible that the Fkh1-Fdo1 interaction is weak enough that small differences in protein abundance or stability in the 2-hybrid assay affect the ability to grow on selective media. If T288 is not essential for the Fkh1-Fdo1 interaction I would use the 2-hybrid assay to further narrow down the interaction region of Fdo1 to simplify the search for relevant threonines, as well as attempt to better define the regions of Fkh1 necessary for interaction.

In addition to defining a possible threonine within Fdo1 required for interaction for Fkh1 I will tag Fdo1 so co-immunoprecipitation experiments can be performed in yeast with wild-type and any mutant versions of the protein. These experiments will provide validation for any results found in the 2-hybrid assays as well as provide a valuable tool for examining the interaction under different conditions in yeast. I was able to observe the Fkh1-Mph1 interaction by co-immunoprecipitation using extracts derived from asynchronously growing yeast. It is possible that I may observe the same result for the Fkh1-Fdo1 interaction. Alternatively, I may only be able to observe the interaction in cells in which a double strand break has been generated by induction of the HO endonuclease or other means. It is also possible that I will see binding in extracts derived from asynchronous cultures but that this interaction will be enhanced in the presence of a double

```
  1 MEENKLSGNK PIQLATWSNQ MGSPENNGNN ANNGSDVQNV IQKALGLIRQ LNNNGLMSPM
 61 EEEHSQPSSS QETLSVDREI NEQGRLRLLM QAKDDNTRKE VGTYSSPMDS AYARENMLNV
121 LQSLVTHLNQ AVSQIQQLKF KNMILTSNEN NIQSRHEVED NLQKQQFERM KCQFLLERQS
181 LKDQLRKREN KIVKYKQKII EKNKKLNNLA KVLNQHAISD TSQIDSFSSS VKKTPSSTTT
241 PQEMKSDMLN TLGILATHVL KDEIDDDSGN QTILQLAAGS ISNDCNTTEL EITCSPEMGR
                                    *
301 TITHNRPNTK DESIQDSHGN RTLQLPKMKS FSTIDGSIKD IK
```

Figure 3-1. Primary amino acid sequence of Fdo1. Interaction with Fkh1 occurs through amino acids 98-342 (shown in italics). This region contains 18 threonines (shown in bold). Known phosphorylation sites (on serines) and ubiquitination sites (on lysines) are underlined in red [133,134]. T288 is marked with a red asterisk.

strand break. This would indicate that the interaction is regulated by events that take place following DNA damage. This may also be the case for the Fkh1-Mph1 interaction and would be worth examining. Interaction could also be observed in live cells before and after induction of a double strand break by high-resolution confocal microscopy in strains expressing Fkh1 and Fdo1/Mph1 that have been tagged with fluorescent proteins.

3.2.2 Examining the role of Fdo1 in DNA repair and DSB biology

Mph1 was a good candidate for a Fkh1 partner protein involved in mating-type switching as it was already known to localize to double strand breaks and have a role in DNA repair [89,115,120]. Unlike Mph1, Fdo1 has not been shown to play a role in any form of DNA repair and its localization upon induction of a double strand break has not been reported. To examine the localization of Fdo1 upon induction of a double strand break I would perform chromatin immunoprecipitation experiments before and after induction of a double strand break at the *MAT* locus. Fluorescence microscopy techniques could also be applied to examine Fdo1 localization in strains expressing Fdo1 that has been tagged with a fluorescent protein and a protein known to localize to DSBs and form foci, such as Rad52, tagged with a different fluorescent protein. Co-localization of the two proteins could then be assessed by microscopy. This technique could be used to examine Fdo1 localization in real time in live cells.

3.2.3 Examining the role of Fdo1 in other areas of Fkh1 biology

I have shown that Fkh1 interacts with Mph1 and Fdo1, and likely many additional proteins, to regulate donor preference during mating-type switching. However, Fkh1 must also, presumably, interact with proteins to accomplish its functions in other areas of biology, including transcription

and DNA replication. Thus far, Fdo1 has no known roles in either of these processes. However, genome-wide studies indicate that levels of *FDO1* mRNA increase upon exposure to hydroxyurea, a DNA replication inhibitor that induces a replication checkpoint [135,136]. Additionally, expression of *FDO1* is cell cycle regulated such that it is more highly expressed during S-phase [4,135]. These results indicate that Fdo1 may play a role in DNA replication. It would be interesting to note if this role is in any way related to the role Fkh1 plays in this process. There are many techniques currently and previously in use in the Fox lab which could be used to observe the effects of *FDO1* mutation on DNA replication timing/efficiency.

3.3 Examining a possible role for CK2 in the Fkh1-Mph1 or Fkh1-Fdo1 interactions

The Haber lab has demonstrated that the essential CK2 kinase is necessary for Fkh1 function in donor preference during mating-type switching [60]. Whereas wild type cells in the Fkh1-dependent mating-type switching assay choose *HML* as a donor ~90% of the time, cells expressing a temperature sensitive CK2 kinase choose *HML* only ~40% of the time. While this reduction in *HML* usage is not as great as that seen upon mutation of Fkh1 (~10% *HML* usage), the data provide evidence that the CK2 kinase plays a critical role in this process. I have shown that Fkh1 is able to interact with Mph1 through one of two threonine residues. Disrupting this interaction by substituting alanine for both threonines (*mph1-2TA*) reduces *HML* preference to ~80%, a 10% reduction. The amino acids surrounding these threonines in Mph1 are highly acidic, similar to other CK2 target sites [119]. To determine if CK2 does phosphorylate Mph1, donor preference can be measured in *mph1-2TA* CK2 mutant yeast. If CK2 does phosphorylate these threonines, then mutation of *MPH1* should not further alter donor preference in a CK2 mutant background. Additionally, co-immunoprecipitation of Fkh1 and Mph1 should be reduced or

abolished in CK2 mutant yeast. The same experiments could be performed in *FDO1* mutant yeast to examine the requirement for CK2 in the Fkh1-Fdo1 interaction.

3.4 Identification of new Fkh1-FHA interaction partners

3.4.1 Rationale

As summarized above, the data I have shown in Chapter 2 demonstrate that a specific Fkh1-FHA-Mph1 interaction plays a role in regulating mating-type switching. However, this interaction does not fully explain the Fkh1 FHA domain's role in mating-type switching or its role in regulating cell cycle transcription. There must be additional, as yet unidentified, protein partners that account for these discrepancies. Additionally, Fkh1 is involved in regulating the activation timing of DNA replication origins [20,69–71,137]. The mechanisms by which Fkh1 regulates this process are unknown and may also involve important FHA-protein interactions. Therefore, defining the Fkh1-FHA-interactome will reveal insights essential to understanding this conserved protein's multipronged role in chromosome structure and function.

The approach many have used for characterizing FHA domains is to perform binding experiments using a peptide library to define the specificity of a given FHA domain. While this approach is useful for general characterization of FHA domains, and to aid in the identification of relevant threonines within known partners, it does not aid in the identification of new protein partners. The results of these peptide binding experiments often show a modest preference for a certain amino acid at one position (i.e. the pT+3 position). With this limited information it is nearly impossible to identify binding targets in the genome with any confidence, as multiple proteins with the identified motif are likely encoded in the genome and many, if not most, likely do not interact

with the FHA domain of interest. To attempt to narrow down the search by only looking at proteins shown to be phosphorylated on the relevant threonines might be misleading due the fact that many phosphorylation sites likely remain uncharacterized. Additionally, because many FHA-protein interactions may be dynamic and involve large semi-stable macromolecular complexes, standard protein-protein interaction approaches have not identified many direct Fkh1 FHA domain partner proteins to date. Therefore, an approach which can simultaneously identify new and existing interaction partners and the relevant threonines required for binding Fkh1 would be ideal.

3.4.2 Phosphoproteomics approach for identifying new Fkh1-FHA partners

To identify new FHA domain interaction partners, the Matrix-Assisted Reader Chromatin Capture (MARCC) method developed in the Denu lab and phosphoproteomic methods developed in the Coon lab could be adapted to define yeast phosphopeptides that bind Fkh1 [138–140] (method schematic shown in Figure 3-2). The identities of interacting phosphopeptides would allow for rapid identification of putative direct Fkh1-FHA interaction partners and simultaneously provide target threonines for mutagenesis. As many of the proteins involved in Fkh1-related functions (such as Mph1) are multifunctional proteins involved in many processes, it is difficult to determine the exact role of an interaction using null alleles alone. Therefore the identification of the exact threonine required for interaction is crucial. Creating a targeted disruption of the FHA-protein partner interface allows a targeted disruption of a discrete cellular role, leaving other known roles unperturbed. Thus the biological role(s) of any putative direct Fkh1-FHA-partner could be rapidly assessed.

Two different Fkh1-FHA domains would be purified from *E.coli* and used in affinity resins for yeast phosphopeptide purification: WT-FHA and Mutant-R80A-FHA. R80A destroys the

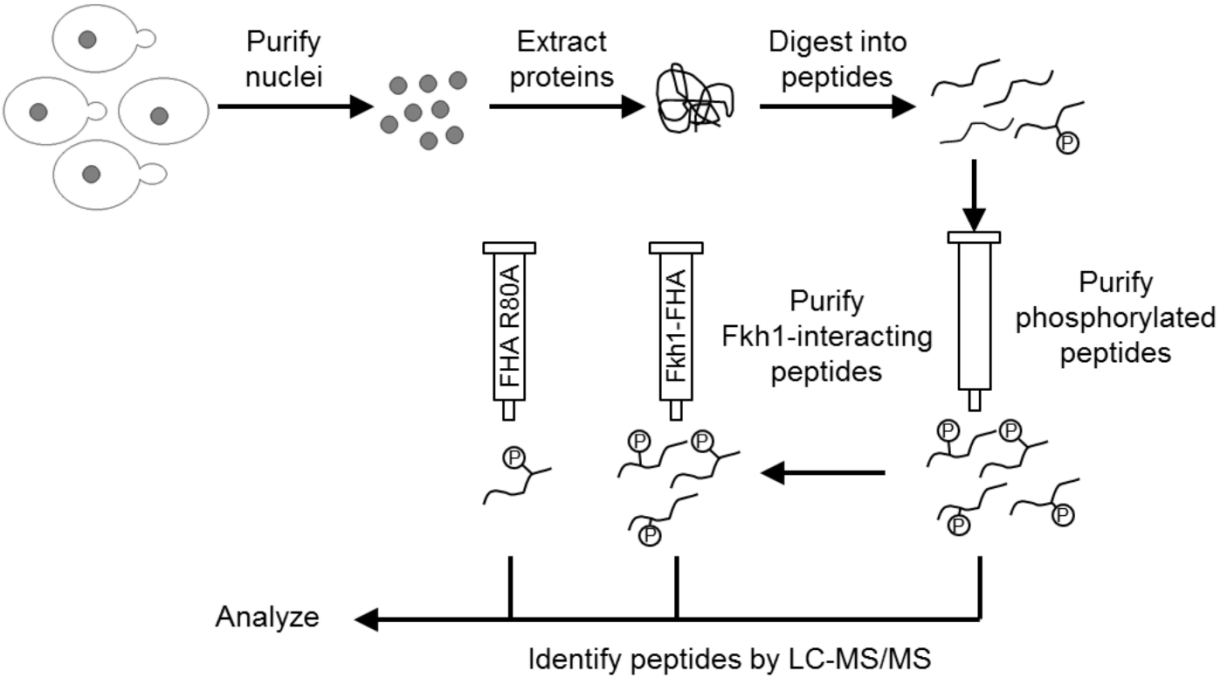

Figure 3-2. Phosphoproteomics approach for purifying Fkh1-FHA-interacting peptides.

phosphothreonine binding pocket in FHA domains and would serve as a negative control [27,37]. To generate a pool of endogenous phosphopeptides for experimentation, yeast protein extracts could be proteolytically digested with trypsin and phosphorylated peptides could be purified using immobilized metal affinity chromatography [140]. These samples would then be split and incubated with WT-FHA affinity resin or Mutant-R80A-FHA resin. Quantitative high resolution nano-LC-MS/MS analysis of the purified phosphopeptides could then be performed. The mass spectral analysis would be used to identify bound phosphopeptides, localize the phosphoryl modification to a single amino acid, and provide quantitative information on the relative amount of each phosphopeptide sequence bound to the WT-FHA resin compared to the negative control resin. These steps would identify phosphopeptide sequences that bind to the WT-FHA domain with specificity and statistical significance. The data these experiments would generate would define candidate protein partners as well as the relevant threonines to target for substitution *in vivo*. Florescence anisotropy on selected phosphopeptides from the bound and unbound fractions would be performed as a quality control measure to test the selectivity for target peptides.

The interacting peptides most relevant to Fkh1-FHA function may be in low abundance. This may be due to low abundance of the interacting protein generally. Additionally, some of these interacting proteins may only be phosphorylated on the relevant threonines at specific stages of the cell cycle or after a specific cellular event, such as the formation of a double strand DNA break. These factors increase the challenge to isolating and detecting these peptides. Thus extracts could also be made from arrested cell cultures or otherwise manipulated cells to enhance the concentration of relevant interacting partners. Peptides could also be purified from nuclear extracts, chromatin-enriched extracts or Fkh1-enriched fractions to increase the likelihood of isolating and detecting Fkh1-FHA interacting peptides.

3.4.3 Potential for contribution to new and existing projects

This technique has the potential to identify multiple new Fkh1 protein partners of great interest to the Fox lab. The lab has experience studying multiple different Fkh1-related biological areas including mating-type switching and DNA replication. Several assays for *FKH1* function that have been performed in the lab could be used to define the cellular roles represented by individual Fkh1-FHA interactors identified in the phosphoproteomics screen.

As the data presented in Chapter 2 suggest, Fkh1 likely requires interaction with multiple proteins via its FHA domain to carry out its function in regulating mating-type switching. The identification of additional protein partners required for Fkh1 function in mating-type switching would solidify this hypothesis and strengthen our knowledge of how Fkh1 regulates donor preference. Peptides could be purified after induction of a double strand break at the *MAT* locus to increase the chances of identifying a relevant partner protein. If new protein partners are identified that play a role in mating-type switching, studies can be conducted to further elucidate the roles of these proteins. Some of these proteins, as is the case for Fdo1, may not previously have been characterized as playing a role in DNA repair. Localization of these proteins after the induction of a double strand break can be assessed through chromatin immunoprecipitation or fluorescence microscopy assays to determine if/when they are recruited to double strand breaks.

The Fox lab is particularly interested in the DNA replication field. Fkh1 has been shown to be involved in regulating replication timing, but the exact mechanisms of this regulation remain elusive [20,69–71,137]. Several models for how Fkh1 regulates timing have been proposed, but there is little supporting evidence for any of these models yet and no indication of what regions of Fkh1 are most critical. It seems reasonable to propose that the FHA domain is important for this function. The identification of new interaction proteins involved in DNA replication would be an

important step in characterizing the mechanisms by which Fkh1 regulates this process. Fkh1 binds to origins in G1 phase, suggesting that Fkh1's role in regulating replication occurs in this phase [20]. Therefore, peptides purified from G1-arrested cultures or from purified DNA replication components may be used to increase the chance of detecting partner proteins relevant to DNA replication. Newly identified partners could then be mutated on the relevant threonines and various replication assays could be performed to determine any defects caused by these mutants. Many different experimental approaches, such as ARS assays and 2D gel electrophoresis, could further define the role that Fkh1 and its partner proteins play in DNA replication.

3.5 Expansion of phosphoproteomics approach for other FHA domains

3.5.1 Rationale

FHA domains act as signaling modulators that transduce information by forming specific phosphothreonine-dependent protein-protein interfaces that in turn control specific cellular responses. However, because FHA-protein interactions are often components of signaling cascades, they are likely transient and/or part of large protein complexes. For these reasons the identities of many proteins that function as direct interaction partners of FHA domains remain unknown. The phosphoproteomics approach proposed to identify new Fkh1-FHA interactors could be expanded to assess the roles of the other FHA domains in yeast (15 FHA domains in 14 different yeast proteins [141–143]), or any FHA domain from any species, and thus develop into a high throughput proteomics project. Given the conservation and obvious biological relevance of FHA domains, this work has the potential to be of transformative value to multiple fields.

3.5.2 Identification of FOXK1 interacting proteins in human muscle cells

FOXK1 is a human ortholog of yeast Fkh1. FOXK1, unlike other Fkh1 orthologs in humans, contains an FHA domain. FOXK1 is required for the proliferation of muscle stem cells and muscle generation [83,84]. A recent study provides evidence for a central role for FOXK1 in mTOR-signaling-controlled transcriptional regulation of autophagy genes [85]. While autophagy research has traditionally focused on cytoplasmic events, it is now clear that highly regulated nuclear events, including major epigenetic changes at autophagy genes, are equally critical. The responsiveness of FOXK1 molecular behavior to mTOR signaling leads to the postulate that interactions between it and partner proteins is important for proper cellular control of autophagy. The role of the FOXK1 FHA domain in this process thus far remains unknown.

To examine the role of the FOXK1 FHA domain in regulating autophagy genes, siRNA knockdowns of FOXK1 and rescue experiments with wild-type and FHA domain-mutant siRNA resistant FOXK1 transgenes could be performed and expression of key autophagy genes could be examined. These experiments would be performed in C2C12 myoblasts, a common cell line used in studies of skeletal muscle cell behavior. It is possible that the FOXK1 FHA domain is important to all of FOXK1's behaviors in controlling the autophagy program. If true, then the Mutant-FHA-FOXK1 would likely be incapable of repressing autophagy genes regardless of mTOR signaling status. Alternatively, Mutant-FHA-FOXK1 may still bind promoters and even repress autophagy genes, but fail to respond to mTOR signaling and leave the nucleus. If true, basal autophagy gene repression would be unaffected but FOXO3-induction of autophagy gene expression would be perturbed.

If the FHA domain is found to be necessary for regulation of autophagy genes, the phosphoproteomics approach developed for yeast Fkh1-FHA could be used to characterize the

FOXK1-FHA-interactome. WT-FOXK1 and Mutant-FHA-FOXK1 proteins would be expressed and purified, and phosphopeptides prepared from extracts of C2C12 cells would be analyzed for binding to these proteins following the approach developed for yeast Fkh1. Protein partners of FOXK1-FHA identified in the phosphoproteomics approach would be examined for their roles in mTOR-regulated autophagy gene expression and FOXK1 molecular behavior using standard siRNA approaches and assays.

Appendix A

Role of the Fkh1-Mph1 interaction in DNA repair and protection against DNA damaging agents

A.1 Introduction to Mph1

Mph1 is a multifunctional DNA helicase that plays a role in many genome maintenance processes. It was first discovered as a deletion mutant that caused an increase in basal mutation rate [144]. Mutants are sensitive to multiple DNA damaging agents including MMS, EMS and 4-NQO [89,115]. Mph1 is able to unwind many different DNA structures *in vitro* (Table A-1), suggesting it may play multiple roles in DNA damage repair and protection. The human homolog of Mph1, FANCM, is one of 17 members of the Fanconi Anemia (FA) group of proteins found to be mutated in human patients with FA, a condition characterized by bone marrow failure, congenital abnormalities and predisposition to cancer [145]. FANCM and Mph1 carry out many of the same biochemical activities (Table A-1). Therefore Mph1 can serve as a model for FANCM function and possibly regulation.

Mph1 activity has been shown to promote or inhibit different mechanisms of DNA repair. For example, Mph1's ability to catalyze displacement loop (D-loop) dissociation affects the rate of crossover during double strand break repair [120]. This dissociation prevents double Holliday

Table A-1. Biochemical activities of Mph1 and FANCM. Adapted from [96].

DNA substrate	Activity	Mph1	FANCM	*In vivo* implications	Reference
Triple helix 	Translocase	ND	✓	Translocate along dsDNA	[146]
3’ overhang 	Unwinding	✓	×	3’ to 5’ DNA helicase	[146,147]
Flap 	Unwinding	✓	×	Lagging strand unwinding	[148]
Movable replication fork 	Fork reversal	✓	✓	Replication fork repair	[99,148,149]
Movable Holliday junction 	Branch migration	✓	✓	Replication fork repair	[99,148,149]
σ structure 	Branch migration	✓	✓	Replication fork repair	[148,149]
Synthetic D-loop 	D-loop unwinding	✓	×	Crossover control	[120]
D-loop 	D-loop dissociation	✓	✓	Crossover control	[120,149]

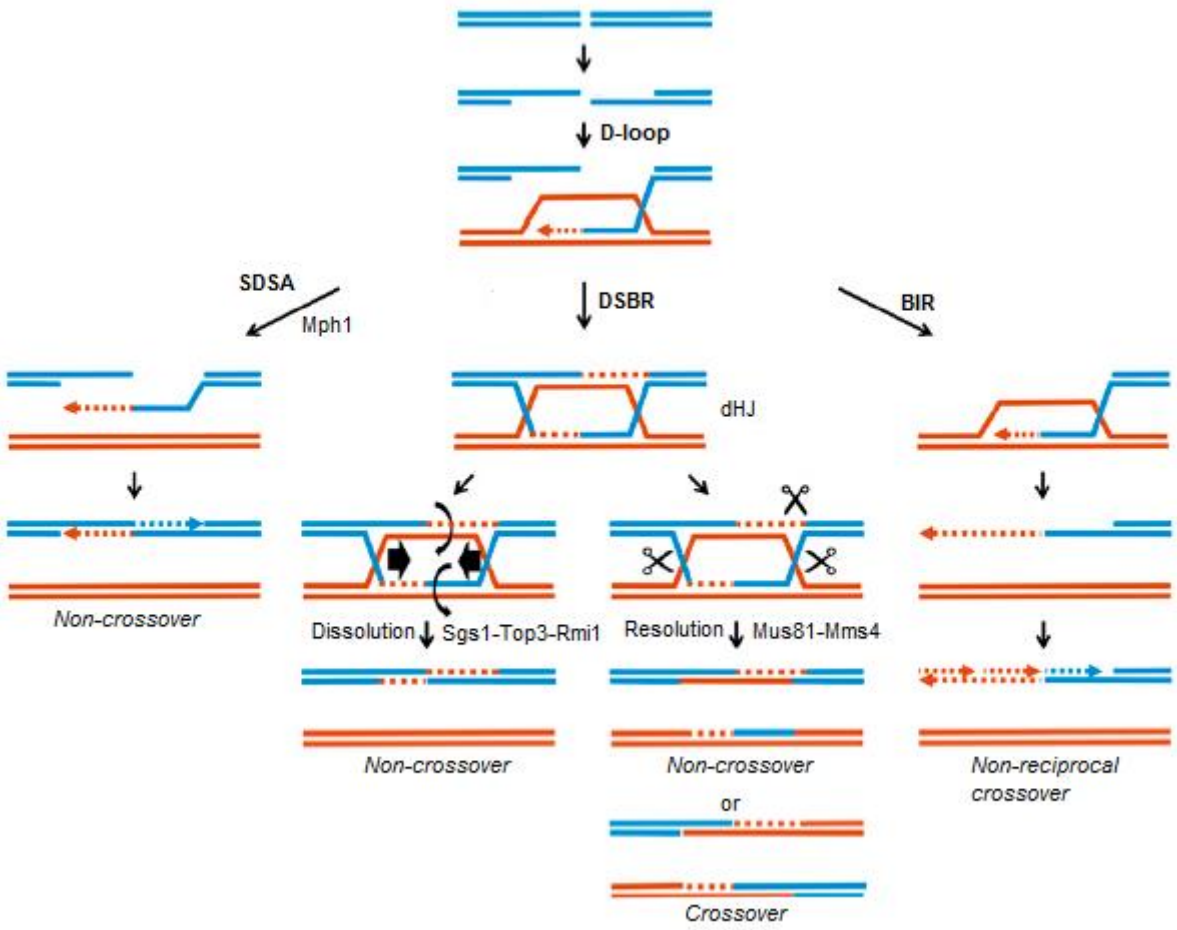

Figure A-1. Double strand break repair pathways in yeast. Mph1 promotes the synthesis dependent strand annealing (SDSA) pathway of double strand break repair, which can only result in non-crossover products. A double Holliday junction can be repaired through dissolution, an unwinding of the dHJ structure by Sgs1, or resolution, in which the dHJ is cut by The Mus81-Mms4 endonuclease. Resolution can lead to crossover events. Break-induced repair (BIR) leads to non-reciprocal crossover and loss of heterozygosity. Modified from [150].

Junction (dHJ) formation and promotes the synthesis-dependent strand annealing (SDSA) pathway of homologous recombinational repair, a pathway that does not produce crossovers (Figure A-1) [122]. D-loop dissociation also inhibits break-induced repair (BIR) at double strand breaks, a process that results in non-reciprocal crossover and loss of heterozygosity [151]. Additionally, Mph1 has recently been implicated in the Recombination Execution Checkpoint (REC) [152]. The REC regulates the choice between standard double strand break repair (DSBR) and BIR based on the homology status of the double strand break ends [153]. If homology is only present for one DNA end, or if the homologous regions for both ends are situated far away or in the wrong orientation, DSBR is blocked and ultimately BIR will be the chosen repair pathway after a significant delay. Deletion of *MPH1* disrupts this checkpoint mechanism and results in reduction in the delay and a preference for DSBR [152]. Whether Mph1 is involved in sensing the homology status of the DNA ends or if its role in dissociating D-loops can fully explain its role in the REC is unknown. Regardless, regulation of Mph1 function has important implications for cellular outcomes after DNA damage.

A.2 Examining the role of the Fkh1-Mph1 interaction in MMS resistance

A.2.1 Background

Deletion of *MPH1* leads to multiple defects related to DNA repair in the cell and produces multiple observable phenotypes. One of the most straight forward phenotypes to assay is sensitivity to DNA damaging agents. Fkh1 has not been implicated previously in protection against DNA damage, so any sensitivity to DNA damaging agents would be a new phenotype observed. As a first step to examine whether the Fkh1-Mph1 interaction is contributing to any of the DNA

repair roles in which Mph1 has been implicated *FKH1* mutant yeast and *MPH1* mutant yeast that do not interact with Fkh1 (*mph1-2TA*) were assayed for sensitivity to the DNA damaging agent MMS.

A.2.2 Deletion of FKH1 *confers sensitivity to MMS*

Unlike *mph1*Δ cells, *mph1-2TA* cells are not sensitive to MMS (Figure A-2A), suggesting that interaction with Fkh1 is not required for protection against MMS-induce damage. However, *fkh1*Δ cells were mildly sensitive to MMS at higher concentrations. Whether or not this sensitivity was additive with that of *mph1*Δ cells was difficult to determine, as *mph1*Δ cells were much more sensitive to MMS. Fkh1 interacts with Mph1 through its FHA domain. Consistent with the result seen with *mph1-2TA,* both *fkh1-fha*Δ and *fkh1-R80A* (a mutant that abolishes Fkh1-Mph1 binding) yeast were not sensitive to MMS (Figure A-2B). Interestingly, cells lacking the Fkh1 DNA binding domain (*fkh1-dbd*Δ) were also not sensitive to MMS.

That the DNA binding domain of Fkh1 can be dispensed without causing MMS sensitivity suggests that loss Fkh1 transcriptional activity is not the cause of MMS sensitivity in *fkh1*Δ cells. However, it is possible that in cells lacking the Fkh1 DBD Fkh2, a Fkh1 paralog that is able to carry out many of the same functions, is able to substitute for some Fkh1 function. Therefore it is possible that sensitivity to MMS in *fkh1*Δ cells is due to a change in transcriptional activity. This transcriptional activity would also have to be independent of the Fkh1 FHA domain, as deletion of this domain also does not lead to MMS sensitivity. I have shown that FHA function is important for Fkh1-regulated transcription, but cannot fully explain its role (see Chapter 2). There is evidence that Fkh2 is able to interact with some partner proteins that regulate transcription through the N-terminus in a region outside of the FHA domain [22], so this fkh1-fhaΔ protein may still be able

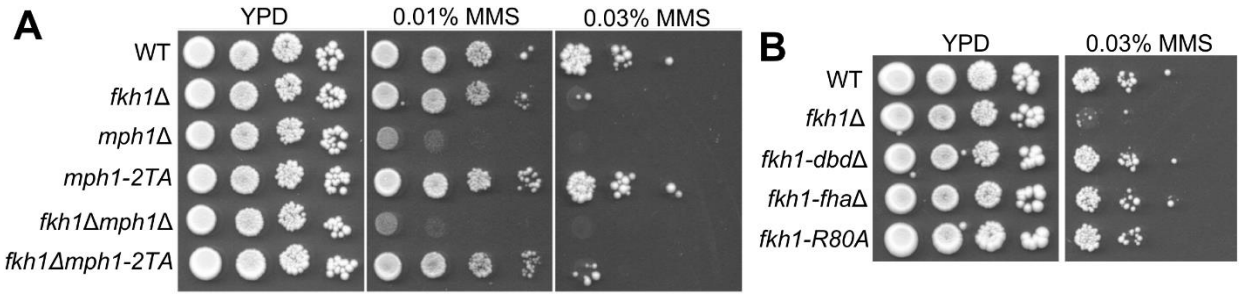

Figure A-2. Sensitivity of *MPH1* and *FKH1* mutants to MMS. (**A-B**) Chronic exposure MMS assay.

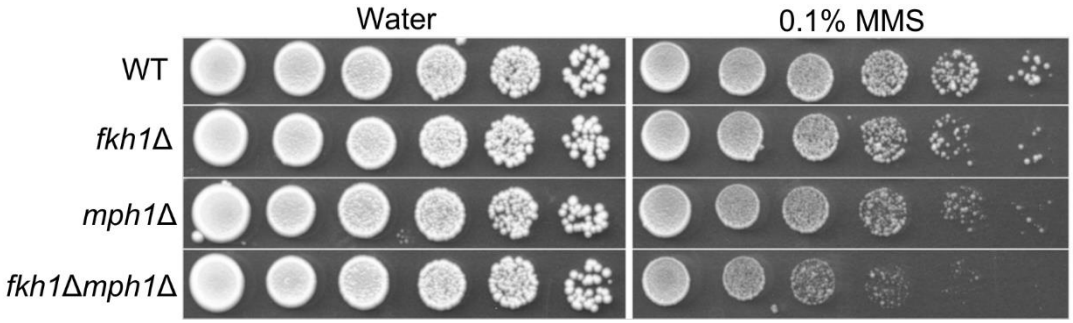

Figure A-3. Sensitivity to MMS in *FKH1* and *MPH1* mutants is additive. Acute exposure MMS assay.

to partially function in transcriptional regulation. Another possible explanation is that Fkh1 binds and sequesters some partner protein through a region outside of the DBD or FHA domain and loss of Fkh1 increases the available concentration of this protein, leading to MMS sensitivity.

A.2.3 fkh1Δ and mph1Δ MMS sensitivity is additive

The epistasis between *FKH1* and *MPH1* mutants under chronic MMS treatment conditions is difficult to assess due to the much higher sensitivity seen in *MPH1* mutants. To better assess the epistatic relationship between *FKH1* and *MPH1*, cells were acutely treated with MMS and assayed for viability. Under acute treatment conditions deletion of *FKH1* and *MPH1* produced similar results, both showing a mild MMS sensitivity phenotype (Figure A-3). Deletion of both *FKH1* and *MPH1* led to a higher degree of MMS sensitivity than deletion of either gene alone. These results suggest that sensitivity to MMS in cells lacking *FKH1* is not likely due to a loss of interaction with Mph1.

A.3 Possible role for Fkh1 in MMM complex

A.3.1 Identification of an Mph1-containing complex involved in ICL repair

Interstrand crosslinks (ICLs) are among the most toxic types of DNA lesions a cell can experience. It has been estimated that even a single unrepaired ICL can kill a yeast cell [154]. To avoid such catastrophic effects, cells contain multiple networks that are able to repair these lesions. The human homolog of Mph1, FANCM, has been shown to be involved in the repair of these DNA lesions [146], however *MPH1* mutants are not sensitive to ICL agents due to the presence of other ICL repair pathways in yeast. Three epistasis groups have been implicated in ICL repair

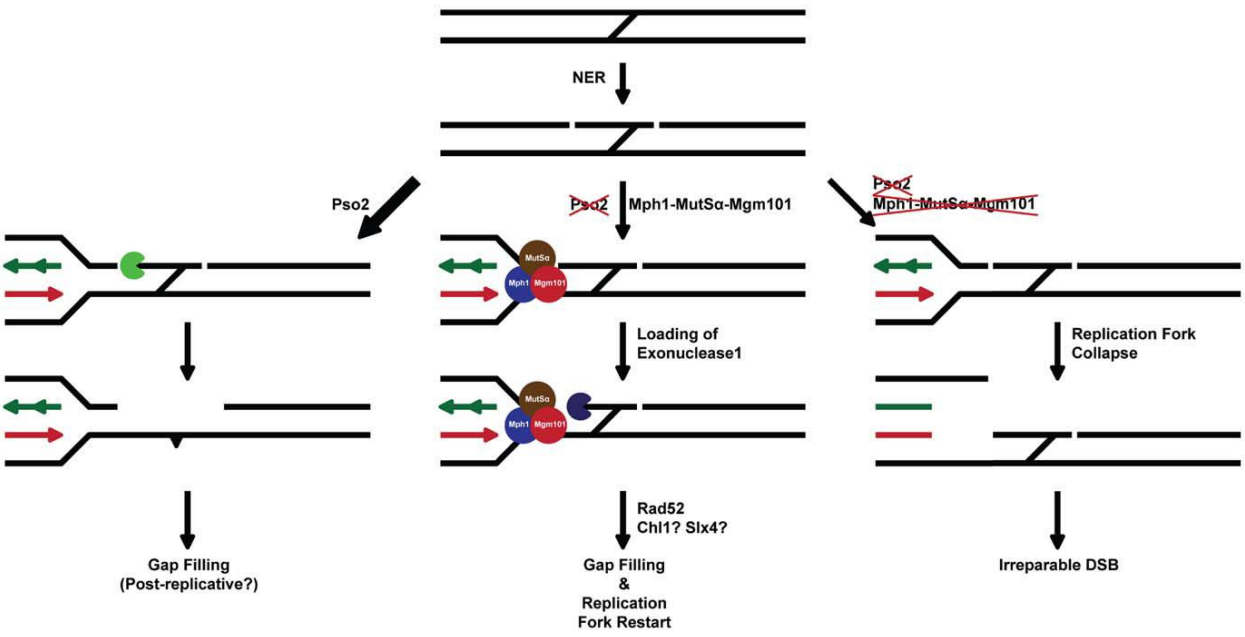

Figure A-4. A model for two ICL repair pathways in yeast. In the absence of Pso2, the MMM (Mph1-MutSα-Mgm101) complex acts as a secondary pathway to repair ICLs. Exo1 acts as the nuclease that degrades the lesion after which the gap is repaired by the HR machinery. From [155].

in yeast – *PSO2*, *RAD52*, and *RAD18* [156]. The precise role that Pso2 plays in this process is not yet worked out in detail, but existing evidence suggests that the Pso2 nuclease is required to degrade the ICL after it has been excised from one strand by other endonucleases [155]. After the ICL has been removed the gap is filled by the post-replicative repair machinery. Although *MPH1* mutants are not sensitive to ICL agents in wild type cells, deletion of *MPH1* does increase sensitivity in *PSO2* mutants, suggesting that Mph1 plays a role in a redundant ICL repair pathway [155]. In fact, Mph1 was found to associate with a complex, which includes Mgm101 and MutSα, that acts upstream of homologous recombination proteins Rad51 and Rad52 in repair of ICLs in the absence of Pso2 (Figure A-4).

A.3.2 Role of the Fkh1-Mph1 interaction in ICL repair is unclear

This Mph1-MutSα-Mgm101 complex was identified after a genome-wide search for proteins that interact with Mgm101. In addition to Mph1 and MutSα, Fkh1 was identified as an Mgm101-interacting protein. To examine whether Fkh1 may play a role in ICL repair, the sensitivity of *MPH1* mutant yeast that are unable to interact with Fkh1 (*mph1-2TA*) to the ICL agent nitrogen mustard (mechlorethamine, or HN2) was examined. After repeated attempts I was unable to replicate published results showing that deletion of *MPH1* increases HN2 sensitivity in a *pso2*Δ or *rad18*Δ background (Figure A-5A) [155]. I found sensitivity to HN2 in all strains to be much higher than what has been previously published, making experiments using high concentrations of HN2 difficult to perform due to the low survival rates. At 100 μM HN2 *pso2*Δ*mph1*Δ strains were more sensitive than *pso2*Δ strains, however this trend failed to hold at higher concentrations (Figure A-5B). *pso2*Δ*mph1-2TA* strains had a survival rate after exposure to 100 μM HN2 that was in between that of *pso2*Δ and *pso2*Δ*mph1*Δ strains, suggesting it may

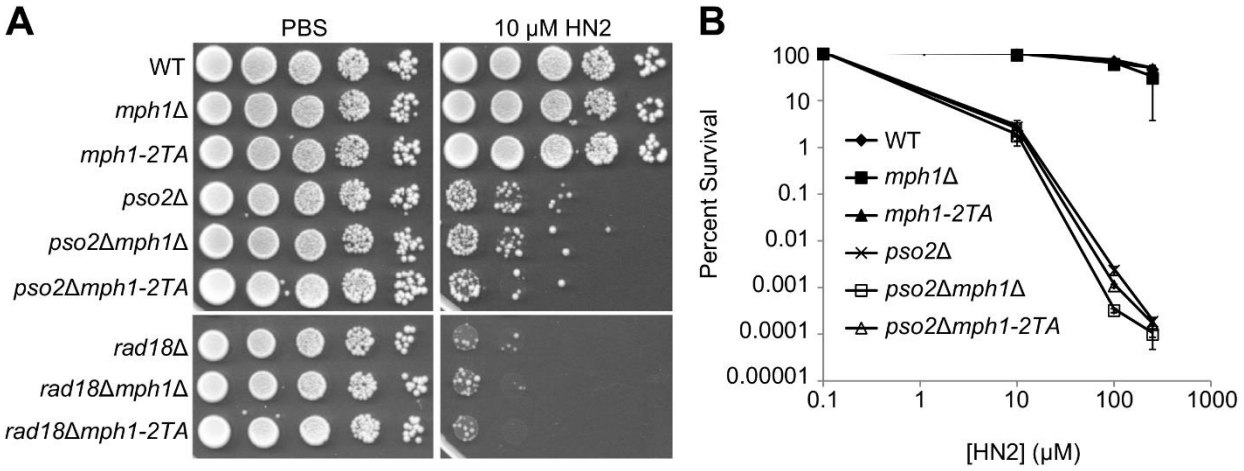

Figure A-5. Sensitivity of *MPH1* mutants to HN2. (**A**) Acute exposure HN2 spot assay. (**B**) Acute exposure HN2 survival curve.

have a slight defect in ICL repair. However, as I was unable to replicate published results it is difficult to conclude anything from the results I obtained.

A.4 Potential regulation of Mph1 fork reversal activity by Fkh1

A.4.1 Regulation of Mph1 fork reversal activity by Smc5/6 and Mhf2

Many proteins have been shown to bind Mph1 and regulate its activity. Most of these interactions occur through the C-terminal region of Mph1, the same region that Fkh1 binds. For example, Mph1 is known to interact with the Smc5/6 complex through direct binding to Smc5 [125]. This binding mainly occurs through amino acids 751-810, a region of Mph1 that overlaps with the Fkh1-interacting region (~amino acids 772-789) [98]. Deletion of *MPH1* rescues the lethality of mutants in the Smc5/6 complex [125], suggesting that Smc5/6 may play a role in attenuating Mph1 functions which result in negative outcomes. Indeed, it has recently been shown that the Smc5/6 complex specifically inhibits Mph1's replication fork reversal activity [99] (Figure A-6). Without attenuation of this biochemical activity excess fork reversal leads to an accumulation of toxic DNA intermediates and ultimately cell death. The histone fold complex, MHF, also binds to Mph1, relieving inhibition of fork reversal activity caused by Smc5/6 binding [100]. Interestingly, neither Smc5/6 nor the MHF complex affect the ratio of crossovers to non-crossovers during double strand break repair, showing that their regulation of Mph1 is specific to fork reversal activity and not D-loop dissociation [99,100].

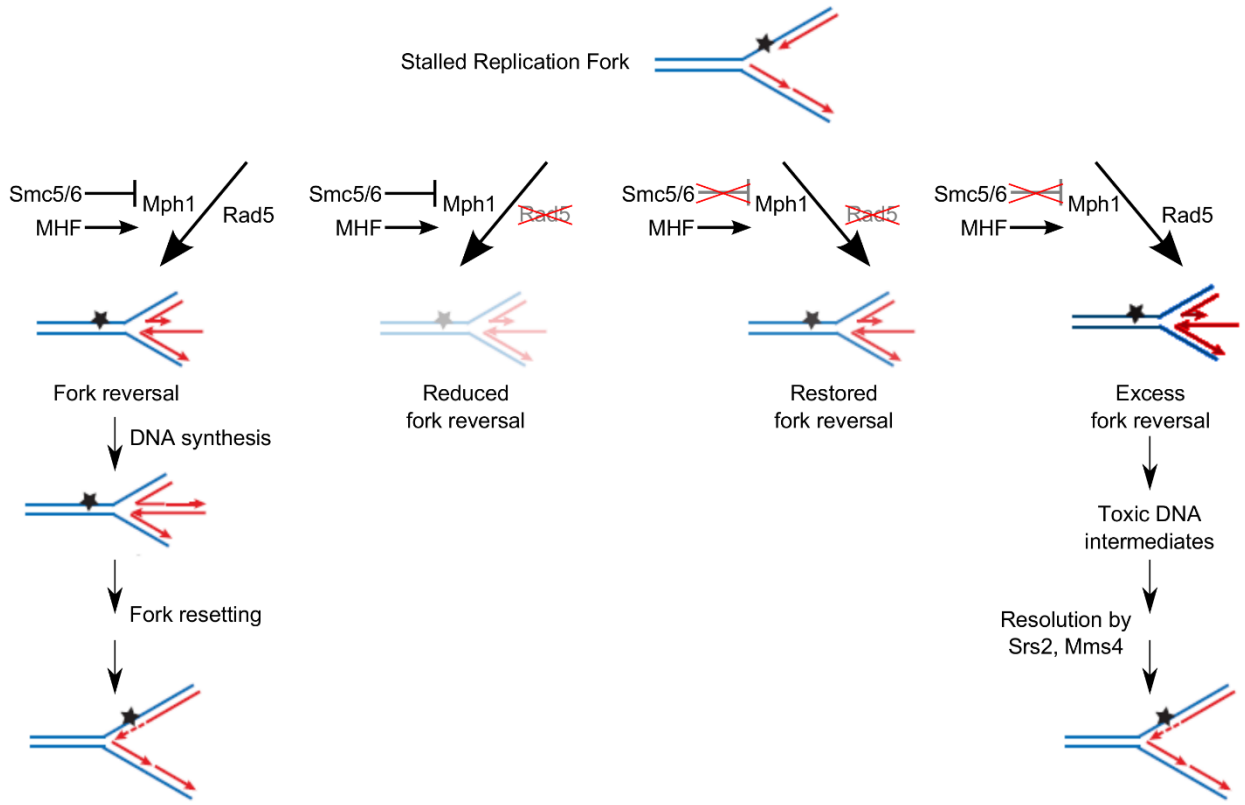

Figure A-6. Function and regulation of Mph1 and Rad5 in replication fork repair. Modified from [96] with information from [99]. Loss of Rad5 replication fork reversal activity leads to a reduction in fork reversal and increased sensitivity to DNA damaging agents. Releasing Smc5/6 inhibition of Mph1 through mutation of *MPH1* partially compensates for the loss of Rad5 fork-reversal. Releasing Smc5/6 inhibition of Mph1 in cells expressing *RAD5* leads to excess fork reversal and the buildup of toxic DNA intermediates that are resolved in part by Srs2 and Mms4.

A.4.2 Examining the role of the Fkh1-Mph1 interaction in regulating Mph1 fork reversal activity

These observations raised the possibility that Fkh1 competes for Mph1 binding with Smc5/6 or the MHF complex and perhaps also regulates the biochemical activity of Mph1. Like Mph1, the DNA helicase Rad5 is also able to catalyze replication fork reversal [157]. Only Mph1 and Rad5 are known to have this catalytic activity in yeast. For this reason, mutation or removal of both *MPH1* and *RAD5* causes extreme sensitivity to DNA damaging agents [115]. However, a strain expressing a mutant version of Mph1 that is unable to interact with Smc5/6 (*mph1*Δ*S1*) partially rescues the MMS sensitivity phenotype seen in a *RAD5* mutant in which Rad5 is unable to catalyze fork reversal (*rad5-DEAA*). This allele of *MPH1* is able to compensate for the loss of Rad5 replication fork reversal activity due to its increased ability to catalyze replication fork reversal without the inhibition of Smc5/6 (Figure A-6) [99]. To examine whether Fkh1 may also play a role in regulating Mph1's fork reversal activity, the effect the *mph1-2TA* mutant has in a *rad5-DEAA* background was examined.

Initial experiments showed that, like the *mph1*Δ*S1* allele that cannot interact with Smc5/6, the *mph1-2TA* allele reduced MMS sensitivity in a *rad5-DEAA* background (Figure A-7A). However, this observation was not seen again after repeating the same experiment (Figure A-7B). Additionally, I was unable to replicate the published results demonstrating that the *mph1*Δ*S1* allele reduces MMS sensitivity in a *rad5-DEAA* background. The previously published results show that the MMS sensitivity of the *mph1*Δ*S1* allele in the *rad5-DEAA* background is variable [99], so it is possible the initial observation of an effect caused by the *mph1-2TA* allele was accurate but that the effect is stochastic. However, as I was unable to repeat the previously published results it is difficult to conclude the effects this allele has. It is also possible that even if the *mph1-2TA* allele has an effect on MMS sensitivity in the *rad5-DEAA* background that this effect is due to a

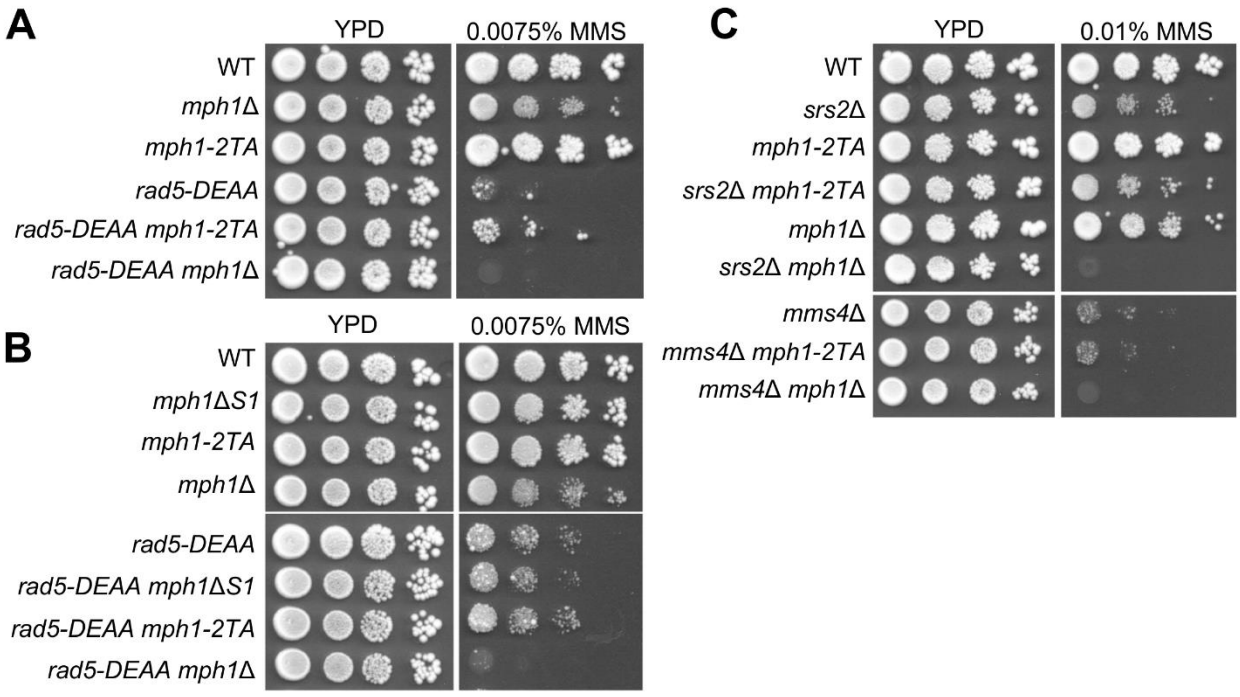

Figure A-7. *mph1-2TA* does not cause excessive fork reversal. (**A-C**) Chronic exposure MMS assays. The *mph1ΔS1* allele is lacking amino acids 751-810.

reduction in interaction with Smc5/6. Yeast-2-hybrid experiments show that this allele still interacts with Smc5, although it may be weakened. *In vitro* experiments measuring Mph1 and mutant Mph1's ability to catalyze fork reversal in the presence of Fkh1 and/or Smc5/6 may be able to clear up this confusion.

Yeast expressing a mutant form of Mph1 that does not interact with Smc5/6 (*mph1ΔS1*) have an increased sensitivity to MMS in both *srs2*Δ and *mms4*Δ mutant backgrounds [99]. This effect is proposed to be due to the DNA repair activities of Srs2 and Mms4. Without inhibition from Smc5/6 the Mph1 fork reversal activity is increased, causing a buildup of toxic DNA recombination intermediates. The activities of Srs2 and Mms4 are required to resolve these intermediates (Figure A-6). I saw no such increase in MMS sensitivity in *mph1-2TA srs2*Δ or *mph1-2TA mms4*Δ cells, suggesting that this allele likely does not lead to excessive replication fork reversal activity (Figure A-7C).

A.5 Genetic interaction between *RAD5* and *FKH1*

The yeast strain used in the Fox lab, w303, contains a mutation in the *RAD5* gene, *rad5-535*, which causes a change in amino acid at position 535 from glycine to arginine [158]. Rad5 is a DNA helicase and ubiquitin ligase that is able to catalyze replication fork reversal and is also involved in post-replication repair [157,159]. Deletion of *RAD5* leads to sensitivity to a number of DNA damaging agents, including MMS [160]. The *rad5-535* mutation leads to a weak DNA repair defect phenotype that is further weakened in certain backgrounds. Very little has been reported about the effects of this allele, however unpublished results from multiple groups suggest that defects observed in *rad5-535* strains are indirect and are due to loss of interaction with chromatin-associated proteins or the transcription machinery (summarized in [161]). MMS

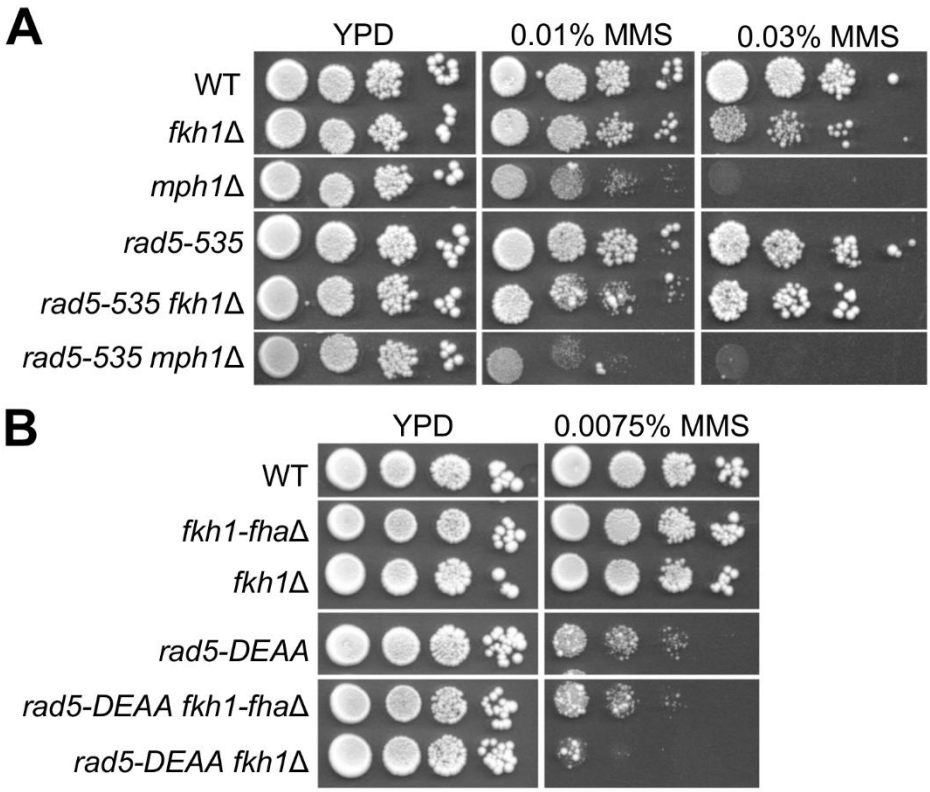

Figure A-8. Genetic effects of *RAD5* and *FKH1* mutation on MMS sensitivity. (**A-B**) Chronic exposure MMS assays. The *fkh1-fha*Δ allele is lacking amino acids 50-202.

sensitivity in *rad5-535 mph1*Δ cells was greater than that of *rad5-535* cells or *mph1*Δ cells (Figure A-8A), suggesting the *rad5-535* mutant causes some defect in an overlapping role with Mph1. Unlike in *RAD5* cells, deletion of *FKH1* in *rad5-535* cells did not lead to MMS sensitivity, suggesting Rad5 activity or interaction with an unknown protein is essential for MMS sensitivity in *fkh1*Δ cells.

Interestingly, deletion of *FKH1* in a *rad5-DEAA* background caused an increase in MMS sensitivity, even at concentrations where deletion of *FKH1* alone causes no sensitivity (Figure A-8B). Removal of only the FHA domain of Fkh1 does not cause the same effect. These results suggest that Fkh1 may play a role in MMS sensitivity that overlaps with Rad5.

A.6 Materials and methods

A.6.1 Yeast strains

Strains were derived from the *Saccharomyces cerevisiae* strain w303. Standard methods were used for yeast growth and strain construction. Strains used in this appendix are listed in Table A-2. Strains have all alleles present in the w303 background (*his3-11, trp1-1, leu2-3,112, ura3-1*) unless otherwise noted.

A.6.2 HN2 and MMS assays

Chronic exposure MMS assays were performed as described in Chapter 2 (see methods section 2.6.7). Acute exposure HN2 assays were performed as described in [155]. Briefly, cells were grown in liquid YPD media to mid-log phase, pelleted, and then resuspended in PBS

Table A-2. Yeast strains used for experiments in Appendix A.

Name	Description	Source
CFY3533	*MATa ADE2+ CAN1+ RAD5+*	This study
CFY3537	*MATa ADE2+ CAN1+ RAD5+ fkh1Δ::HisG*	This study
CFY3539	*MATa ADE2+ CAN1+ RAD5+ mph1Δ::KanMX*	This study
CFY3541	*MATa ADE2+ CAN1+ RAD5+ fkh1Δ::HisG mph1Δ::KanMX*	This study
CFY3612	*MATa ADE2+ CAN1+ rad5-535*	This study
CFY3613	*MATa ADE2+ CAN1+ rad5-535 mph1Δ::KanMX*	This study
CFY3622	*MATa ADE2+ CAN1+ rad5-535 fkh1Δ::HisG*	This study
CFY3952	*MATa ADE2+ CAN1+ RAD5+ pso2Δ::TRP1 mph1Δ::KanMX*	This study
CFY3956	*MATa ADE2+ CAN1+ RAD5+ fkh1-R80A*	This study
CFY3969	*MATa ADE2+ CAN1+ RAD5+ fkh1Δ50-202*	This study
CFY4034	*MATa ADE2+ CAN1+ RAD5+ fkh1-dbdΔ*	Modified from [9]
CFY4038	*MATa ADE2+ CAN1+ RAD5+ mph1-2TA*	This study
CFY4092	*MATa ADE2+ CAN1+ RAD5+ pso2Δ::TRP1 mph1-2TA*	This study
CFY4268	*MATa ADE2+ CAN1+ RAD5+ fkh1Δ::HisG mph1-2TA*	This study
CFY4270	*MATa ADE2+ CAN1+ RAD5+ pso2Δ::TRP1*	This study
CFY4295	*MATa ADE2+ CAN1+ rad5-DEAA mph1Δ::KanMX*	Modified from [99]
CFY4297	*MATa ADE2+ CAN1+ rad5-DEAA mph1-2TA*	Modified from [99]
CFY4299	*MATa ADE2+ CAN1+ RAD5+ srs2Δ::TRP1*	Modified from [99]
CFY4301	*MATa ADE2+ CAN1+ RAD5+ srs2Δ::TRP1 mph1Δ::KanMX*	Modified from [99]
CFY4303	*MATa ADE2+ CAN1+ RAD5+ srs2Δ::TRP1 mph1-2TA*	Modified from [99]
CFY4304	*MATa ADE2+ CAN1+ RAD5+ mms4Δ::KanMX*	Modified from [99]
CFY4306	*MATa ADE2+ CAN1+ RAD5+ mms4Δ::KanMX mph1Δ::KanMX*	Modified from [99]
CFY4308	*MATa ADE2+ CAN1+ RAD5+ mms4Δ::KanMX mph1-2TA*	Modified from [99]
CFY4313	*MATa ADE2+ CAN1+ RAD5+ rad18Δ::KanMX*	*rad18*Δ allele courtesy X. Zhao
CFY4315	*MATa ADE2+ CAN1+ RAD5+ rad18Δ::KanMX mph1Δ::KanMX*	*rad18*Δ allele courtesy X. Zhao
CFY4317	*MATa ADE2+ CAN1+ RAD5+ rad18Δ::KanMX mph1-2TA*	*rad18*Δ allele courtesy X. Zhao
CFY4335	*MATa ADE2+ CAN1+ rad5-DEAA*	Modified from [99]
CFY4355	*MATa ADE2+ CAN1+ rad5-DEAA fkh1Δ::HisG*	Modified from [99]
CFY4356	*MATa ADE2+ CAN1+ rad5-DEAA fkh1Δ50-202*	Modified from [99]
CFY4389	*MATa ADE2+ CAN1+ RAD5+ mph1ΔS1 (Δ751-810)*	Modified from [99]
CFY4392	*MATa ADE2+ CAN1+ rad5-DEAA mph1ΔS1 (Δ751-810)*	Modified from [99]

supplemented with the indicated concentration of HN2 and incubated at 30°C for 1 hour. Acute exposure MMS assays were performed identically except that cells were resuspended in water and incubated at 30°C for 2 hours. Cells were then spotted onto YPD agar media and imaged after two or three days growth. For survival assays cells were plated onto YPD agar media and colonies were counted to calculate viability.

Appendix B

Examining the Fkh2-Mph1 interaction and the role of Fkh2 in DNA damage avoidance

B.1 Examining the Fkh2-Mph1 interaction

Fkh1 and Fkh2 have very similar amino acid sequences. Every residue in the Fkh1 FHA domain that I have shown to be required for Mph1 binding is also present in the Fkh2 FHA domain (Figure B-1A). This led to the prediction that Fkh2 is likely able to bind many, if not all, Fkh1 interacting proteins I identified in the 2-hybrid screen. Indeed, Fkh2 is able to bind Mph1, Ecm30, and Gln3 in 2-hybrid assays, although these interactions appear weaker than interactions between these proteins and Fkh1 (Figure B-1B). Interaction with these proteins also required the Fkh2 FHA domain. Unlike Fkh1, Fkh2 was unable to interact with Ure2 or Fdo1. These results suggest that the Fkh1-Ure2 and Fkh1-Fdo1 interactions may require other amino acids in Fkh1 that are not also present in Fkh2. This is consistent with my other results showing that the FHA domain of Fkh1 was not sufficient to interact with Fdo1. It is also possible that small differences in protein abundance or stability in the 2-hybrid context reduce the levels of Fkh2 binding with Ure2 and/or Fdo1 such that interaction is not observable by 2-hybrid. However, whether Fkh2 binds these proteins in extracts remains to be explored.

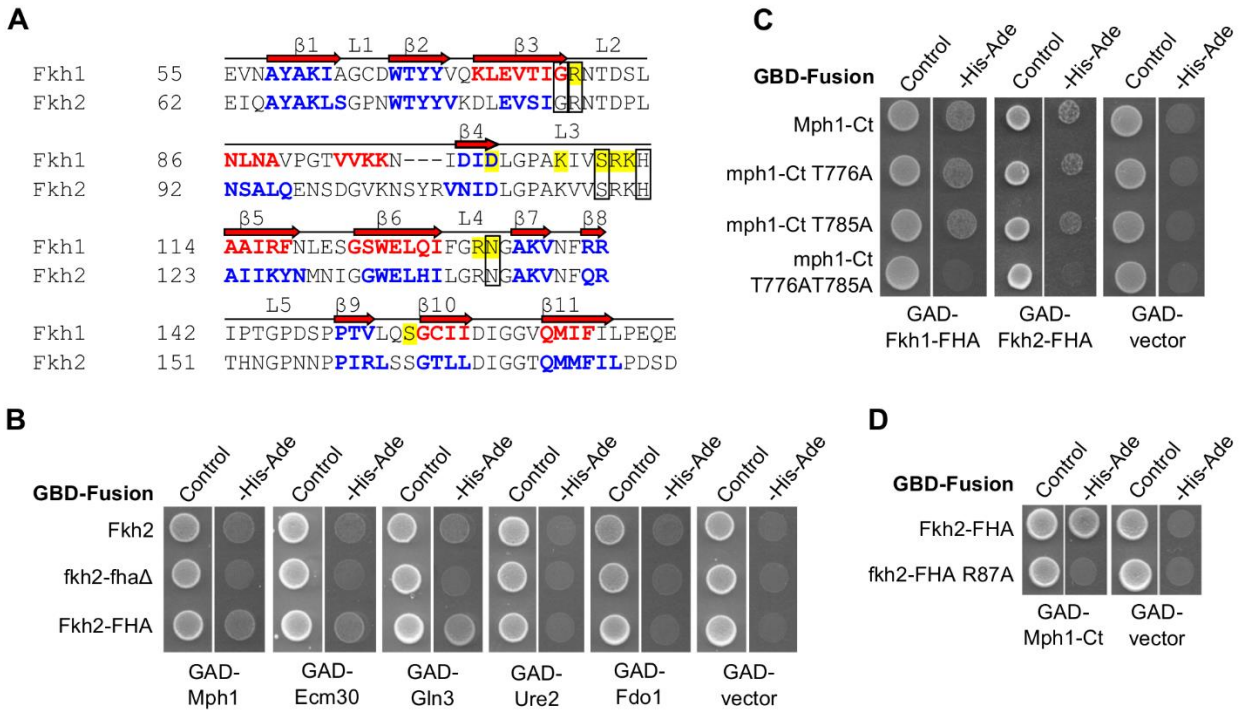

Figure B-1. The Fkh2 FHA domain interacts with many of the same proteins as the Fkh1 FHA domain. (**A**) Alignment of the Fkh1 and Fkh2 FHA domains. Alignment was generated using structural predictions of the Fkh1 FHA domain, which include a combination of the Rad53-based homology model and secondary structure prediction, and secondary structure prediction of the Fkh2 FHA domain [104] (See Figure 2-3 and section 2.6.3 for details). Conserved FHA domain β-strands and the loops which comprise the peptide binding site are labeled [38]. Fkh1 β-strands predicted in the homology model are shown in red and those predicted from secondary structure prediction are shown in blue. The five conserved FHA residues that comprise the phosphothreonine binding pocket are boxed. Fkh1 residues shown to be required for binding to Mph1 are highlighted yellow. (**B**) Yeast-2-hybrid assay using different forms of Fkh2 as bait and Fkh1 interactors described in Chapter 2 as prey. The Fkh2 FHA domain in these assays is defined as amino acids 57-212. (**C-D**) 2-hybrid assays using mutant forms of Fkh2 and Mph1. The FHA domain of Fkh2 is defined as amino acids 1-214 in these assays.

Further examination of the Fkh2-Mph1 interaction by 2-hybrid revealed that the same two threonines in Mph1 that are required for binding Fkh1 are also required for binding Fkh2 (Figure B-1C). These two threonines are also redundant for interaction with Fkh2, as both need to be substituted with alanine to see a loss of interaction. The phosphothreonine binding capability of Fkh2 is required for this interaction, as substitution of alanine for R87 (the analogous residue to Fkh1 R80) also abolishes binding to Mph1 (Figure B-1D). These results suggest that Fkh2 binds Mph1 with the same mechanism as Fkh1. However, I have not shown that Fkh2 and Mph1 interact in extracts. These proteins are overexpressed in the 2-hybrid system and it is possible that in normal cells in which Fkh1 is present Fkh2 and Mph1 do not interact.

B.2 Deletion of *FKH2* leads to MMS sensitivity in *RAD5* or *MPH1* mutant backgrounds

Unlike deletion of *FKH1*, deletion of *FKH2* in wild-type cells did not lead to MMS sensitivity. However, deletion of *FKH2* did lead to MMS sensitivity in both an *mph1*Δ background and a *rad-535* background, suggesting that deletion of *FKH2* causes a defect in a role overlapping with Mph1 and Rad5. Whether or not this role is a direct role in DNA repair or the by-product of altered cell cycle transcription is currently unknown.

B.3 Materials and methods

B.3.1 Yeast strains and plasmids

Strains were derived from the *Saccharomyces cerevisiae* strain w303. Standard methods were used for yeast growth and strain construction. Strains used in this appendix are listed in Table B-1. Strains have all alleles present in the w303 background (*his3-11, trp1-1, leu2-3,112, ura3-1*)

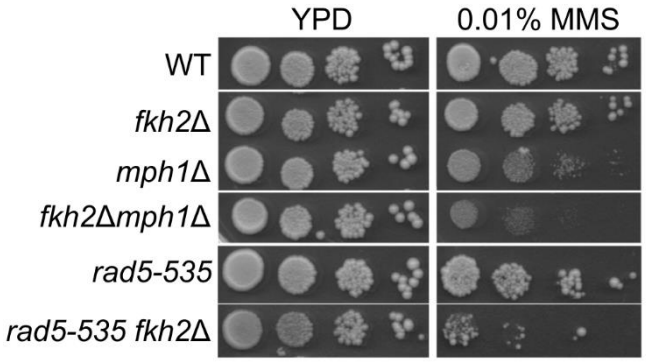

Figure B-2. Effect of *FKH2* mutation on MMS sensitivity in different genetic backgrounds. Cells were grown to mid-log phase in YPD and then spotted onto plates with the indicated concentration of MMS.

Table B-1. Yeast strains used for experiments in Appendix B.

Name	Description	Source
PJ69-4A	*MATa trp1-901 leu2-3,112 ura3-52 his3-200 gal4Δ gal80Δ GAL2-ADE2 LYS2::GAL1-HIS3 met2::GAL7-lacZ*	[88]
CFY3533	*MATa ADE2+ CAN1+ RAD5+*	This study
CFY3539	*MATa ADE2+ CAN1+ RAD5+ mph1Δ::KanMX*	This study
CFY3549	*MATa ADE2+ CAN1+ RAD5+ fkh2Δ::HisG*	This study
CFY3555	*MATa ADE2+ CAN1+ RAD5+ fkh2Δ::HisG mph1Δ::KanMX*	This study
CFY3612	*MATa ADE2+ CAN1+ rad5-535*	This study
CFY4368	*MATa ADE2+ CAN1+ rad5-535 fkh2Δ::HisG*	This study

Table B-2. Plasmids used for experiments in Appendix B.

Name	Description	Source
pGBDU-C1	Yeast-2-hybrid vector-Gal4 DNA Binding Domain	[88]
pGAD-C1	Yeast-2-hybrid vector-Gal4 Activation Domain	[88]
pCF2106	pGBDU-C1 Fkh1-FHA(50-202)	This study
pCF2123	pGBDU-C1 Fkh2-FHA(1-214)	This study
pCF2130	pGBDU-C1 Dun1-FHA(3-170)	This study
pCF2131	pGBDU-C1 Vps64-FHA(133-324)	This study
pCF2132	pGBDU-C1 Tos4-FHA(52-218)	This study
pCF2183	pGBDU-C1 Fkh1-FHA(50-202)	This study
pCF2185	pGAD-C1 Mph1 (762-993)	This study
pCF2280	pGAD-C1 Fkh2-FHA(1-214)	This study
pCF2559	pGAD-C3 Ecm30 (1005-1183)	[88]
pCF2561	pGAD-C1 Gln3 (20-189)	[88]
pCF2568	pGAD-C2 Ure2 (84-354)	[88]
pCF2570	pGAD-C2 Fdo1 (98-342)	[88]
pCF2776	pGBDU-C1 Fkh2	This study
pCF2892	pGBDU-C1 Fkh2(1-214) R87A	This study
pCF4016	pGBDU-C1 fkh2-fhaΔ (Δ57-212)	This study
pCF4045	pGBDU-C1 Fkh2-FHA (aa 57-212)	This study

unless otherwise noted. Plasmids were constructed using standard techniques and are listed in Table B-2.

B.3.2 Structure-based sequence alignment

Alignment was generated based on Fkh1 structural predictions (see section 2.6.3 for details) and secondary structure prediction of the Fkh2 FHA domain. Secondary structure prediction was generated by J-Pred [104].

B.3.3 2-hybrid assays

Yeast-2-hybrid assays were performed as described in Chapter 2 (section 2.6.2).

B.3.4 MMS assays

Chronic exposure MMS assays were performed as described in Chapter 2 (section 2.6.7).

References

1. Koch C, Nasmyth K. Cell cycle regulated transcription in yeast. Curr Opin Cell Biol. 1994;6: 451–459.

2. Mendenhall MD, Hodge AE. Regulation of Cdc28 cyclin-dependent protein kinase activity during the cell cycle of the yeast *Saccharomyces cerevisiae*. Microbiol Mol Biol Rev. 1998;62: 1191–1243.

3. Remus D, Diffley JFX. Eukaryotic DNA replication control: lock and load, then fire. Curr Opin Cell Biol. 2009;21: 771–777. doi:10.1016/j.ceb.2009.08.002

4. Spellman PT, Sherlock G, Zhang MQ, Iyer VR, Anders K, Eisen MB, et al. Comprehensive identification of cell cycle-regulated genes of the yeast *Saccharomyces cerevisiae* by microarray hybridization. Mol Biol Cell. 1998;9: 3273–3297.

5. Chant J, Herskowitz I. Genetic control of bud site selection in yeast by a set of gene products that constitute a morphogenetic pathway. Cell. 1991;65: 1203–1212. doi:10.1016/0092-8674(91)90015-Q

6. Lydall D, Ammerer G, Nasmyth K. A new role for *MCM1* in yeast: cell cycle regulation of *SW15* transcription. Genes Dev. 1991;5: 2405–2419.

7. Maher M, Cong F, Kindelberger D, Nasmyth K, Dalton S. Cell cycle-regulated transcription of the *CLB2* gene is dependent on Mcm1 and a ternary complex factor. Mol Cell Biol. 1995;15: 3129–3137. doi:10.1128/MCB.15.6.3129

8. Althoefer H, Schleiffer A, Wassmann K, Nordheim A, Ammerer G. Mcm1 is required to coordinate G2-specific transcription in *Saccharomyces cerevisiae*. Mol Cell Biol. 1995;15: 5917–5928.

9. Hollenhorst PC, Bose ME, Mielke MR, Müller U, Fox CA. Forkhead genes in transcriptional silencing, cell morphology and the cell cycle. Overlapping and distinct functions for *FKH1* and *FKH2* in *Saccharomyces cerevisiae*. Genetics. 2000;154: 1533–1548.

10. Kumar R, Reynolds DM, Shevchenko A, Shevchenko A, Goldstone SD, Dalton S. Forkhead transcription factors, Fkh1p and Fkh2p, collaborate with Mcm1p to control transcription required for M-phase. Curr Biol. 2000;10: 896–906.

11. Zhu G, Spellman PT, Volpe T, Brown PO, Botstein D, Davis TN, et al. Two yeast forkhead genes regulate the cell cycle and pseudohyphal growth. Nature. 2000;406: 90–94. doi:10.1038/35017581

12. Koranda M, Schleiffer A, Endler L, Ammerer G. Forkhead-like transcription factors recruit Ndd1 to the chromatin of G2/M-specific promoters. Nature. 2000;406: 94–98. doi:10.1038/35017589

13. Pic A, Lim FL, Ross SJ, Veal EA, Johnson AL, Sultan MR, et al. The forkhead protein Fkh2 is a component of the yeast cell cycle transcription factor SFF. EMBO J. 2000;19: 3750–3761. doi:10.1093/emboj/19.14.3750

14. Surana U, Robitsch H, Price C, Schuster T, Fitch I, Futcher AB, et al. The role of *CDC28* and cyclins during mitosis in the budding yeast *S. cerevisiae*. Cell. 1991;65: 145–161.

15. Fitch I, Dahmann C, Surana U, Amon A, Nasmyth K, Goetsch L, et al. Characterization of four B-type cyclin genes of the budding yeast *Saccharomyces cerevisiae*. Mol Biol Cell. 1992;3: 805–818.

16. Hollenhorst PC, Pietz G, Fox CA. Mechanisms controlling differential promoter-occupancy by the yeast forkhead proteins Fkh1p and Fkh2p: implications for regulating the cell cycle and differentiation. Genes Dev. 2001;15: 2445–2456. doi:10.1101/gad.906201

17. Altschul SF, Gish W, Miller W, Myers EW, Lipman DJ. Basic local alignment search tool. J Mol Biol. 1990;215: 403–410. doi:10.1016/S0022-2836(05)80360-2

18. Pic-Taylor A, Darieva Z, Morgan BA, Sharrocks AD. Regulation of cell cycle-specific gene expression through cyclin-dependent kinase-mediated phosphorylation of the forkhead transcription factor Fkh2p. Mol Cell Biol. 2004;24: 10036–10046. doi:10.1128/MCB.24.22.10036-10046.2004

19. Boros J, Lim F-L, Darieva Z, Pic-Taylor A, Harman R, Morgan BA, et al. Molecular determinants of the cell-cycle regulated Mcm1p-Fkh2p transcription factor complex. Nucleic Acids Res. 2003;31: 2279–2288.

20. Ostrow AZ, Nellimoottil T, Knott SRV, Fox CA, Tavaré S, Aparicio OM. Fkh1 and Fkh2 bind multiple chromosomal elements in the *S. cerevisiae* genome with distinct specificities and cell cycle dynamics. PLoS ONE. 2014;9: e87647. doi:10.1371/journal.pone.0087647

21. Linke C, Klipp E, Lehrach H, Barberis M, Krobitsch S. Fkh1 and Fkh2 associate with Sir2 to control *CLB2* transcription under normal and oxidative stress conditions. Front Physiol. 2013;4: 173. doi:10.3389/fphys.2013.00173

22. Veis J, Klug H, Koranda M, Ammerer G. Activation of the G2/M-Specific Gene *CLB2* Requires Multiple Cell Cycle Signals. Mol Cell Biol. 2007;27: 8364–8373. doi:10.1128/MCB.01253-07

23. Voth WP, Yu Y, Takahata S, Kretschmann KL, Lieb JD, Parker RL, et al. Forkhead proteins control the outcome of transcription factor binding by antiactivation. EMBO J. 2007;26: 4324–4334. doi:10.1038/sj.emboj.7601859

24. Loy CJ, Lydall D, Surana U. *NDD1*, a high-dosage suppressor of *cdc28-1N*, is essential for expression of a subset of late-S-phase-specific genes in *Saccharomyces cerevisiae*. Mol Cell Biol. 1999;19: 3312–3327.

25. Reynolds D, Shi BJ, McLean C, Katsis F, Kemp B, Dalton S. Recruitment of Thr 319-phosphorylated Ndd1p to the FHA domain of Fkh2p requires Clb kinase activity: a mechanism for *CLB* cluster gene activation. Genes Dev. 2003;17: 1789–1802. doi:10.1101/gad.1074103

26. Darieva Z, Pic-Taylor A, Boros J, Spanos A, Geymonat M, Reece RJ, et al. Cell cycle-regulated transcription through the FHA domain of Fkh2p and the coactivator Ndd1p. Curr Biol. 2003;13: 1740–1745.

27. Durocher D, Jackson SP. The FHA domain. FEBS Lett. 2002;513: 58–66. doi:10.1016/S0014-5793(01)03294-X

28. Mahajan A, Yuan C, Lee H, Chen ES-W, Wu P-Y, Tsai M-D. Structure and function of the phosphothreonine-specific FHA domain. Sci Signal. 2008;1: re12. doi:10.1126/scisignal.151re12

29. Mermershtain I, Glover JNM. Structural mechanisms underlying signaling in the cellular response to DNA double strand breaks. Mutat Res. 2013;750: 15–22. doi:10.1016/j.mrfmmm.2013.07.004

30. Mohammad DH, Yaffe MB. 14-3-3 proteins, FHA domains and BRCT domains in the DNA damage response. DNA Repair. 2009;8: 1009–1017. doi:10.1016/j.dnarep.2009.04.004

31. Reinhardt HC, Yaffe MB. Phospho-Ser/Thr-binding domains: navigating the cell cycle and DNA damage response. Nat Rev Mol Cell Biol. 2013;14: 563–580. doi:10.1038/nrm3640

32. Hofmann K, Bucher P. The FHA domain: a putative nuclear signaling domain found in protein kinases and transcription factors. Trends Biochem Sci. 1995;20: 347–349.

33. Maser RS, Zinkel R, Petrini JHJ. An alternative mode of translation permits production of a variant NBS1 protein from the common Nijmegen breakage syndrome allele. Nat Genet. 2001;27: 417–421. doi:10.1038/86920

34. Yata K, Lloyd J, Maslen S, Bleuyard J-Y, Skehel M, Smerdon SJ, et al. Plk1 and CK2 act in concert to regulate Rad51 during DNA double strand break repair. Mol Cell. 2012;45: 371–383. doi:10.1016/j.molcel.2011.12.028

35. Zhou R, Niwa S, Guillaud L, Tong Y, Hirokawa N. A Molecular Motor, KIF13A, Controls Anxiety by Transporting the Serotonin Type 1A Receptor. Cell Rep. 2013;3: 509–519. doi:10.1016/j.celrep.2013.01.014

36. Havranek O, Spacek M, Hubacek P, Mocikova H, Markova J, Trneny M, et al. Alterations of CHEK2 forkhead-associated domain increase the risk of Hodgkin lymphoma. Neoplasma. 2011;58: 392–395.

37. Durocher D, Henckel J, Fersht AR, Jackson SP. The FHA domain is a modular phosphopeptide recognition motif. Mol Cell. 1999;4: 387–394.

38. Huang YM, Chang CA. Achieving peptide binding specificity and promiscuity by loops: Case of the Forkhead-Associated Domain. PLoS ONE. 2014;9: e98291. doi:10.1371/journal.pone.0098291

39. Durocher D, Taylor IA, Sarbassova D, Haire LF, Westcott SL, Jackson SP, et al. The molecular basis of FHA domain:phosphopeptide binding specificity and implications for phospho-dependent signaling mechanisms. Mol Cell. 2000;6: 1169–1182.

40. Lee H, Yuan C, Hammet A, Mahajan A, Chen ES-W, Wu M-R, et al. Diphosphothreonine-specific interaction between an SQ/TQ cluster and an FHA domain in the Rad53-Dun1 kinase cascade. Mol Cell. 2008;30: 767–778. doi:10.1016/j.molcel.2008.05.013

41. Byeon I-JL, Li H, Song H, Gronenborn AM, Tsai M-D. Sequential phosphorylation and multisite interactions characterize specific target recognition by the FHA domain of Ki67. Nat Struct Mol Biol. 2005;12: 987–993. doi:10.1038/nsmb1008

42. Li J, Williams BL, Haire LF, Goldberg M, Wilker E, Durocher D, et al. Structural and functional versatility of the FHA domain in DNA-damage signaling by the tumor suppressor kinase Chk2. Mol Cell. 2002;9: 1045–1054.

43. Huen MSY, Grant R, Manke I, Minn K, Yu X, Yaffe MB, et al. RNF8 Transduces the DNA-Damage Signal via Histone Ubiquitylation and Checkpoint Protein Assembly. Cell. 2007;131: 901–914. doi:10.1016/j.cell.2007.09.041

44. Mahajan A, Yuan C, Pike BL, Heierhorst J, Chang C-F, Tsai M-D. FHA Domain−Ligand Interactions: Importance of Integrating Chemical and Biological Approaches. J Am Chem Soc. 2005;127: 14572–14573. doi:10.1021/ja054538m

45. Li H, Byeon IJL, Ju Y, Tsai MD. Structure of human Ki67 FHA domain and its binding to a phosphoprotein fragment from hNIFK reveal unique recognition sites and new views to the structural basis of FHA domain functions. J Mol Biol. 2004;335: 371–381.

46. Chaurushiya MS, Lilley CE, Aslanian A, Meisenhelder J, Scott DC, Landry S, et al. Viral E3 Ubiquitin Ligase-Mediated Degradation of a Cellular E3: Viral Mimicry of a Cellular Phosphorylation Mark Targets the RNF8 FHA Domain. Mol Cell. 2012;46: 79–90. doi:10.1016/j.molcel.2012.02.004

47. Nott TJ, Kelly G, Stach L, Li J, Westcott S, Patel D, et al. An intramolecular switch regulates phosphoindependent FHA domain interactions in *Mycobacterium tuberculosis*. Sci Signal. 2009;2: ra12. doi:10.1126/scisignal.2000212

48. Matthews LA, Selvaratnam R, Jones DR, Akimoto M, McConkey BJ, Melacini G, et al. A novel non-canonical forkhead-associated (FHA) domain-binding interface mediates the interaction between Rad53 and Dbf4 proteins. J Biol Chem. 2014;289: 2589–2599. doi:10.1074/jbc.M113.517060

49. Strathern JN, Herskowitz I. Asymmetry and directionality in production of new cell types during clonal growth: the switching pattern of homothallic yeast. Cell. 1979;17: 371–381.

50. Haber JE. Mating-type gene switching in *Saccharomyces cerevisiae*. Annu Rev Genet. 1998;32: 561–599. doi:10.1146/annurev.genet.32.1.561

51. Haber JE. Mating-type genes and *MAT* switching in *Saccharomyces cerevisiae*. Genetics. 2012;191: 33–64. doi:10.1534/genetics.111.134577

52. Sil A, Herskowitz I. Identification of asymmetrically localized determinant, Ash1p, required for lineage-specific transcription of the yeast *HO* gene. Cell. 1996;84: 711–722.

53. Bobola N, Jansen RP, Shin TH, Nasmyth K. Asymmetric accumulation of Ash1p in postanaphase nuclei depends on a myosin and restricts yeast mating-type switching to mother cells. Cell. 1996;84: 699–709.

54. Weiler KS, Broach JR. Donor locus selection during *Saccharomyces cerevisiae* mating type interconversion responds to distant regulatory signals. Genetics. 1992;132: 929–942.

55. Wu X, Haber JE. A 700 bp cis-acting region controls mating-type dependent recombination along the entire left arm of yeast chromosome III. Cell. 1996;87: 277–285.

56. Sun K, Coïc E, Zhou Z, Durrens P, Haber JE. *Saccharomyces* forkhead protein Fkh1 regulates donor preference during mating-type switching through the recombination enhancer. Genes Dev. 2002;16: 2085–2096. doi:10.1101/gad.994902

57. Weiss K, Simpson RT. Cell type-specific chromatin organization of the region that governs directionality of yeast mating type switching. EMBO J. 1997;16: 4352–4360. doi:10.1093/emboj/16.14.4352

58. Wu C, Weiss K, Yang C, Harris MA, Tye B-K, Newlon CS, et al. Mcm1 regulates donor preference controlled by the recombination enhancer in *Saccharomyces* mating-type switching. Genes Dev. 1998;12: 1726–1737. doi:10.1101/gad.12.11.1726

59. Coïc E, Sun K, Wu C, Haber JE. Cell cycle-dependent regulation of *Saccharomyces cerevisiae* donor preference during mating-type switching by SBF (Swi4/Swi6) and Fkh1. Mol Cell Biol. 2006;26: 5470–5480. doi:10.1128/MCB.02443-05

60. Li J, Coïc E, Lee K, Lee C-S, Kim J-A, Wu Q, et al. Regulation of budding yeast mating-type switching donor preference by the FHA domain of Fkh1. PLoS Genet. 2012;8: e1002630. doi:10.1371/journal.pgen.1002630

61. Watanabe Y, Maekawa M. Spatiotemporal regulation of DNA replication in the human genome and its association with genomic instability and disease. Curr Med Chem. 2010;17: 222–233.

62. Natsume T, Müller CA, Katou Y, Retkute R, Gierliński M, Araki H, et al. Kinetochores coordinate pericentromeric cohesion and early DNA replication by Cdc7-Dbf4 kinase recruitment. Mol Cell. 2013;50: 661–674. doi:10.1016/j.molcel.2013.05.011

63. Bell SP, Stillman B. ATP-dependent recognition of eukaryotic origins of DNA replication by a multiprotein complex. Nature. 1992;357: 128–134. doi:10.1038/357128a0

64. Vashee S, Cvetic C, Lu W, Simancek P, Kelly TJ, Walter JC. Sequence-independent DNA binding and replication initiation by the human origin recognition complex. Genes Dev. 2003;17: 1894–1908. doi:10.1101/gad.1084203

65. Cvetic C, Walter JC. Eukaryotic origins of DNA replication: could you please be more specific? Semin Cell Dev Biol. 2005;16: 343–353. doi:10.1016/j.semcdb.2005.02.009

66. Ding Q, MacAlpine DM. Defining the replication program through the chromatin landscape. Crit Rev Biochem Mol Biol. 2011;46: 165–179. doi:10.3109/10409238.2011.560139

67. Müller P, Park S, Shor E, Huebert DJ, Warren CL, Ansari AZ, et al. The conserved bromo-adjacent homology domain of yeast Orc1 functions in the selection of DNA replication origins within chromatin. Genes Dev. 2010;24: 1418–1433. doi:10.1101/gad.1906410

68. Hoggard T, Shor E, Müller CA, Nieduszynski CA, Fox CA. A Link between ORC-origin binding mechanisms and origin activation time revealed in budding yeast. PLoS Genet. 2013;9: e1003798. doi:10.1371/journal.pgen.1003798

69. Knott SRV, Peace JM, Ostrow AZ, Gan Y, Rex AE, Viggiani CJ, et al. Forkhead transcription factors establish origin timing and long-range clustering in *S. cerevisiae*. Cell. 2012;148: 99–111. doi:10.1016/j.cell.2011.12.012

70. Lõoke M, Kristjuhan K, Värv S, Kristjuhan A. Chromatin-dependent and -independent regulation of DNA replication origin activation in budding yeast. EMBO Rep. 2012;14: 191–198. doi:10.1038/embor.2012.196

71. Peace JM, Villwock SK, Zeytounian JL, Gan Y, Aparicio OM. Quantitative BrdU immunoprecipitation method demonstrates that Fkh1 and Fkh2 are rate-limiting activators of replication origins that reprogram replication timing in G1 phase. Genome Res. 2016; gr.196857.115. doi:10.1101/gr.196857.115

72. Kaufmann E, Knöchel W. Five years on the wings of fork head. Mech Dev. 1996;57: 3–20.

73. Jackson BC, Carpenter C, Nebert DW, Vasiliou V. Update of human and mouse forkhead box (FOX) gene families. Hum Genomics. 2010;4: 345–352.

74. Lalmansingh AS, Karmakar S, Jin Y, Nagaich AK. Multiple modes of chromatin remodeling by Forkhead box proteins. Biochim Biophys Acta. 2012;1819: 707–715. doi:10.1016/j.bbagrm.2012.02.018

75. Myatt SS, Lam EW-F. The emerging roles of forkhead box (Fox) proteins in cancer. Nat Rev Cancer. 2007;7: 847–859. doi:10.1038/nrc2223

76. Hannenhalli S, Kaestner KH. The evolution of Fox genes and their role in development and disease. Nat Rev Genet. 2009;10: 233–240. doi:10.1038/nrg2523

77. Tuteja G, Kaestner KH. SnapShot:Forkhead Transcription Factors I. Cell. 2007;130: 1160.e1-1160.e2. doi:10.1016/j.cell.2007.09.005

78. Tuteja G, Kaestner KH. Forkhead transcription factors II. Cell. 2007;131: 192. doi:10.1016/j.cell.2007.09.016

79. Dong X-Y, Chen C, Sun X, Guo P, Vessella RL, Wang R-X, et al. FOXO1A is a candidate for the 13q14 tumor suppressor gene inhibiting androgen receptor signaling in prostate cancer. Cancer Res. 2006;66: 6998–7006. doi:10.1158/0008-5472.CAN-06-0411

80. Singh B, Gogineni SK, Sacks PG, Shaha AR, Shah JP, Stoffel A, et al. Molecular cytogenetic characterization of head and neck squamous cell carcinoma and refinement of 3q amplification. Cancer Res. 2001;61: 4506–4513.

81. Rodriguez S, Khabir A, Keryer C, Perrot C, Drira M, Ghorbel A, et al. Conventional and array-based comparative genomic hybridization analysis of nasopharyngeal carcinomas from the Mediterranean area. Cancer Genet Cytogenet. 2005;157: 140–147. doi:10.1016/j.cancergencyto.2004.08.017

82. Heselmeyer K, Macville M, Schröck E, Blegen H, Hellström AC, Shah K, et al. Advanced-stage cervical carcinomas are defined by a recurrent pattern of chromosomal aberrations revealing high genetic instability and a consistent gain of chromosome arm 3q. Genes Chromosomes Cancer. 1997;19: 233–240.

83. Garry DJ, Meeson A, Elterman J, Zhao Y, Yang P, Bassel-Duby R, et al. Myogenic stem cell function is impaired in mice lacking the forkhead/winged helix protein MNF. Proc Natl Acad Sci. 2000;97: 5416–5421. doi:10.1073/pnas.100501197

84. Meeson AP, Hawke TJ, Graham S, Jiang N, Elterman J, Hutcheson K, et al. Cellular and molecular regulation of skeletal muscle side population cells. Stem Cells. 2004;22: 1305–1320. doi:10.1634/stemcells.2004-0077

85. Bowman CJ, Ayer DE, Dynlacht BD. Foxk proteins repress the initiation of starvation-induced atrophy and autophagy programs. Nat Cell Biol. 2014;16: 1202–1214. doi:10.1038/ncb3062

86. Dummer AM, Su Z, Cherney R, Choi K, Denu J, Zhao X, et al. Binding of the Fkh1 Forkhead Associated domain to a phosphopeptide within the Mph1 DNA helicase regulates mating-type switching in budding yeast. PLoS Genet. 2016;In Press.

87. Ercan S, Reese JC, Workman JL, Simpson RT. Yeast Recombination Enhancer Is Stimulated by Transcription Activation. Mol Cell Biol. 2005;25: 7976–7987. doi:10.1128/MCB.25.18.7976-7987.2005

88. James P, Halladay J, Craig EA. Genomic libraries and a host strain designed for highly efficient two-hybrid selection in yeast. Genetics. 1996;144: 1425–1436.

89. Scheller J, Schürer A, Rudolph C, Hettwer S, Kramer W. *MPH1*, a yeast gene encoding a DEAH protein, plays a role in protection of the genome from spontaneous and chemically induced damage. Genetics. 2000;155: 1069–1081.

90. Mitchell AP, Magasanik B. Regulation of glutamine-repressible gene products by the *GLN3* function in *Saccharomyces cerevisiae*. Mol Cell Biol. 1984;4: 2758–2766.

91. Courchesne WE, Magasanik B. Regulation of nitrogen assimilation in *Saccharomyces cerevisiae*: roles of the *URE2* and *GLN3* genes. J Bacteriol. 1988;170: 708–713.

92. Lussier M, White AM, Sheraton J, di Paolo T, Treadwell J, Southard SB, et al. Large scale identification of genes involved in cell surface biosynthesis and architecture in *Saccharomyces cerevisiae*. Genetics. 1997;147: 435–450.

93. Giaever G, Chu AM, Ni L, Connelly C, Riles L, Véronneau S, et al. Functional profiling of the *Saccharomyces cerevisiae* genome. Nature. 2002;418: 387–391. doi:10.1038/nature00935

94. Ho Y, Gruhler A, Heilbut A, Bader GD, Moore L, Adams S-L, et al. Systematic identification of protein complexes in *Saccharomyces cerevisiae* by mass spectrometry. Nature. 2002;415: 180–183. doi:10.1038/415180a

95. Whitby MC. The FANCM family of DNA helicases/translocases. DNA Repair. 2010;9: 224–236. doi:10.1016/j.dnarep.2009.12.012

96. Xue X, Sung P, Zhao X. Functions and regulation of the multitasking FANCM family of DNA motor proteins. Genes Dev. 2015;29: 1777–1788. doi:10.1101/gad.266593.115

97. Banerjee S, Smith S, Oum J-H, Liaw H-J, Hwang J-Y, Sikdar N, et al. Mph1p promotes gross chromosomal rearrangement through partial inhibition of homologous recombination. J Cell Biol. 2008;181: 1083–1093. doi:10.1083/jcb.200711146

98. Chavez A, Agrawal V, Johnson FB. Homologous recombination-dependent rescue of deficiency in the structural maintenance of chromosomes (Smc) 5/6 complex. J Biol Chem. 2011;286: 5119–5125. doi:10.1074/jbc.M110.201608

99. Xue X, Choi K, Bonner J, Chiba T, Kwon Y, Xu Y, et al. Restriction of Replication Fork Regression Activities by a Conserved SMC Complex. Mol Cell. 2014;56: 436–445. doi:10.1016/j.molcel.2014.09.013

100. Xue X, Choi K, Bonner JN, Szakal B, Chen Y-H, Papusha A, et al. Selective modulation of the functions of a conserved DNA motor by a histone fold complex. Genes Dev. 2015;29: 1000–1005. doi:10.1101/gad.259143.115

101. Arnold K, Bordoli L, Kopp J, Schwede T. The SWISS-MODEL workspace: a web-based environment for protein structure homology modelling. Bioinformatics. 2006;22: 195–201. doi:10.1093/bioinformatics/bti770

102. Kiefer F, Arnold K, Künzli M, Bordoli L, Schwede T. The SWISS-MODEL Repository and associated resources. Nucleic Acids Res. 2009;37: D387-392. doi:10.1093/nar/gkn750

103. Guex N, Peitsch MC, Schwede T. Automated comparative protein structure modeling with SWISS-MODEL and Swiss-PdbViewer: a historical perspective. Electrophoresis. 2009;30 Suppl 1: S162-173. doi:10.1002/elps.200900140

104. Cole C, Barber JD, Barton GJ. The Jpred 3 secondary structure prediction server. Nucleic Acids Res. 2008;36: W197-201. doi:10.1093/nar/gkn238

105. Benkert P, Biasini M, Schwede T. Toward the estimation of the absolute quality of individual protein structure models. Bioinformatics. 2011;27: 343–350. doi:10.1093/bioinformatics/btq662

106. Stavridi ES, Huyen Y, Loreto IR, Scolnick DM, Halazonetis TD, Pavletich NP, et al. Crystal structure of the FHA domain of the Chfr mitotic checkpoint protein and its complex with tungstate. Struct Lond Engl 1993. 2002;10: 891–899.

107. Cai Z, Chehab NH, Pavletich NP. Structure and activation mechanism of the CHK2 DNA damage checkpoint kinase. Mol Cell. 2009;35: 818–829. doi:10.1016/j.molcel.2009.09.007

108. Ali AAE, Jukes RM, Pearl LH, Oliver AW. Specific recognition of a multiply phosphorylated motif in the DNA repair scaffold XRCC1 by the FHA domain of human PNK. Nucleic Acids Res. 2009;37: 1701–1712. doi:10.1093/nar/gkn1086

109. Bernstein NK, Williams RS, Rakovszky ML, Cui D, Green R, Karimi-Busheri F, et al. The molecular architecture of the mammalian DNA repair enzyme, polynucleotide kinase. Mol Cell. 2005;17: 657–670. doi:10.1016/j.molcel.2005.02.012

110. Yuan C, Yongkiettrakul S, Byeon IJ, Zhou S, Tsai MD. Solution structures of two FHA1-phosphothreonine peptide complexes provide insight into the structural basis of the ligand specificity of FHA1 from yeast Rad53. J Mol Biol. 2001;314: 563–575. doi:10.1006/jmbi.2001.5140

111. Byeon IJ, Yongkiettrakul S, Tsai MD. Solution structure of the yeast Rad53 FHA2 complexed with a phosphothreonine peptide pTXXL: comparison with the structures of

FHA2-pYXL and FHA1-pTXXD complexes. J Mol Biol. 2001;314: 577–588. doi:10.1006/jmbi.2001.5141

112. Liao H, Byeon IJ, Tsai MD. Structure and function of a new phosphopeptide-binding domain containing the FHA2 of Rad53. J Mol Biol. 1999;294: 1041–1049. doi:10.1006/jmbi.1999.3313

113. Li J, Lee GI, Van Doren SR, Walker JC. The FHA domain mediates phosphoprotein interactions. J Cell Sci. 2000;113 Pt 23: 4143–4149.

114. Gabrielse C, Miller CT, McConnell KH, DeWard A, Fox CA, Weinreich M. A Dbf4p BRCA1 C-terminal-like domain required for the response to replication fork arrest in budding yeast. Genetics. 2006;173: 541–555. doi:10.1534/genetics.106.057521

115. Schürer KA, Rudolph C, Ulrich HD, Kramer W. Yeast *MPH1* gene functions in an error-free DNA damage bypass pathway that requires genes from Homologous recombination, but not from postreplicative repair. Genetics. 2004;166: 1673–1686.

116. Nishino T, Komori K, Tsuchiya D, Ishino Y, Morikawa K. Crystal structure and functional implications of *Pyrococcus furiosus* hef helicase domain involved in branched DNA processing. Structure. 2005;13: 143–153. doi:10.1016/j.str.2004.11.008

117. Liang X, Van Doren SR. Mechanistic Insights into Phosphoprotein-Binding FHA Domains. Acc Chem Res. 2008;41: 991–999. doi:10.1021/ar700148u

118. Hall BM, Ma C-X, Liang P, Singh KK. Fluctuation analysis CalculatOR: a web tool for the determination of mutation rate using Luria-Delbruck fluctuation analysis. Bioinformatics. 2009;25: 1564–1565. doi:10.1093/bioinformatics/btp253

119. Meggio F, Pinna LA. One-thousand-and-one substrates of protein kinase CK2? FASEB J. 2003;17: 349–368. doi:10.1096/fj.02-0473rev

120. Prakash R, Satory D, Dray E, Papusha A, Scheller J, Kramer W, et al. Yeast Mph1 helicase dissociates Rad51-made D-loops: implications for crossover control in mitotic recombination. Genes Dev. 2009;23: 67–79. doi:10.1101/gad.1737809

121. Polo SE, Jackson SP. Dynamics of DNA damage response proteins at DNA breaks: a focus on protein modifications. Genes Dev. 2011;25: 409–433. doi:10.1101/gad.2021311

122. Krejci L, Altmannova V, Spirek M, Zhao X. Homologous recombination and its regulation. Nucleic Acids Res. 2012;40: 5795–5818. doi:10.1093/nar/gks270

123. Miné-Hattab J, Rothstein R. Increased chromosome mobility facilitates homology search during recombination. Nat Cell Biol. 2012;14: 510–517. doi:10.1038/ncb2472

124. Muhlrad D, Hunter R, Parker R. A rapid method for localized mutagenesis of yeast genes. Yeast. 1992;8: 79–82. doi:10.1002/yea.320080202

125. Chen Y-H, Choi K, Szakal B, Arenz J, Duan X, Ye H, et al. Interplay between the Smc5/6 complex and the Mph1 helicase in recombinational repair. Proc Natl Acad Sci. 2009;106: 21252–21257. doi:10.1073/pnas.0908258106

126. The PyMOL Molecular Graphics System. Schrödinger, LLC;

127. Roth V. Doubling Time [Internet]. 2006. Available: http://www.doubling-time.com/compute.php

128. Zhang T, Lei J, Yang H, Xu K, Wang R, Zhang Z. An improved method for whole protein extraction from yeast *Saccharomyces cerevisiae*. Yeast. 2011;28: 795–798. doi:10.1002/yea.1905

129. Casey L, Patterson EE, Müller U, Fox CA. Conversion of a replication origin to a silencer through a pathway shared by a forkhead transcription factor and an S phase cyclin. Mol Biol Cell. 2008;19: 608–622. doi:10.1091/mbc.E07-04-0323

130. Lang GI, Murray AW. Estimating the per-base-pair mutation rate in the yeast *Saccharomyces cerevisiae*. Genetics. 2008;178: 67–82. doi:10.1534/genetics.107.071506

131. Lõoke M, Kristjuhan K, Kristjuhan A. Extraction of genomic DNA from yeasts for PCR-based applications. BioTechniques. 2011;50: 325–328. doi:10.2144/000113672

132. Schneider CA, Rasband WS, Eliceiri KW. NIH Image to ImageJ: 25 years of image analysis. Nat Methods. 2012;9: 671–675. doi:10.1038/nmeth.2089

133. Albuquerque CP, Smolka MB, Payne SH, Bafna V, Eng J, Zhou H. A multidimensional chromatography technology for in-depth phosphoproteome analysis. Mol Cell Proteomics MCP. 2008;7: 1389–1396. doi:10.1074/mcp.M700468-MCP200

134. Swaney DL, Beltrao P, Starita L, Guo A, Rush J, Fields S, et al. Global analysis of phosphorylation and ubiquitylation cross-talk in protein degradation. Nat Methods. 2013;10: 676–682. doi:10.1038/nmeth.2519

135. Travesa A, Kuo D, de Bruin RAM, Kalashnikova TI, Guaderrama M, Thai K, et al. DNA replication stress differentially regulates G1/S genes via Rad53-dependent inactivation of Nrm1. EMBO J. 2012;31: 1811–1822. doi:10.1038/emboj.2012.28

136. Alvino GM, Collingwood D, Murphy JM, Delrow J, Brewer BJ, Raghuraman MK. Replication in hydroxyurea: it's a matter of time. Mol Cell Biol. 2007;27: 6396–6406. doi:10.1128/MCB.00719-07

137. Aparicio OM. Location, location, location: it's all in the timing for replication origins. Genes Dev. 2013;27: 117–128. doi:10.1101/gad.209999.112

138. Su Z, Denu JM. MARCC (Matrix-Assisted Reader Chromatin Capture): An Antibody-Free Method to Enrich and Analyze Combinatorial Nucleosome Modifications. Curr Protoc Mol Biol. 2015;111: 21.32.1-21.32.21. doi:10.1002/0471142727.mb2132s111

139. Grimsrud PA, Carson JJ, Hebert AS, Hubler SL, Niemi NM, Bailey DJ, et al. A quantitative map of the liver mitochondrial phosphoproteome reveals posttranslational control of ketogenesis. Cell Metab. 2012;16: 672–683.

140. Ficarro SB, Adelmant G, Tomar MN, Zhang Y, Cheng VJ, Marto JA. Magnetic Bead Processor for Rapid Evaluation and Optimization of Parameters for Phosphopeptide Enrichment. Anal Chem. 2009;81: 4566–4575. doi:10.1021/ac9004452

141. Schultz J, Milpetz F, Bork P, Ponting CP. SMART, a simple modular architecture research tool: Identification of signaling domains. Proc Natl Acad Sci. 1998;95: 5857–5864.

142. Letunic I, Doerks T, Bork P. SMART: recent updates, new developments and status in 2015. Nucleic Acids Res. 2015;43: D257–D260. doi:10.1093/nar/gku949

143. Shima H, Suzuki M, Shinohara M. Isolation and Characterization of Novel *xrs2* Mutations in *Saccharomyces cerevisiae*. Genetics. 2005;170: 71–85. doi:10.1534/genetics.104.037580

144. Entian KD, Schuster T, Hegemann JH, Becher D, Feldmann H, Güldener U, et al. Functional analysis of 150 deletion mutants in *Saccharomyces cerevisiae* by a systematic approach. Mol Gen Genet. 1999;262: 683–702.

145. Wang AT, Smogorzewska A. SnapShot: Fanconi Anemia and Associated Proteins. Cell. 2015;160: 354–354.e1. doi:10.1016/j.cell.2014.12.031

146. Meetei AR, Medhurst AL, Ling C, Xue Y, Singh TR, Bier P, et al. A human ortholog of archaeal DNA repair protein Hef is defective in Fanconi anemia complementation group M. Nat Genet. 2005;37: 958–963. doi:10.1038/ng1626

147. Prakash R, Krejci L, Van Komen S, Anke Schürer K, Kramer W, Sung P. *Saccharomyces cerevisiae MPH1* gene, required for homologous recombination-mediated mutation avoidance, encodes a 3’ to 5’ DNA helicase. J Biol Chem. 2005;280: 7854–7860. doi:10.1074/jbc.M413898200

148. Zheng X-F, Prakash R, Saro D, Longerich S, Niu H, Sung P. Processing of DNA structures via DNA unwinding and branch migration by the *S. cerevisiae* Mph1 protein. DNA Repair. 2011;10: 1034–1043. doi:10.1016/j.dnarep.2011.08.002

149. Gari K, Décaillet C, Delannoy M, Wu L, Constantinou A. Remodeling of DNA replication structures by the branch point translocase FANCM. Proc Natl Acad Sci. 2008; doi:10.1073/pnas.0804777105

150. Stafa A, Donnianni RA, Timashev LA, Lam AF, Symington LS. Template switching during break-induced replication is promoted by the Mph1 helicase in *Saccharomyces cerevisiae*. Genetics. 2014;196: 1017–1028. doi:10.1534/genetics.114.162297

151. Luke-Glaser S, Luke B. The Mph1 Helicase Can Promote Telomere Uncapping and Premature Senescence in Budding Yeast. PLoS ONE. 2012;7: e42028. doi:10.1371/journal.pone.0042028

152. Jain S, Sugawara N, Mehta A, Ryu T, Haber JE. Sgs1 and Mph1 Helicases Enforce the Recombination Execution Checkpoint During DNA Double-Strand Break Repair in *Saccharomyces cerevisiae*. Genetics. 2016; genetics.115.184317. doi:10.1534/genetics.115.184317

153. Jain S, Sugawara N, Haber JE. Role of Double-Strand Break End-Tethering during Gene Conversion in *Saccharomyces cerevisiae*. PLoS Genet. 2016;12: e1005976. doi:10.1371/journal.pgen.1005976

154. Magaña-Schwencke N, Henriques JA, Chanet R, Moustacchi E. The fate of 8-methoxypsoralen photoinduced crosslinks in nuclear and mitochondrial yeast DNA: comparison of wild-type and repair-deficient strains. Proc Natl Acad Sci. 1982;79: 1722–1726.

155. Ward TA, Dudášová Z, Sarkar S, Bhide MR, Vlasáková D, Chovanec M, et al. Components of a Fanconi-Like Pathway Control Pso2-Independent DNA Interstrand Crosslink Repair in Yeast. PLoS Genet. 2012;8: e1002884. doi:10.1371/journal.pgen.1002884

156. Grossmann KF, Ward AM, Matkovic ME, Folias AE, Moses RE. *S. cerevisiae* has three pathways for DNA interstrand crosslink repair. Mutat Res Repair. 2001;487: 73–83. doi:10.1016/S0921-8777(01)00106-9

157. Blastyák A, Pintér L, Unk I, Prakash L, Prakash S, Haracska L. Yeast Rad5 protein required for postreplication repair has a DNA helicase activity specific for replication fork regression. Mol Cell. 2007;28: 167–175. doi:10.1016/j.molcel.2007.07.030

158. Fan HY, Cheng KK, Klein HL. Mutations in the RNA polymerase II transcription machinery suppress the hyperrecombination mutant hpr1 delta of *Saccharomyces cerevisiae*. Genetics. 1996;142: 749–759.

159. Gangavarapu V, Haracska L, Unk I, Johnson RE, Prakash S, Prakash L. Mms2-Ubc13-dependent and -independent roles of Rad5 ubiquitin ligase in postreplication repair and translesion DNA synthesis in *Saccharomyces cerevisiae*. Mol Cell Biol. 2006;26: 7783–7790. doi:10.1128/MCB.01260-06

160. Chang M, Bellaoui M, Boone C, Brown GW. A genome-wide screen for methyl methanesulfonate-sensitive mutants reveals genes required for S phase progression in the presence of DNA damage. Proc Natl Acad Sci. 2002;99: 16934–16939. doi:10.1073/pnas.262669299

161. Rothstein R, Bärtsch S. CommunityW303.html - SGD-Wiki [Internet]. [cited 13 Apr 2016]. Available: http://wiki.yeastgenome.org/index.php/CommunityW303.html